

---

[All ETDs from UAB](#)

[UAB Theses & Dissertations](#)

---

2012

## Development of Electrospun Bone-Mimetic Matrices for Bone Regenerative Applications

Matthew Christopher Phipps  
*University of Alabama at Birmingham*

Follow this and additional works at: <https://digitalcommons.library.uab.edu/etd-collection>

---

### Recommended Citation

Phipps, Matthew Christopher, "Development of Electrospun Bone-Mimetic Matrices for Bone Regenerative Applications" (2012). *All ETDs from UAB*. 2724.  
<https://digitalcommons.library.uab.edu/etd-collection/2724>

This content has been accepted for inclusion by an authorized administrator of the UAB Digital Commons, and is provided as a free open access item. All inquiries regarding this item or the UAB Digital Commons should be directed to the [UAB Libraries Office of Scholarly Communication](#).

DEVELOPMENT OF ELECTROSPUN BONE-MIMETIC MATRICES FOR BONE  
REGENERATIVE APPLICATIONS

by

MATTHEW CHRISTOPHER PHIPPS

SUSAN L. BELLIS, COMMITTEE CHAIR  
MARCAS M. BAMMAN  
STUART J. FRANK  
SHAWN R. GILBERT  
JACK E. LEMONS

A DISSERTATION

Submitted to the graduate faculty of The University of Alabama at Birmingham,  
in partial fulfillment of the requirements for the degree of  
Doctor of Philosophy

BIRMINGHAM, ALABAMA

2012

# DEVELOPMENT OF ELECTROSPUN BONE-MIMETIC MATRICES FOR BONE REGENERATIVE APPLICATIONS

MATTHEW CHRISTOPHER PHIPPS

CELLULAR AND MOLECULAR PHYSIOLOGY

## ABSTRACT

Although bone has a dramatic capacity for regeneration, certain injuries and procedures present defects that are unable to heal properly, requiring surgical intervention to induce and support osteoregeneration. Our research group has hypothesized that the development of a biodegradable material that mimics the natural composition and architecture of bone extracellular matrix has the potential to provide therapeutic benefit to these patients. Utilizing a process known as electrospinning, our lab has developed a bone-mimetic matrix (BMM) consisting of composite nanofibers of the mechanically stable polymer polycaprolactone (PCL), and the natural bone matrix molecules type-I collagen and hydroxyapatite nanocrystals (HA). We herein show that BMMs supported greater adhesion, proliferation, and integrin activation of mesenchymal stem cells (MSCs), the multipotent bone-progenitor cells within bone marrow and the periosteum, in comparison to electrospun PCL alone. These cellular responses, which are essential early steps in the process of bone regeneration, highlight the benefits of presenting cells with natural bone molecules. Subsequently, evaluation of new bone formation in a rat cortical tibia defect showed that BMMs are highly osteoconductive. However, these studies also revealed the inability of endogenous cells to migrate within electrospun matrices due to the inherently small pore sizes. To address this limitation, which will negatively impact the rate of scaffold-to-bone turnover and inhibit vascularization, sacrificial fibers were added to the matrix. The removal of these fibers after fabrication resulted in BMMs with larger pores,

leading to increased infiltration of MSCs and endogenous bone cells. Lastly, we evaluated the potential of our matrices to stimulate the recruitment of MSCs, a vital step in bone healing, through the sustained delivery of platelet derived growth factor-BB (PDGF-BB). BMMs were found to adsorb and subsequently release greater quantities of PDGF-BB, compared to PCL scaffolds, over an 8-week interval. The released PDGF-BB retained its bioactivity, stimulating MSC chemotaxis in two separate assays. Collectively, these results suggest that electrospun matrices incorporating the bone matrix molecules collagen I and HA, with sacrificial fibers, provide a favorable scaffold for MSC survival and infiltration as well as the ability to sequester PDGF-BB from solution, leading to sustained local delivery and MSC chemotaxis.

## ACKNOWLEDGEMENTS

I would like to sincerely thank everyone who has helped me become who I am today. First and foremost, I thank my family, for providing me with the foundation necessary for me to achieve my goals. I will never forget all that they have done for me. Secondly, I appreciate everyone at UAB who has contributed to my success, including friends, collaborators, and fellow lab mates. Specifically, I would like to thank my committee members for all of the advice they have given me as well as for putting up with my incessant emails. I would like to especially thank Dr. Shawn Gilbert for all of the times he let me follow him around in the hospital, and Dr. Jack Lemons for taking time out of his day to meet with me personally on multiple occasions, Dr. Marcas Bamman for checking in on me while passing in the halls, and Dr. Stuart Frank for his jokes during committee meetings.

Of course I cannot say enough about my mentor, Dr. Susan Bellis. She is the reason I came to UAB for graduate school. I enjoyed my time in her lab so much as a summer REU student I decided to come back for an extended stay. She has helped me grow as a scientist in every way, and was always there to give me advice. I know that I was very fortunate to have a mentor who cared so much about their graduate students.

Lastly, I thank the most important person in my life, my fiancé, LeeAnn. She's made each day better than the last and I can't wait to see where the future takes us.

## TABLE OF CONTENTS

	<i>Page</i>
ABSTRACT .....	ii
ACKNOWLEDGEMENTS .....	iv
LIST OF TABLES .....	vii
LIST OF FIGURES.....	viii
INTRODUCTION.....	1
Human Skeletal System .....	1
Bone Cells .....	2
Mesenchymal Stem Cells .....	3
Osteoblasts and Osteocytes .....	4
Osteoclasts.....	4
Chondrocytes.....	5
Other Cells Present in Bone .....	5
Bone Regeneration and Complications .....	6
Bone Graft Materials .....	7
Engineered Bone Biomaterials.....	8
Hydrogels .....	9
Solvent Casting .....	9
Electrospinning.....	10
Cellular Responses to Electrospun Biomaterials .....	12
Cell Recruitment .....	13
Cell Adhesion.....	13
Cell Differentiation .....	14
Cell Infiltration.....	15
Strategies for Improving Electrospun Orthopedic Implant Materials.....	16
Incorporation of Cell Ligands .....	16
Increased Porosity .....	17
Delivery of Therapeutic Agents .....	18
Research Objectives .....	21

TABLE OF CONTENTS (Continued)

	<i>Page</i>
MESENCHYMAL STEM CELL RESPONSES TO BONE-MIMETIC ELECTROSPUN MATRICES COMPOSED OF POLYCAPROLACTONE, COLLAGEN I AND NANOPARTICULATE HYDROXYAPATITE.....	28
INCREASING THE PORE SIZES OF BONE-MIMETIC ELECTROSPUN SCAFFOLDS COMPRISED OF POLYCAPROLACTONE, COLLAGEN I AND HYDOXYAPATITE TO ENHANCE CELL INFILTRATION.....	56
DELIVERY OF PLATELET-DERIVED GROWTH FACTOR AS A CHEMOTACTIC FACTOR FOR MESENCHYMAL STEM CELLS BY BONE-MIMETIC ELCTROSPUN SCAFFOLDS .....	92
CONCLUSIONS.....	118
GENERAL LIST OF REFERENCES.....	131
APPENDIX	
A    INSTITUTIONAL REVIEW BOARD FOR HUMAN USE APPROVAL FORM .....	146
B    INSTITUTIONAL ANIMAL CARE AND USE COMMITTEE APPROVAL FORMS .....	148

## LIST OF TABLES

<i>Table</i>		<i>Page</i>
	MESENCHYMAL STEM CELL RESPONSES TO BONE-MIMETIC ELECTROSPUN MATRICES COMPOSED OF POLYCAPROLACTONE, COLLAGEN I AND NANOPARTICULATE HYDROXYAPATITE	
1	Tensile properties of dry and hydrated scaffolds .....	38



## LIST OF FIGURES

<i>Figure</i>		<i>Page</i>
INTRODUCTION		
1	Bone microstructure .....	25
2	Diagram of electrospinning apparatus.....	26
3	Integrin mediated cell adhesion and signaling cascades .....	27
MESENCHYMAL STEM CELL RESPONSES TO BONE-MIMETIC ELECTROSPUN MATRICES COMPOSED OF POLYCAPROLACTONE, COLLAGEN I AND NANOPARTICULATE HYDROXYAPATITE		
1	SEM images of MSCs cultured on nanofibrous scaffolds for 24 hours.....	51
2	Live cell imaging of GFP-expressing MSCs seeded onto electrospun scaffolds .....	52
3	MTS assay quantifying cell proliferation on electrospun scaffolds of PCL, PCL/HA or PCL/col/HA .....	53
4	Adsorption of FN and VN by electrospun scaffolds .....	54
5	Immunostaining for phosphorylated focal adhesion kinase.....	55
INCREASING THE PORE SIZES OF BONE-MIMETIC ELECTROSPUN SCAFFOLDS COMPRISED OF POLYCAPROLACTONE, COLLAGEN I AND HYDROXYAPATITE TO ENHANCE CELL INFILTRATION		
1	PCL/col/HA scaffolds (“TRI”), or scaffolds composed of 100% PCL, were implanted into a cortical defect in a rat tibia for seven days.....	84
2	SEM images of selective cleavage of collagen I present in TRI scaffolds .....	85
3	Pre-treating scaffolds with collagenase does not facilitate cell infiltration of MSCs <i>in vitro</i> .....	86
4	Decreasing the packing density of electrospun fibers.....	87
5	Removal of sacrificial electrospun fibers.....	88

LIST OF FIGURES (Continued)

<i>Figure</i>	<i>Page</i>
6	Mean pore size analysis of electrospun TRI and TRI/PEO scaffolds ..... 89
7	Electrospun scaffolds created with PEO fibers support cell infiltration of MSCs <i>in vitro</i> ..... 90
8	Electrospun scaffolds created with PEO fibers support infiltration of endogenous cells from calvarial organ cultures ..... 91
<p>DELIVERY OF PLATELET-DERIVED GROWTH FACTOR AS A            CHEMOTACTIC FACTOR FOR MESENCHYMAL STEM CELLS BY            BONE-MIMETIC ELECTROSPUN SCAFFOLDS</p>	
1	Standard curve of GFP fluorescent signal from lysed GFP-MSCs..... 112
2	Chemotactic responses of MSCs..... 113
3	Adsorption and release of PDGF-BB from scaffolds..... 114
4	PDGF-BB released from PCL/col/HA scaffolds stimulates MSC chemotaxis... 115
5	Mitogenic effects of PDGF-BB..... 116
6	Released PDGF-BB induces chemotaxis of MSCs in a stringent migration assay ..... 117

## INTRODUCTION

### Human Skeletal System

The human skeletal system provides our bodies with essential mechanical support, protection of vital organs, a reservoir of growth factors and minerals, and the necessary microenvironment for hematopoiesis [1]. Mature skeletal bone is composed of both an inorganic and organic phase. The inorganic phase is primarily carbonated hydroxyapatite (HA) crystals  $\text{Ca}_{10}(\text{PO}_4)_6(\text{OH})_2$ , making up approximately two thirds of the total bone weight. The organic phase primarily consists of type I collagen, but also lesser amounts of other proteins, such as bone sialoprotein, and osteocalcin, as well as proteoglycans. Mature lamellar bone is made up of highly aligned collagen fibrils with interspersed HA crystals (Figure 1). Concentric layers of lamellar fibrils combine to form osteons, cylindrical structures that surround blood vessels and nerves in the bone. This highly organized structure combining organic and inorganic materials contributes to the extraordinary mechanical properties of bone. The skeletal system is made up of five general categories of bones: long bones, short bones, flat bones, sesamoid bones and irregular bones [1].

Flat bones, such as the cranium, form through the process of intramembranous ossification. This process is initiated by the differentiation of mesenchymal stem cells (MSCs), the multipotent stem cells found in the bone marrow and periosteum, into osteoblasts, the primary bone-building cells, and the formation of an ossification center. These cells then secrete an osteoid matrix, primarily consisting of type I collagen. This osteoid

matrix is subsequently mineralized by osteoblasts to form woven bone, a quickly forming but mechanically weaker form of bone. Over time, the less-organized woven bone is replaced with mature lamellar bone. As more bone formation occurs, some osteoblasts become trapped in the mineralized matrix, becoming osteocytes [2].

Other bone types, such as long bones (femur) and short bones (carpals), form through a combination of intramembranous and endochondral ossification. In endochondral ossification, the formation of mineralized tissue is preceded by chondrocyte production of a hyaline cartilage matrix. A thin membrane of connective tissue containing bone progenitor cells, known as the periosteum, then forms around the cartilage template, and a primary ossification center begins to form with the invasion of blood vessels into the cartilage as well as the differentiation of mesenchymal stem cells to osteoblasts. Chondrocytes begin the process of matrix calcification before undergoing apoptosis. Osteoblasts then enter the cavity left by the chondrocytes and secrete osteoid. Osteoclasts, the primary bone-resorption cells, work in conjunction with osteoblasts to convert the calcified cartilage and osteoid into mature lamellar bone. Ultimately, cancellous bone, a form of bone with high surface area and vascularization, is formed to house the bone marrow cavity and hematopoiesis. This cavity is surrounded by the more compact cortical bone, which provides the mechanical strength of bone [2].

### Bone Cells

The bone marrow, periosteum, and bone matrix house numerous cell types. These cells are vital for not only maintaining and healing bone, but also for the replenishing of blood cells through hematopoiesis. Although initially believed that only bone-building

cells were vital to the process of bone healing, research has shown that multiple cell types work in conjunction to return a skeletal defect to its original strength and shape.

### *Mesenchymal Stem Cells*

Researchers have studied the various cell types in the bone marrow for many decades, but it wasn't until the end of the 20<sup>th</sup> century that the multipotent nature of bone marrow stromal cells was truly realized. Arnold Caplan first introduced the term mesenchymal stem cell (MSC) in 1991 [3], although they are also referred to as marrow stromal stem cells, mesenchymal progenitor cells, and multipotent stromal cells. Pittenger et al. [4], among others [5, 6], were among the earliest to definitively demonstrate the ability of MSCs to differentiate along adipogenic, chondrogenic and osteogenic lineages.

MSCs are adherent-dependent multipotent cells residing in the bone marrow and periosteum, among other tissues. About one out of every 100,000-500,000 cells in the bone marrow is an undifferentiated MSC [5], capable of differentiating along adipocytic, chondrocytic, osteoblastic, and potentially other cell lineages [7-9]. Although believed to be quiescent *in vivo* under normal conditions, MSCs are capable of undergoing rapid proliferation following physiological changes to their environment. Following a bone injury, MSCs are recruited to the defect site in response to factors released during the inflammation stage, such as platelet-derived growth factor (PDGF) [10, 11]. Once at the site of the defect, MSCs proliferate and differentiate into chondrocytes and osteoblasts. The differentiation of MSCs is mediated by various growth factors, such as bone-morphogenic proteins (BMPs), fibroblast growth factors (FGF), and transforming growth factors (TGF) [10, 12].

MSCs are of especial interest in the tissue-engineering field due to their ability to differentiate into multiple cell types and their relative ease in harvesting and culturing *in vitro* [13]. Their importance in the bone healing process makes it essential to investigate the interactions between MSCs and bone biomaterials. Additionally, many biomaterials have the potential to serve as carriers for the delivery of exogenously expanded MSCs into a bone defect.

### *Osteoblasts and Osteocytes*

Osteoblasts are the primary cells responsible for synthesizing new bone matrix. Mature osteoblasts have a cuboidal morphology with a large nuclei, enlarged Golgi structures, and extensive endoplasmic reticulum. They are typically found lining the bone in conjunction with osteoblast precursors. Activated osteoblasts secrete the protein matrix osteoid, composed of type I collagen and other matrix proteins, such as osteopontin, osteocalcin, and bone sialoprotein [1]. Osteoblasts then mineralize this osteoid matrix, ultimately converting the matrix into lamellar bone. During the bone building process, some osteoblasts become trapped within the bone matrix. These cells, known as osteocytes, remain isolated in lacunae and are believed to signal to other osteocytes and osteoblasts in response to mechanosensory stimuli and bone injuries [14].

### *Osteoclasts*

Osteoclasts are multi-nucleated cells formed by the fusion of monocyte-macrophage precursor cells [15]. RANK ligand (RANKL), expressed on the surface of osteoblasts, and macrophage colony-stimulated factor (M-CSF) are necessary for osteo-

clast formation and activation. Once activated, osteoclasts attach to the bone matrix (sealing zone) and create a resorptive pit known as a Howship's Lacunae. The cell membrane in contact with the bone matrix forms a ruffled border to increase the surface area, and hydrogen ions are then released into the resorptive pit in order to acidify the cavity and facilitate the dissolution of the hydroxyapatite crystals [1]. Additionally, the osteoclasts secrete proteases, such as cathepsin K, to degrade the bone matrix proteins [15].

### *Chondrocytes*

Chondrocytes produce cartilaginous matrix through the secretion of collagen and proteoglycans. The only cell present in cartilage, chondrocytes are also essential to the process of endochondral ossification. Chondrocytic production of collagen type II and X is necessary for the growth of long bones [16] and is important in the healing of many bone defects [17]. The matrix produced by chondrocytes acts as a template for osteoblast bone matrix production.

### *Other Cells Present in Bone*

The bone marrow cavity is home to hematopoiesis, and specifically hematopoietic stem cells. The blood vessels, consisting of endothelial cells and pericytes, present throughout the bone make it possible for hematopoiesis to occur, and angiogenesis following bone fracture is necessary for the healing process. Other cell types, such as adipocytes and lymphocytes are also present in the bone marrow.

## Bone Regeneration and Complications

In response to a skeletal injury, such as a fracture, the bone healing process is initiated with an inflammation stage. In the first few hours after the injury, a blood clot will form and restriction of the blood vessels will prevent further bleeding. Growth factors released during this stage initiate the chemotaxis of various cell types, including immune cells such as macrophages and giant cells, fibroblasts, and MSCs, into the defect [18]. Additionally, new blood vessels begin to form during this stage, bringing in oxygen and nutrients and removing waste. In the following days, the migrated MSCs will multiply and differentiate into chondrocytes and osteoblasts, and begin laying down hyaline cartilage and woven bone, respectively. This newly formed tissue, known as the fracture callus, stabilizes the fracture site [19]. Over time, the loosely organized fracture callus is replaced with lamellar bone through endochondral ossification and creeping substitution, restoring most of the inherent strength [2]. The defect site will continue to undergo remodeling for several years in order to finally return the bone to its original shape and strength.

Although skeletal bone has a dramatic capacity for regeneration, cases of significant bone loss or other extenuating circumstances may exceed the body's natural healing capabilities. These defects require surgical intervention in order to assist in the healing process, often utilizing fixators and bone grafts [20]. Fixation is necessary to provide mechanical stability to the bone during the healing process. Depending on the location of the bone injury, various fixation techniques can be used. These include external fixators, intramedullary nails, bridging plates, and cast immobilization, among others [19]. A lack of mechanical stability during the healing process will lead to excessive fibrous scar tissue,



inhibiting new bone growth. In contrast, excessively rigid fixation may inhibit fracture callus formation, increasing the time necessary for the bone to heal.

### Bone Graft Materials

Depending on the severity of the skeletal defect, bone grafts may be used to 1) provide an osteoconductive matrix to serve as a framework for new bone growth, 2) deliver cells with osteogenic potential, and/or 3) deliver an osteoinductive molecule to stimulate new bone formation [21]. Numerous types of bone grafts are used clinically, with autograft, bone harvested from the patient, being the current gold standard.

Although autograft possesses all three of the previously mentioned uses of bone grafts, thereby making it very effective, its use has numerous limitations. Autograft is typically harvested from the iliac crest of the patient's pelvic bone, requiring a secondary surgery and increased operating time, often leading to donor site morbidity [22]. In some patients, such as those suffering from osteoporosis or diabetes, the quality of harvestable bone may not be optimal for use as a bone graft. Additionally, the limited supply of harvestable bone may not meet the needs of severe defects [20, 23].

In attempt to alleviate the need for harvesting a patient's own bone tissue, clinicians have the option of using allograft, or bone transplanted from other humans. In order to reduce the risk of disease transmission and immune rejection, these grafts must be processed to destroy all bone cells, drastically reducing their osteogenic potential [19]. Allogenic bone graft comes in multiple forms, such as bone chips, bulk allograft, cortical struts, and demineralized bone graft [21]. First published by Urist in 1965, demineralization of allograft bone was found to expose osteoinductive molecules, such as BMP-2,

within the underlying matrix [24]. Although allografts provide benefit to some patients with bone defects, the successful fusion rate of procedures using allograft is still lower than that of autogenous grafts, creating the need for improved graft materials.

Clinicians and researchers have also investigated the use of synthetic alternatives with the potential to support new bone growth. These biomaterials include (but are not limited to) calcium-containing biomaterials such as HA, tri-calcium phosphate (TCP), calcium sulphate (plaster of Paris), as well as collagen sponges, and combinations of these materials [21, 25]. These products are typically considered only osteoconductive, and therefore have limited use, such as a bone graft extender when used in conjunction with autograft [20]. Despite the numerous products available, a suitable alternative to completely replace autogenous bone grafting has yet to be developed.

### Engineered Bone Biomaterials

The steadily increasing occurrence of bone grafting procedures has created a major clinical need for a material capable of stimulating new bone formation, thereby reducing the necessity of harvesting a patient's own bone. In response to this demand, interdisciplinary researchers in the field of tissue engineering have made considerable advances, with materials evolving from bioinert, to biodegradable, to being capable of stimulating cellular responses at the molecular level [25]. To this end, biodegradable materials capable of supporting cell adhesion, proliferation, controlled differentiation and tissue-ingrowth, ultimately being replaced by native bone, are currently being developed. These materials typically mimic the natural structure and composition of bone through the incorporation of natural bone molecules or bio-mimetic peptides. Additionally, many labs

are currently investigating novel methods to deliver bioactive molecules and growth factors capable of stimulating bone formation.

### *Hydrogels*

A hydrogel is a general term used to describe highly absorbent cross-linked polymers. These gel-like materials are very flexible and malleable, allowing them to conform to a desired space. Therefore, most hydrogels are injectable, a beneficial property for non-invasive surgeries [26]. The aqueous environment of a hydrogel allows it to easily deliver cells [27] or therapeutic agents locally, making it a potential delivery vehicle [28]. However, hydrogels can be difficult to sterilize, and typically lack biological components. Many researchers are investigating ways to functionalize hydrogels in order to increase their biological activity, such as the inclusion of cell attachment mediators and incorporation of calcium phosphate minerals [29].

### *Solvent Casting*

Another popular engineering technique is solvent casting. In this technique, polymers are dissolved in an organic solvent, and the solution is then added to a mold. After the solvent evaporates, the resulting polymer material will have adopted the architecture of the mold, thereby allowing control of the structure on the macro-scale. Additionally, particles and/or proteins can be added to the polymer solution prior to casting, thereby creating advanced composites [30]. For instance, the addition of porogens, such as salt particles or microspheres [31, 32], has been used as a sacrificial material to increase the porosity of the resulting scaffold. After casting, the material can be placed in a bath to dissolve the porogens, leaving pores in their place [33, 34].

Although solvent casting is a versatile technique, it does present some potential drawbacks and limitations. Deposits of the solvent left over after fabrication may be toxic to cells and tissues. Furthermore, the most common methods for increasing the porosity of the material, such as salt leaching, do not guarantee the formation of interconnected pores, limiting the effectiveness of the pores *in vivo*.

### *Electrospinning*

A promising technique capable of creating biodegradable, nanofibrous scaffolds is electrospinning [35-38]. Originally developed in the textile industry, the process of electrospinning has received steadily increasing attention since it was demonstrated to produce fibrous meshes that mimic the architecture found in native extracellular matrix [39, 40]. An electrospinning set-up (Figure 2) consists of a polymer or composite solution pumped from a syringe into a positively charged metal needle. Once the electrostatic repulsion of the charged particles overcomes the surface tension of the solution, a cone forms at the tip of the needle, called a Taylor cone, and a thin fiber is expelled from the tip of the cone, which travels through the air towards a grounded collecting plate [36]. As the fiber travels, electrostatic repulsion causes the fiber to whip around, the solvent used evaporates and the fiber elongates and thins out prior to deposition, where the charge dissipates. The resulting matrix consists of fibers with diameters in the nano- to micrometer range (similar to collagen bundles [41]), with a large surface-to-volume ratio and interconnected pores.

The adjustment of processing parameters during electrospinning allows for the tailoring of fiber diameter size and arrangement. For instance, increasing the voltage ap-

plied to the solution or the distance between the needle and the collecting plate has been shown to decrease the average fiber diameter [38]. The arrangement of the collecting fibers can also be controlled in a variety of ways, such as using different types of collecting plates. Cylindrical collecting plates rotating with high angular velocity on an axis perpendicular to the direction of the electrospun fibers have been shown to align the arrangement of the collecting fibers [42]. These highly aligned matrices may provide benefit in applications where maximum mechanical properties are needed in a uniaxial direction, such as tendon tissue engineering. However, it is postulated that these aligned matrices decrease the porosity of the scaffold, thereby hindering cellular infiltration.

A large portion of the current literature on electrospun biomaterials has focused on using 100% synthetic polymers, such as polycaprolactone (PCL) [43-45], polyglycolic acid (PGA) [46], and polylactic acid (PLA) [47, 48], due to the relative ease of electrospinning these molecules and controlling their fiber architecture and orientation. However, these polymers do not provide biological signals to cells, and are therefore poor substrates for cell adhesion. Consequently, many researchers have investigated coating polymer scaffolds with hydroxyapatite [49, 50], collagen mimetic peptides[51] or full-length collagen I [52, 53] in order to provide biological factors for cells. Although benefits to cell adhesion and survival have been reported in these studies, passively coating the surface of meshes consisting of polymer fibers creates a heterogeneous matrix, with interior fibers receiving little if any biological modification. Therefore, after the exterior layers of the scaffold degrade and cells migrate within the scaffold, the cells will only be exposed to 100% polymer fibers, providing no biological signals to the cells. In this study, we hypothesized that electrospinning a solution of collagen I and hydroxyapatite nanoparticles

with polycaprolactone (PCL) will create a matrix consisting entirely of bone-mimetic, biodegradable nanofibers. Using nanohydroxyapatite particles with average diameters of 50nm, we can obtain an even dispersion of HA throughout the matrix, with little agglomeration [54]. Therefore, our matrices present infiltrating cells with bone-like extracellular matrix (ECM) throughout the scaffold, even after the outer layers of the scaffold have degraded. We chose PCL, an aliphatic polyester with a degradation rate slower than that of collagen, to provide mechanical stability to the scaffolds and control the rate of resorption [55]. PCL is a biodegradable polymer that has received FDA approval for many applications, including drug delivery devices [56] and sutures [57].

### Cellular Responses to Electrospun Biomaterials

Biodegradable materials designed for bone regeneration must provide cells that have been recruited into the bone defect with a matrix that supports cell adhesion and proliferation. Additionally, the ability of a matrix to influence cell differentiation has been reported by many [58-60], and therefore biomaterials capable of supporting or even stimulating osteogenic differentiation of bone progenitor cells offer increased therapeutic benefit. The implant must also biodegrade, allowing bone cells to turn over the temporary scaffolding material into new bone. Biomaterials capable of supporting the infiltration of bone cells into the interior of the scaffold will help facilitate this process by allowing new bone formation throughout the implant [25]. This will ultimately increase the rate at which the defect is replaced with native bone, allowing the patient to return to normal activities sooner. An ideal bone regenerative biomaterial will support all of these various

cellular responses, spanning from initial cell attachment to deposition of mineralized matrix, providing a framework for new bone formation.

### *Cell Recruitment*

In response to skeletal injury, the chemotaxis of numerous cells into the site of the defect is essential for proper healing. These include neutrophils, macrophages, fibroblasts and MSCs. The recruitment of MSCs from the neighboring bone marrow and periosteum is vital to the healing process, since they are the progenitors for chondrocytes and osteoblasts. Therefore, stimulating the migration of MSCs has the potential to provide therapeutic benefit in cases of insufficient bone healing. Many researchers have investigated the propensity of chemokines, growth factors, and small molecules to stimulate MSC migration *in vitro* and *in vivo* [61-64]. Incorporation of one or more of these factors onto electrospun biomaterials may ultimately lead to improved patient prognosis.

### *Cell Adhesion*

The ability of a biomaterial to facilitate the cellular adhesion of invading cells is an important step in the bone healing process. The binding of cell surface integrins, heterodimeric transmembrane glycoproteins consisting of an  $\alpha$  and  $\beta$  subunit, to ligands in the ECM such as collagen I, leads to the formation of protein complexes at the cytosolic integrin tails. These protein complexes activate cell signaling cascades, ultimately influencing cell adhesion, proliferation and differentiation (Figure 3) [65-68]. Therefore, it is important for biomaterials to present anchorage dependent cells, such as MSCs, with integrin ligands.

In addition to incorporating integrin ligands, such as collagen I, into bone biomaterials, the ability of a biomaterial to adsorb proadhesive proteins from the surrounding microenvironment provides an additional method for facilitating cell adhesion. It is known that high levels of proadhesive proteins, such as fibronectin (FN) and vitronectin (VN), are present in blood and serum. Once a biomaterial is implanted into a patient, it quickly becomes covered in the patient's blood, thereby exposing it to these proteins. It has been shown that HA containing biomaterials are capable of adsorbing vast quantities of FN and VN from serum and the bone microenvironment, and these adsorbed proteins facilitate increased MSC adhesion over uncoated HA [69-71].

### *Cell Differentiation*

MSCs are multipotent stem cells, capable of differentiating along multiple cell lineages, notably adipocytes, chondrocytes and osteoblasts. The commitment to a specific lineage is dependent on soluble molecular cues and the extracellular matrix. Culturing MSCs in media supplemented with ascorbic acid-2-phosphate (AsAP),  $\beta$ -glycerolphosphate ( $\beta$ -GP), and dexamethasone (Dex), has been shown to induce osteoblastic differentiation *in vitro* [72]. Numerous other factors, including BMP-2 [73], BMP-7 [74], bFGF [75], TGF- $\beta$  [76], parathyroid hormone [77], and platelet derived growth factor-BB (PDGF-BB) [78] have all been reported to induce MSC differentiation into osteoblasts *in vitro*, either alone or in conjunction with other molecules.

MSC differentiation along the osteoblastic lineage is initially characterized by an alteration of cell morphology, from a small body with long, thin extended processes to a cuboidal shape with large amounts of rough endoplasmic reticulum. The early stages of



differentiation also include an increase in alkaline phosphatase activity and the upregulation of the transcription factors RUNX2 and Osterix [79]. The later stages of differentiation involve increased production of the bone matrix proteins collagen I, bone sialoprotein, osteocalcin, and osteopontin. Induced MSCs will also begin to form mineralized nodules through the seeding of nanocrystalline calcium phosphate molecules into the secreted protein matrix in late stages of differentiation [80].

The properties and composition of the extracellular matrix exposed to MSCs have also been shown to play an important role in cellular fate. For instance, matrix stiffness is capable of influencing MSC commitment along cell specific lineages, with more rigid surfaces promoting osteoblastic cell phenotype [58]. In addition to its role in MSC adhesion, collagen I has also been reported to induce the osteoblastic differentiation of MSCs through the  $\alpha_2\beta_1$  integrin, leading to increased matrix mineralization and upregulation of osteoblastic genes [81, 82]. Therefore, incorporation of collagen I in bone biomaterials has the potential to positively influence cell adhesion and subsequent MSC differentiation.

### *Cell Infiltration*

The infiltration of bone cells into a biodegradable implant is a crucial step in the replacement of the temporary scaffold with new bone through a process known as creeping substitution. Additionally, vascularization of the biomaterial is important to bring nutrients and oxygen to the bone cells [83]. It has been shown that non-porous materials, such as some metals, inhibit bone ingrowth, thereby reducing the strength of the implant/bone interface [19]. The ideal pore size for bone ingrowth into a biomaterial is con-

troversial, however interconnected pores with sizes ranging from 30-100 $\mu$ m have been shown to facilitate substantial cell infiltration and biointegration [84, 85].

In addition to the presence of pores created in the biomaterial during fabrication, degradation of the implant *in vivo* will also influence cell infiltration. Ideally, a bone biomaterial will resorb at a similar rate as new bone formation, facilitating a natural turnover of implant/bone. Materials that resorb too slow or too quickly will negatively affect the healing process [86].

## Strategies for Improving Electrospun Orthopedic Implant Materials

### *Incorporation of Cell Ligands*

Although 100% polymer scaffolds possess favorable tensile properties, the lack of biological cues presented to cells limits cell adhesion and the activation of cellular signaling cascades, which leads to proliferation and differentiation. By incorporating natural cellular ligands into electrospun polymer matrices, a composite material can be created that more closely mimics the natural ECM of the target tissue. It is believed that these biomimetic matrices will be able to influence cellular responses as well as provide mechanical stability. A variety of proteins have been investigated for their ability to positively influence cellular behavior when incorporated into electrospun fibers, including collagens [87], gelatin [88], chitosan [89], silk fibroin [90], laminin [91] and elastin [92]. In this study, the primary goal was to create a biomimetic bone matrix, therefore we investigated the benefits of including two of the largest constituents of natural bone, collagen I and HA.

### *Increased Porosity*

Recent literature from our lab as well as others has brought to light the inability of cells to infiltrate into standard electrospun matrices *in vitro* and *in vivo* [44, 83, 93, 94]. Although the fibrous meshes present a high porosity with interconnected pores, the mean pore size is too small to facilitate cell infiltration. Therefore recent work in the field has attempted to address this key limitation through a variety of methods. One such method involves the use of unique, patterned collecting plates, which are capable of controlling fiber alignment and packing density. This method has been successfully reported with PCL fibers in a concave shell with embedded metallic needles [95], PCL fibers onto patterned flat collecting plates, including metal wire meshes [96], and PLGA fibers onto a rotating frame with horizontal metal struts [97]. All studies reported significant increases in cell infiltration in comparison to standard electrospinning set-ups. Alternatively, Nam et al. [98] and Wright et al. [99] both reported on the incorporation of salt crystals during the electrospinning process. After electrospinning, the salt particles were washed away, leaving voids in their place, which facilitated increased cellular infiltration of CFK2 cells into PCL matrices and MC3T3-E1 cells into PLLA matrices, respectively. Similarly, Leong et al. constructed an electrospinning environment that supported spontaneous ice crystal formation within collecting electrospun fibers of PLA [100]. After the ice crystals were melted away, the resulting matrices promoted cell infiltration of fibroblasts *in vitro* and *in vivo* in subcutaneous skin pouches. Instead of using sacrificial particles, Baker et al. [101] and Milleret et al. [102] reported increasing the mean pore sizes of electrospun scaffolds via the incorporation of sacrificial fibers of water-soluble polymers during matrix fabrication, with subsequent removal of the fibers by washing the scaffolds in water.

It should be noted that the vast majority of studies investigating ways to increase the porosity of electrospun scaffolds has been performed with 100% polymer solutions. Therefore a major goal of the current study was to examine possible mechanisms for increasing the mean pore sizes of our bone mimetic matrices.

### *Delivery of Therapeutic Agents*

In order to increase the therapeutic potential of bone biomaterials, many researchers have investigated using them as delivery vehicles for recombinant proteins and other molecules to promote endogenous repair mechanisms. By locally delivering these molecules, a higher concentration and extended duration of the therapeutic agent can be achieved at the defect site [103]. Additionally, limiting systemic exposure has the potential to reduce the occurrence of unwanted side effects. Depending on the delivery vehicle and therapeutic agent chosen for delivery, specific consideration must be given to protein stability, loading dose and release kinetics. Numerous mechanisms have been explored for loading growth factors and other molecules to electrospun matrices and similar biomaterials, with varied levels of success.

*Bone Morphogenic Protein-2.* BMP-2 is a member of the TGF- $\beta$  superfamily and a powerful inducer of osteoblastic differentiation *in vitro* and new bone formation *in vivo* [104]. BMP-2 has been approved for use in certain clinical applications of bone healing, specifically in Medtronic's Infuse<sup>®</sup> bone graft for the treatment of lumbar spinal fusions, tibia fractures and sinus augmentation. The Infuse<sup>®</sup> bone graft consists of a collagen I sponge scaffold soaked in BMP-2 prior to implantation [105]. The degradation of colla-

gen I sponges *in vivo* leads to the rapid release of adsorbed BMP-2, and therefore high initial loading doses of BMP-2 protein are necessary. Recently, the Infuse<sup>®</sup> product has fallen under controversy from off-label use and subsequent side effects caused by the dissemination of large doses of BMP-2 [106, 107]. It has become apparent that better delivery vehicles are needed to deliver BMP-2, offering greater control over the release kinetics and ultimately allowing for the use of smaller doses.

*Bone Morphogenic Protein-7.* Another member of the TGF- $\beta$  superfamily, BMP-7, also known as osteogenic protein-1 (OP-1), has shown similar potential to that of BMP-2. Treatment of MSCs with BMP-7 leads to the expression of osteoblastic genes in MSCs cultured *in vitro* [108]. A product from Olympus Biotech, Opgenra<sup>®</sup> (formerly OP-1 from Stryker), combines BMP-7 with bovine collagen I and carboxymethylcellulose sodium to form a putty for use in spinal fusions and tibia fractures [109]. Its use has also been controversial in the USA, where it has struggled to gain complete approval by the Food and Drug Administration (FDA), although it has been approved for spinal fusions in much of Europe. As a means to control the delivery of BMP-7, other researchers have investigated the use of delivery vehicles such as poly-D, L-lactic-acid (PDLLA) pellets [110] and poly(lactic-co-glycolic acid) (PLGA) nanospheres [111], with both studies reporting the induction of ectopic bone formation *in vivo*.

*Insulin-like Growth Factor-1.* IGF-1 is a hormone that plays a very important role in childhood growth, particularly the extension of long bones [104]. During endochondral ossification, IGF-1 stimulates the proliferation of chondrocytes and subsequent extracel-

lular matrix production, thereby lengthening the cartilage template in growing bones. IGF-1 is primarily released by the liver in response to growth hormone secreted from the pituitary gland. However, it has been reported that numerous tissue specific cell types are also capable of secreting IGF-1, such as osteoblasts [103]. Xian et al. have also reported the ability of IGF-1 to induce osteoblastic differentiation of MSCs [112]. Recent work has explored the effects of locally delivered IGF-1 on healing skeletal defects and periodontal tissues. In attempt to extend the delivery of IGF-1, Wang et al incorporated the protein into PLGA microspheres to sustain its release in a model of dental implantation in diabetic rats [113] and noted improved osseointegration. Similarly, increased periodontal tissue regeneration was reported when IGF-1 release was sustained locally using dextran-co-gelatin microspheres [114]

*Platelet-Derived Growth Factor-BB.* PDGFs are mitogenic and chemotactic agents for cells of mesenchymal origin, as well as inducers of angiogenesis, making them key molecules in the repair of many tissue types [115]. The PDGF family consists of 4 distinct subunits that are secreted as disulfide linked homo- or heterodimers. Primarily synthesized and released by platelets in response to tissue injury, PDGFs are also produced by numerous other cell types, including macrophages, chondrocytes, and fibroblasts [10]. PDGF-BB is the only isoform capable of activating all three known receptors of PDGF, and therefore is considered the most biologically active isoform [11]. PDGF-BB has been shown to be present at the site of skeletal defects during the inflammation stage, and its local delivery has led to an increase in the rate of bone healing [116]. PDGF-BB has been studied in a wide range of preclinical models for safety [117] and is

currently FDA approved for delivery from  $\beta$ -tricalcium phosphate (TCP) in periodontal procedures (GEM21S<sup>®</sup> Osteohealth). The use of PDGF-BB with  $\beta$ -TCP (Augment Bone Graft<sup>®</sup>, Biomimetic Therapeutics, Inc) in foot and ankle fusions is currently under review for approval by the FDA. However, the dissemination of PDGF-BB from these  $\beta$ -TCP particles is extremely rapid *in vitro* and *in vivo*. After implantation in a rat cranial defect, approximately 90% of PDGF had been released by 72hrs [118]. It has been hypothesized that extended release of PDGF-BB will help encourage angiogenesis in addition to MSC migration and proliferation. Therefore, novel vehicles for delivering PDGF are needed to extend the delivery time *in vivo*, curtailing unwanted dissemination and potentially reducing the amount of PDGF-BB loaded onto the biomaterial.

### Research Objectives

To address the ever-growing clinical need for bone grafts, the primary objective of this dissertation was to develop a synthetic material capable of supporting robust bone regeneration. We hypothesized that the most successful material for achieving this goal would mimic the structure and composition of natural bone matrix. To create such a material, we chose to combine the natural bone molecules collagen I and HA with the FDA approved biodegradable polymer PCL into a nanofibrous matrix using the process of electrospinning. The initial goals of this work included developing the apparatus for electrospinning and determining the optimal parameters for material construction.

In order to analyze a material for its potential use as a bone biomaterial, our lab and others have shown the importance of studying the initial cellular responses of MSCs [70, 71, 87, 119, 120]. In order to support new bone formation and proper osseointegra-

tion, MSCs must be able to firmly adhere and proliferate on a material. Initially, we investigated the response of MSCs to 100% electrospun collagen I scaffolds. We hypothesized that these matrices, consisting entirely of the natural bone protein collagen I, would provide cells with an excellent matrix for cell adhesion. However, it was found that the poor mechanical properties and rapid degradation of 100% collagen I scaffolds inhibited cell adhesion, and subsequently cell survival [87]. Based on these findings, we hypothesized that combining collagen I with the biodegradable polymer PCL would increase the mechanical properties and degradation times of the scaffolds, and therefore investigated the MSC responses between our bone-mimetic matrices (BMMs), consisting of PCL, collagen I, and nanoparticulate HA, and 100% PCL matrices, allowing us to evaluate how the presence of natural bone molecules affects cellular behavior. These experiments showed that BMMs were able to retain the mechanical stability of PCL, yet provided cells with biological cues leading to increases in MSC integrin activation, firm adhesion, and proliferation. Additionally, BMMs adsorbed greater amounts of proadhesive proteins, from both serum and the bone microenvironment, than PCL scaffolds. Previously, our lab has shown that HA containing biomaterials are capable of adsorbing vast quantities of proadhesive proteins from solution, and that these proteins help facilitate cell adhesion [70].

The second overarching goal of this project was to develop a straightforward, reproducible way to increase the pore sizes of our BMMs. Previous results revealed that although BMMs were able to support robust new bone formation *in vivo*, the mean pore sizes of our BMMs were not large enough to promote cellular infiltration into the bio-



material. We therefore investigated possible techniques for increasing the average pore size in our BMMs.

Initially, we posited that the collagen present in the BMMs could be a target for controlled degradation, thereby increasing pore sizes. MSCs and other cells would potentially be able to use the collagen as a ligand for integrins, and subsequently release proteases capable of cleaving the collagen fibers, opening pores for their migration. Using collagenase as a model protease *in vitro*, we pretreated both BMMs and PCL matrices to evaluate changes in pore size and subsequent cell infiltration. Although collagenase was able to successfully cleave fibers in the BMM matrix, these fiber breakages were unable to facilitate cell infiltration.

Alternatively, we attempted to decrease the packing density of the electrospun fibers during the fabrication process. We hypothesized that by using a unique collecting plate consisting of a flat polystyrene surface with metallic probes perpendicularly exiting the plate, it could be possible to reduce the density at which the fibers collect. The resulting matrices for PCL showed an advanced architecture with large pores and deep channels, however this could not be recapitulated with our BMMs.

As a final means of increasing the mean pore size of electrospun scaffolds, we tested the inclusion of sacrificial fibers during the fabrication process. Specifically, we examined the possibility of electrospinning distinct fibers of the water-soluble polymer polyethylene oxide (PEO) during the fabrication of our BMMs. We anticipated that the resulting matrices could be soaked in water in order to remove the PEO fibers, thereby increasing the size of the pores between the BMM fibers. BMMs with PEO fibers re-

moved showed significant increases in mean pore size, and supported the infiltration of MSCs *in vitro* and endogenous bone cells *ex vivo*.

Lastly, our final objective was aimed at increasing the therapeutic potential of our BMMs by evaluating their ability to deliver a chemotactic agent for MSCs. We hypothesized that local sustained delivery of such a factor from our BMMs could potentially stimulate an increase in the number of bone building cells at a skeletal defect. This would lead to an accelerated healing process, providing benefit to the patient. Initial studies revealed that platelet-derived growth factor-BB had the greatest effect on MSC chemotaxis *in vitro*, and was successfully able to stimulate MSC migration when adsorbed and subsequently released from BMMs.

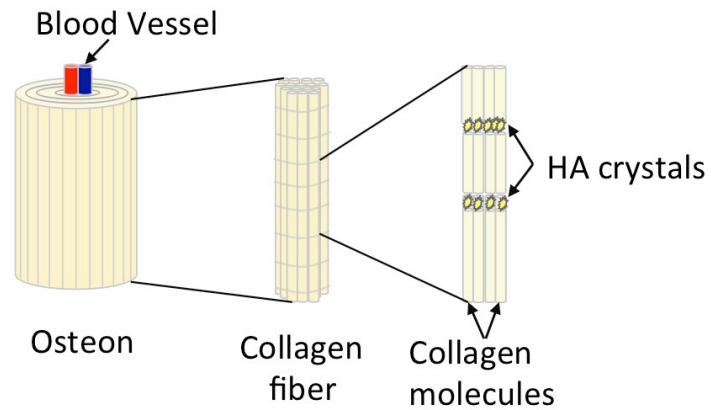


Figure 1. Bone microstructure. Mature skeletal bone consists of highly organized collagen I molecules with interspersed hydroxyapatite nanocrystals. These constructs combine to form collagen fiber bundles. Aligned collagen fiber bundles combine into lamellar sheets, which create the concentric layers of the osteon. The osteon houses blood vessels and nerves in the bone.

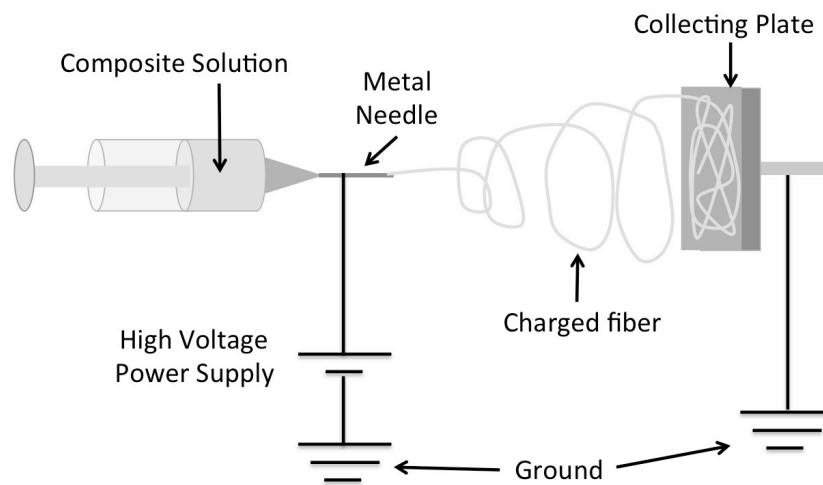


Figure 2. Diagram of electrospinning apparatus. A polymer or composite solution is loaded into a syringe and the needle of the syringe is attached to a high voltage power supply. Once the solution enters the needle, it becomes positively charged, causing a thin fiber to eject from the tip of the needle and travel through the air towards the grounded collecting plate. As the fiber travels, electrostatic repulsion causes the fibers to whip around and the solvent to evaporate, resulting in the deposition of fibers in the nano- to micro-meter diameter.

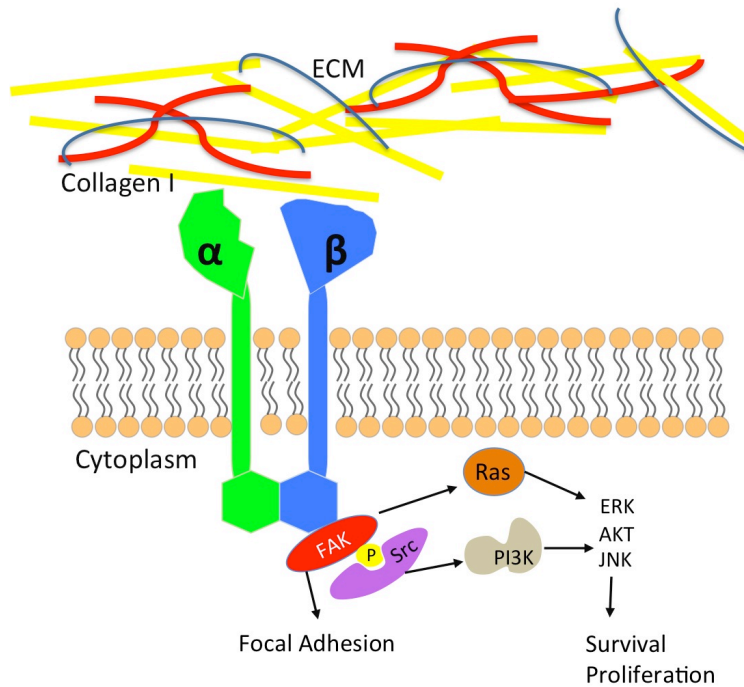


Figure 3. Integrin mediated cell adhesion and signaling cascades. Integrins on the cell surface consist of an alpha and beta subunit. When bound by their specific ligand, such as collagen I in the extracellular matrix, conformational changes lead to the recruitment of various cytosolic proteins, such as focal adhesion kinase (FAK) to the integrin tail. These proteins typically become phosphorylated, and interact with other proteins to activate downstream signaling cascades. Ultimately, integrin ligand interactions can lead to the activation of transcription factors, leading to cell survival, proliferation, and focal adhesion among other cell fates.

MESENCHYMAL STEM CELL RESPONSES TO BONE-MIMETIC ELECTROSPUN  
MATRICES COMPOSED OF POLYCAPROLACTONE, COLLAGEN I AND  
NANOPARTICULATE HYDROXYAPATITE

by

MATTHEW C. PHIPPS, WILLIAM C. CLEM, SHANE A. CATLEDGE, YUANYUAN  
XU, KRISTIN M. HENNESSY, VINOY THOMAS, MICHAEL J. JABLONSKY,  
SHAFIUL CHOWDHURY, ANDREI V. STANISHEVSKY, YOGESH K. VOHRA,  
SUSAN L. BELLIS

*PLoS ONE*, 2011 February; 6(2) e16813

Copyright  
2011  
by  
Phipps et al.

Format adapted for dissertation

## Abstract

The performance of biomaterials designed for bone repair depends, in part, on the ability of the material to support the adhesion and survival of mesenchymal stem cells (MSCs). In this study, a nanofibrous bone-mimicking scaffold was electrospun from a mixture of polycaprolactone (PCL), collagen I, and hydroxyapatite (HA) nanoparticles with a dry weight ratio of 50/30/20 respectively (PCL/col/HA). The cytocompatibility of this tri-component scaffold was compared with three other scaffold formulations; 100% PCL (PCL), 100% collagen I (col), and a bi-component scaffold containing 80%PCL/20%HA (PCL/HA). Scanning electron microscopy, fluorescent live cell imaging, and MTS assays showed that MSCs adhered to the PCL, PCL/HA and PCL/col/HA scaffolds, however more rapid cell spreading and significantly greater cell proliferation was observed for MSCs on the tri-component bone-mimetic scaffolds. In contrast, the col scaffolds did not support cell spreading or survival, possibly due to the low tensile modulus of this material. PCL/col/HA scaffolds adsorbed a substantially greater quantity of the adhesive proteins, fibronectin and vitronectin, than PCL or PCL/HA following in vitro exposure to serum, or placement into rat tibiae, which may have contributed to the favorable cell responses to the tri-component substrates. In addition, cells seeded onto PCL/col/HA scaffolds showed markedly increased levels of phosphorylated FAK, a marker of integrin activation and a signaling molecule known to be important for directing cell survival and osteoblastic differentiation. Collectively these results suggest that electrospun bone-mimetic matrices serve as promising degradable substrates for bone regenerative applications.

## Introduction

Bone is the second most transplanted tissue in the body (after blood transfusions). Autografting of bone is extensively employed in orthopedic and dental surgeries; however the harvesting of the patient's own bone requires a second surgery that can greatly increase the time and cost for the procedure. Additionally, nonunion at the repair site is a common problem, and iliac crest harvest can lead to complications in as many as 20% of patients [1-3]. Another limitation is that the supply of bone material from the iliac crest may be inadequate when a large amount of graft material is required [4]. For these reasons, there is an immediate need for a biomaterial that can either substitute for autografted bone or serve as a temporary matrix that induces regeneration of native bone at implant sites.

It is hypothesized that the most successful biomaterials for bone repair will be those that mimic the natural extracellular matrix, thereby minimizing foreign body or fibrotic responses. Mature bone matrix is composed of 65% mineral and 35% protein. The mineral phase is a calcium phosphate mixture that is predominantly hydroxyapatite (HA). The organic phase consists of 90% collagen I fibers, and the remaining 10% is composed of various proteoglycans and other proteins [5]. Many investigators have attempted to model the natural matrix by producing materials containing HA [6-9] and/or collagen I [10-13], and in vitro studies suggest that these matrices are usually highly osteoconductive [14, 15]. There are currently several commercial products that utilize collagen in combination with other molecules, such as growth factors, to stimulate or guide bone regeneration. However, in order to prevent rapid degradation, these collagen-based materials must be cross-linked, which unfortunately has some disadvantages [16].



First, the use of chemical cross-linking agents, such as glutaraldehyde, has been shown to produce prolonged toxic effects [17]. In addition, cross-linking collagen biomaterials greatly reduces the average pore size, delaying vascularization of the biomaterial and the tissue in-growth necessary for complete healing [18]. As an alternative to cross-linking, combining collagen with a synthetic polymer such as polycaprolactone (PCL) can be used to improve the mechanical properties. PCL is a semicrystalline, aliphatic polyester that has a much lower rate of degradation than collagen, and is useful in a composite scaffold for increasing mechanical strength, and fine-tuning the rate of resorbability [19-21].

Electrospinning is a particularly promising technique for synthesizing biomimetic matrices [22-26]. With this approach, scaffolds can be produced with nanoscale fibers that mimic the size and arrangement of native collagen fibers [27]. Additionally, electrospun scaffolds have a high surface to volume ratio, and interconnecting pores, which facilitate cell adhesion and formation of cell-cell junctions. In a prior study we described the synthesis and characterization of a tri-component electrospun scaffold composed of PCL, collagen I, and nanoparticulate HA [28]. The average fiber diameter of the scaffold was  $180 \pm 50$  nm, which approximates the collagen fiber bundle diameter characteristic of the native extracellular matrix of bone [29]. Moreover, a uniform dispersion of nanoscale HA particles along the fiber length was observed, with only minor agglomeration. Due to problems with agglomeration, many groups have alternately explored deposition of an HA layer onto the surface of electrospun scaffolds. One benefit of electrospinning HA along with PCL and collagen I is that the presence of HA nanoparticles throughout the scaffold provides a continuous bone-like matrix to cells

as the scaffold degrades *in vivo*. In the current investigation we evaluated mesenchymal stem cell (MSC) responses to the bone-like tri-component PCL/col/HA scaffolds (50%PCL/30%col I/20% HA), in direct comparison with three other scaffold formulations; 100% PCL, 100% collagen I, and a PCL/HA composite (80%PCL/20%HA).

## Materials and Methods

### *Preparation of Electrospun Scaffolds*

Four types of scaffolds were produced by electrospinning as described previously [28]: (1) 100% PCL, (2) 80wt% PCL + 20wt% HA, (3) 50wt% PCL + 30wt% collagen I + 20wt% HA, and (4) 100% collagen I. Solutions were made by adding hexafluoroisopropanol (HFP, Sigma-Aldrich) to each mixture such that the solid weight was 7.5% of the total solution weight. PCL (MW = 110,000 Da) was purchased from Birmingham Polymers, lyophilized calf skin collagen I was from MP Biomedicals, and HA nanoparticles (10 – 50 nm particle size) were synthesized as described [28]. The solutions were magnetically stirred at room temperature for 1h before loading into disposable syringes. Voltages between 15 and 25 kV were applied using a high-voltage power supply (Gamma High Voltage Research, Ormond Beach, FL). Higher voltages were found to be necessary in order to effectively spin the collagen-based mixtures without fiber beading. The grounded aluminum collection foil was located 12cm from the tip of the electrically charged 27-gauge needle. A syringe pump was used to feed polymer solution into the needle at a feed rate of 2mL/h. The resulting samples were randomly arranged fibers de-

posited as a sheet with estimated thickness between 50 and 100  $\mu\text{m}$ . No chemical or radiation-induced cross-linking of PCL or collagen fibers was performed.

Following electrospinning, samples were placed under vacuum for 48 hours to remove the residual HFP solvent. To quantify residual HFP, a 25 mg sample of each scaffold was dissolved in 1 mL of deuterated chloroform (Cambridge Isotope, Andover, MA).  $^{19}\text{F}$  NMR data were collected on a Bruker DRX400 spectrometer at ambient temperature with the following parameters:  $30^\circ$  pulse width, 64 scans, 100 ppm spectral width, 4.6 second recycle time. A 1.0 Hz line broadening was applied before the Fourier transform. The results were compared to a standard of 10 ppm HFP in d-chloroform, and it was found that following the 48-hour vacuuming step, the amount of HFP was below the limit of detection ( $< 1$  ppm).

### *Tensile Testing of Scaffolds*

The bulk tensile properties of each scaffold formulation were determined under wet and dry conditions. The scaffolds were cut into rectangular strips (50 mm  $\times$  6 mm). The thickness of the fibrous specimen was measured at 3 different positions and the average thickness was taken to calculate the cross sectional area of the specimen. Each sample (n = 5 specimens) was loaded into the tensile testing fixture of a dynamic mechanical analyzer (DMA, TA Instruments Inc., DE) and subjected to a load of 18N in the ramp force mode [30]. A ramp force of 0.1 N/mm was applied. Displacement was measured with an optical encoder. The stress vs. strain curve was generated and the elastic modulus was determined from the initial 10% strain at the linear regime for each specimen. The stress

at maximum from the stress vs. strain curve was taken as the tensile strength of the specimen. The data were reported as average value  $\pm$  standard deviation.

#### *Isolation and Culture of MSCs*

Human MSCs were isolated from bone marrow donations, as previously described [31]. Briefly, cells were pelleted by centrifugation, resuspended in Dulbecco's Modified Eagle Medium (DMEM), and then applied to a Histopaque-1077 column (Sigma, St. Louis, MO). A density gradient was generated by centrifugation at 500g for 30 min. Cells from the DMEM/Histopaque interface were extracted with a syringe and seeded onto tissue culture dishes and cultured in DMEM containing 10% fetal bovine serum. For fluorescent live cell imaging studies, lentivirus-transduced human MSCs constitutively-expressing green fluorescent protein (GFP) were provided by the Tulane Center for Gene Therapy (New Orleans, LA). The GFP-MSCs were selected for stable GFP expression by the vendor. The protocols for isolation and propagation of MSCs were approved by the Univ. of Alabama Institutional Review Board, which determined that our studies qualified for the "No Human Subjects" designation and therefore did not require informed consent (approval # N060810001).

#### *Scanning Electron Microscopy (SEM) Analysis of MSC Morphology:*

MSCs grown on scaffolds for 24 h were fixed in 2.5% glutaraldehyde and then dried in a gradient of ethanol in water, followed by a gradient of hexamethyldisilazane (HMDS) in ethanol. SEM imaging was performed on a Philips 515 SEM with an accelerating voltage of 15kV.

### *Live Cell Imaging of GFP-Labeled MSCs*

Scaffolds were placed into sterile 24-well CellCrown™ inserts (Scaffdex, Tampere, Finland) to prevent sample floating or deformation. The effective area of the scaffold when placed in a 24-well CellCrown™ is 0.8cm<sup>2</sup>. Scaffolds were sterilized in 70% EtOH prior to cell seeding. GFP-labeled MSCs were seeded at a density of 9,000 cells/cm<sup>2</sup> (~7,500 cells/scaffold) and cultured in growth media (DMEM containing 4.5 g/L glucose, supplemented with 10% fetal bovine serum) at 37°C, exchanging media every 2-3 days. Visualization of the GFP-expressing cells was performed using a Nikon 80i stereomicroscope.

### *MSC Proliferation on Electrospun Scaffolds*

Scaffolds were placed into sterile 48-well CellCrown™ inserts as described above. The effective area of the scaffold when placed in a 48-well CellCrown™ is 0.4cm<sup>2</sup>. MSCs were seeded at a density of 10,000 cells/cm<sup>2</sup> and cultured in growth media at 37°C, exchanging media every 2-3 days. At time points of 1 and 4 days, a modified MTS assay (Promega, Madison, WI) was performed to calculate relative cellular proliferation rates. After incubation in media containing MTS reagents, scaffolds were removed from the CellCrown™ and washed in PBS. The scaffolds were then boiled in 1% TX-100 lysis buffer to ensure MTS product was removed from the scaffolds and cells. The supernatant was then read for absorbance at 490nm on a BioTek Synergy 2 microplate reader. Experiments were performed three separate times, with each independent experiment performed in duplicate, and values were normalized to cell proliferation on PCL scaffolds at

day one. Error bars indicate Standard Error of the Mean. Statistical analysis between groups was performed using an unpaired student t-test. Differences were considered significant for probability values less than 0.05.

### *Protein Adsorption on Scaffolds*

Scaffolds were either coated overnight with FBS, or placed into rat tibial defects for 30 minutes as previously reported [32]. For the tibial implants, male Sprague-Dawley rats were anesthetized with a 4% isoflurane/oxygen mixture. Under a sterile field, a 1mm round defect was made in the proximal right tibia, and a scaffold was inserted. After 30 minutes, the scaffolds were retrieved and washed extensively to remove loosely bound proteins. Proteins remaining on the FBS-coated, or tibial-implanted, scaffolds were solubilized in boiling sodium dodecyl sulfate (SDS)-buffer (50mM Tris, 2% SDS, 5%  $\beta$ -mercaptoethanol) for 30 minutes, with constant agitation. The supernatants were collected and stored at -80°C. Desorbed proteins were resolved on a 7% polyacrylamide gel. Proteins were transferred to a polyvinylidene difluoride (PVDF) membrane, and exposed to antibodies for fibronectin (Chemicon AB1954, 1:1000), or vitronectin (Abcam MAB 1945, 1:2500); followed by an HRP-conjugated secondary antibody (Amersham Life Sciences, NA934V, 1:5000, and NA931V, 1:2500). Proteins were detected using chemiluminescence reagents (Amersham Life Sciences or Millipore).

Experiments involving male Sprague-Dawley rats were carried out in strict accordance with the recommendations in the Guide for the Care and Use of Laboratory Animals of the National Institutes of Health. The protocol was approved by the Institutional Animal Care and Use Committee at the University of Alabama at Birmingham (approval #

091107667). Surgeries were performed under isoflurane anesthesia, and all efforts were made to minimize suffering. Two independent runs of this experiment were performed with one animal per scaffold for each run. Western blot images are representative of both runs.

#### *Immunocytochemical Staining for Phosphorylated Focal Adhesion Kinase*

Scaffold solutions were electrospun onto cover slips in order to create a coating of electrospun nanofibers. Coated cover slips were placed into low-adhesion wells of a 24-well plate and sterilized with 70% EtOH. MSCs were seeded onto substrates at a density of 800 cells/cm<sup>2</sup> and allowed to adhere for 5 hours. After this time point, cells were fixed in 4% formaldehyde and permeabilized in a 0.1% TX-100 solution. Immunostaining was performed using primary rabbit antibodies against phosphorylated Focal Adhesion Kinase (pFAK Y397, Invitrogen 44-624G, 1:400 dilution); followed by an Alexa Fluor 568 conjugated secondary anti-rabbit antibody (Invitrogen A10042, 1:400, dilution). Cells were counterstained with DAPI (Invitrogen 1:20,000) in order to show cell nuclei.

## Results and Discussion

#### *Tensile Properties of Electrospun Composites*

One of the benefits in mixing PCL with collagen I is that it allows tuning of scaffold tensile strength. This is important in light of recent evidence demonstrating that cells exhibit poor adhesion and survival on matrices that lack sufficient stiffness [33, 34]. Accordingly, we tested the mechanical properties of the four electrospun formulations. The tensile properties of the scaffolds under both dry and wet conditions are given in Table 1.

Dry properties provide information regarding durability in surgical handling, whereas wet properties represent the physiological condition experienced by cells. As shown in Table 1, the wet modulus of the PCL, PCL/HA and PCL/col/HA substrates ranged from 13.4 - 8.4 MPa, and the wet tensile strength was 6.5 - 2.6 MPa. Notably, the hydrated scaffolds composed of 100% collagen I were markedly more fragile; in fact, scaffolds broke apart immediately upon applying force, therefore values could not be recorded. Similar findings have been reported by Shields et al., claiming that electrospinning of collagen disrupts the natural intermolecular cross-linking of collagen which in turn leads to dissolution of the scaffolds when placed in aqueous solutions [35]. In comparison, blending collagen I with PCL (as represented by the PCL/col/HA scaffolds) significantly increased scaffold strength relative to scaffolds composed of collagen I alone, thus providing a useful alternative to chemical cross-linking of collagen fibers.

Table 1

*Tensile Properties of dry and hydrated scaffolds.* Values represent the average  $\pm$  standard deviation calculated in the linear portion at 10% strain. The hydrated collagen scaffolds have very low mechanical properties and could not be measured by this technique.

SCAFFOLD	TENSILE STRENGTH (MPa)		TENSILE MODULUS (MPa)		TENSILE STRAIN (%)	
	Dry	Wet	Dry	Wet	Dry	Wet
PCL	6.5 $\pm$ 0.74	6.46 $\pm$ 0.34	14.63 $\pm$ 0.85	13.37 $\pm$ 1.40	73.96 $\pm$ 3.5	87.35 $\pm$ 3.20
PCL/HA	3.99 $\pm$ 0.31	3.03 $\pm$ 0.98	9.14 $\pm$ 1.15	9.23 $\pm$ 1.88	93.82 $\pm$ 8.3	51.48 $\pm$ 4.2
PCL/col/HA	4.67 $\pm$ 0.82	2.62 $\pm$ 0.92	13.93 $\pm$ 4.94	8.38 $\pm$ 0.29	70.64 $\pm$ 7.98	75.3 $\pm$ 15.69
col	1.46 $\pm$ 0.35	---	18.26 $\pm$ 3.14	---	20.0 $\pm$ 5.0	---

Note: From “Mesenchymal Stem Cell Responses to Bone-Mimetic Electrospun Matrices Composed of Polycaprolactone, Collagen I and Nanoparticulate Hydroxyapatite” by M.C. Phipps, W.C. Clem, S. A. Catledge, Y. Xu, K.M. Hennessy, V. Thomas, M. J. Jablonsky, S. Chowdhury, A. V. Stanishevsky, Y. K. Vohra, S. L. Bellis, 2011, *PLoS ONE*, 6, e16813. Copyright 2011 by Phipps et al. Reprinted with permission.



*MSCs adhere and spread on scaffolds composed of PCL, PCL/HA and PCL/col/HA, but not col I*

As a first step toward evaluating scaffold cytocompatibility, human MSCs were seeded onto the substrates, and evaluated 24 hrs later for attachment and spreading using scanning electron microscopy (SEM). As shown in Fig. 1A, cells were able to adhere and spread on scaffolds composed of PCL, PCL/HA, and PCL/col/HA, however, MSCs on col scaffolds remained very rounded, suggesting poor cell adhesion. While there are several factors that could account for the lack of cell spreading on col, one possibility was that some inhibitory factor may have been released from the col scaffolds. To test this hypothesis, electrospun col scaffolds (without cells) were incubated in culture media at 37°C to allow for the potential release of soluble factors into the media, and after 24 hours, the media was collected. MSCs were then suspended into this media and seeded onto PCL scaffolds. After 24 hours of adhesion to PCL scaffolds (while in conditioned media from col scaffolds), SEM images were collected (Fig 1B). These results showed extensive cell spreading, indicating that the poor response of MSCs to the electrospun col scaffolds was not due to any cytotoxic factors released from the substrate.

#### *Growth of MSCs on Scaffolds*

In order to assess cell responses to the scaffolds over more extended culture periods, GFP-expressing MSCs were seeded onto the scaffolds and subjected to live cell imaging at varying time points. The value of this approach is that real-time changes in cell morphology and survival can be monitored on the same samples over the course of their

culture, and in addition, using a low magnification allows simultaneous visualization of nearly the entire scaffold surface. Thus, live cell imaging experiments reduce the chance of bias associated with fixing cells at designated time points and then selecting individual representative fields for study. At 7 h following the seeding of GFP-expressing MSCs, adherent cells were apparent on all four of the scaffold formulations (Fig 2A). The cells adopted a slightly spread morphology on the PCL, PCL/HA and col scaffolds, however spreading was noticeably more extensive on the PCL/col/HA scaffolds at 7 h (see Fig 2B), suggesting that the tri-component scaffolds provided cells with unique cues that influenced cytoskeletal reorganization. At 24 h, the cells were spread on PCL, PCL/HA and PCL/col/HA scaffolds, and more cells were apparent on the PCL/HA and PCL/col/HA scaffolds as compared with PCL alone. In contrast, only a few very rounded cells, and some cell aggregates, were observed on the col scaffolds at this time point, consistent with the SEM images shown in Fig 1. At one week following seeding, cells had survived on PCL, PCL/HA and PCL/col/HA scaffolds, although again there appeared to be greater numbers of cells on PCL/HA and PCL/col/HA substrates as compared with PCL. In fact cells were confluent on the PCL/col/HA scaffolds, suggesting that an increased level of proliferation occurred on these substrates. In marked contrast, no cells were apparent on the col scaffolds at one week, reflecting poor survival.

The reason for the lack of cell attachment and survival on col scaffolds is not currently understood. We speculate that this response may be due to the low substrate tensile properties when hydrated. Others have also reported the very low mechanical properties of non-cross-linked electrospun collagen when placed in an aqueous solution, such as cell culture media [18, 35, 36]. A burgeoning literature is revealing that substrate stiffness

has a dramatic effect on cell survival and differentiation status [37]. For example, it has been reported that tactile sensing of substrate stiffness by cells feeds back on cell adhesion and cytoskeletal organization [33, 38], and in addition, substrates that are too elastic can cause cell apoptosis [38]. The most common method of increasing the mechanical properties of collagen biomaterials is to use chemical cross-linking agents [16, 17, 35, 36, 39-41]. However, residual cross-linking agent in the biomaterial has been shown to be cytotoxic [16] and it has been reported that chemical cross-links created by glutaraldehyde, the most common cross-linking agent, can degrade and release cytotoxic aldehydes into the environment [42, 43]. Additionally, Haydarkhan-Hagvall et al. reported that cross-linking of electrospun scaffolds drastically reduces the porosity of the scaffolds, which negatively impacted cell seeding [18]. As an alternative approach to cross-linking, the incorporation of a synthetic polymer to electrospun collagen scaffolds can be used to increase the mechanical properties [18]. Our results clearly show that scaffolds incorporating both PCL and col stimulate greater cell spreading and survival as compared with either PCL or col alone. Elucidating the exact mechanism underlying this result will require future studies, however col substrates were not studied further in the current investigation due to the poor mechanical properties and unfavorable cell responses.

#### *Cells Exhibit Greater Proliferation on Tri-Component Scaffolds*

To quantify the proliferation of MSCs adherent to the scaffolds, an MTS assay was performed (Fig 3). At 1 day following cell seeding, greater numbers of cells were observed on PCL/col/HA and PCL/HA scaffolds as compared to PCL alone ( $p < .05$ ), consistent with better cell adhesion to these substrates. At day four, the cell number on

PCL/col/HA scaffolds was significantly higher than either PCL or PCL/HA, suggesting that the PCL/col/HA surfaces supported the highest rate of proliferation. MTS is a very common method for monitoring cell proliferation, and is useful because it specifically detects viable cells, in contrast to many other labeling protocols that do not discriminate between live and dead cells. Although it is possible for MTS readings to be influenced by changes in cellular metabolic activity, the MTS results shown in Fig 3 are in excellent agreement with the GFP-labeled cell imaging studies, which are not influenced by metabolic activity and show that cells are confluent on PCL/col/HA, but not PCL or PCL/HA, scaffolds at 7 days following seeding (Fig 2).

The quantitative MTS assays lend support for the hypothesis that the addition of col and HA in electrospun scaffolds provides a favorable matrix for MSC attachment and growth. Other groups have seen similar benefits when including collagen or HA in nanofibrous biomaterials. For example, Lee et al. reported significant increases in cellular proliferation of osteoblasts grown on PCL/collagen I electrospun scaffolds compared to PCL alone [44]. Likewise, the addition of HA in PCL electrospun scaffolds by Chuenjitkuntaworn et al. leads to significantly higher levels of primary bone cell growth compared to scaffolds of PCL alone [45]. One of the advances provided by the current study is that both col and HA were incorporated into polymeric electrospun scaffolds, and as previously reported, we were able to minimize agglomeration of the HA particles, thus achieving excellent dispersion of nanoscale HA crystals that approximate the size of native bone HA crystals [28].

### *Tri-Component Scaffolds Adsorb Greater Amounts of Adhesion Molecules*

The adsorption of bioactive proteins within the tissue microenvironment to the biomaterial surface is known to influence cell/material interactions. This is especially important upon implantation of a biomaterial in a patient, where it is immediately coated with blood and other bodily fluids that contain large amounts of pro-adhesive proteins. Given that HA is known to have a high capacity for protein adsorption, we hypothesized that the incorporation of HA into the scaffolds would increase the amounts of fibronectin (FN) and vitronectin (VN) adsorbed from serum in the media, which in turn would be expected to stimulate integrin-dependent behaviors such as cell adhesion and survival. To test this hypothesis, we monitored the amount of FN and VN bound to the scaffolds following incubation in fetal bovine serum (FBS). Protein adsorption was assessed by Western blot analysis of proteins that were desorbed by incubation in boiling SDS buffer. As shown in Fig. 4A, the PCL/HA scaffolds adsorbed greater amounts of FN and VN from FBS than PCL alone, as expected. However, markedly greater protein adsorption was apparent on PCL/col/HA scaffolds when compared with either of the other two formulations, indicating that the inclusion of collagen I into the scaffolds increased protein adsorption beyond that observed with HA. This is likely due to the fact that col is known to have specific binding interactions with both FN and VN [46, 47]. The enhanced adsorption of FN and VN from serum may have contributed to the increased cell adhesion and proliferation observed on tri-component scaffolds (Figs 2 and 3).

The adsorption of FN and VN has clinical relevance since implanted biomaterials are immediately exposed to the patient's bodily fluids. Once FN and VN are adsorbed onto a biomaterial, they provide adhesive ligands for MSCs that infiltrate into the wound

site. It is well established that FN and VN promote integrin-dependent cell adhesion, survival and proliferation [48] and these molecules have also been implicated in osteoblastic differentiation [14, 15, 49]. To evaluate protein adsorption in a *bona fide* implant site, scaffolds were implanted into rat tibiae for 30 minutes to allow endogenous protein adsorption from the bone microenvironment. As shown in Fig 4B, substantially greater amounts of FN and VN were bound to the retrieved tri-component scaffolds. Collectively these results suggest that in vivo, tri-component scaffolds will provide a surface rich in integrin-binding proteins, such as col, FN, and VN, that in turn can direct binding of osteogenic cells to the material surface.

#### *Tri-Component Scaffolds Promote the Phosphorylation and Activation of Focal Adhesion Kinase*

Anchorage-dependent cells, such as MSCs, rely on the binding of integrins to ligands in order to promote cell survival through downstream signaling cascades. Upon integrin attachment to proteins within the extracellular matrix, one of the early intracellular events to occur is the autophosphorylation of FAK [50]. Activation of FAK, a protein tyrosine kinase, initiates numerous signal transduction pathways that ultimately lead to increased MSC survival and proliferation [15, 51]. To evaluate the capacity of the matrices to induce integrin-associated signaling, MSCs were seeded onto PCL, PCL/HA, or PCL/col/HA scaffolds, and then immunostained for phosphorylated FAK. Cells were also counterstained with DAPI to show cell nuclei. It was apparent that cells seeded on tri-component scaffolds showed markedly increased levels of pFAK, as well as greater cell spreading, as compared with PCL or PCL/HA (Figure 5). Some weak and diffuse

cytosolic pFAK staining was evident for cells on PCL/HA scaffolds, but not on PCL. The limited activation of pFAK observed on cells attached to PCL/HA scaffolds may be due to the HA in the scaffolds adsorbing pro-adhesive proteins such as FN and VN from the FBS in the media, as shown previously (Figure 4). As with collagen I, integrin binding to FN and VN induces FAK phosphorylation [52]. Of note, it was observed that the pFAK staining pattern for cells adherent to PCL/col/HA was more punctate than the classic focal adhesion-type staining observed with cells adherent to FBS-coated glass cover slips (Figure 5). These results are consistent with other studies reporting punctate pFAK staining for cells grown in 3-dimensional matrices such as collagen gels [53], rather than 2D tissue culture substrates. The higher levels of FAK phosphorylation observed in cells adherent to PCL/col/HA suggest stronger activation of integrin-dependent signaling cascades, which in turn are important for cell survival and osteoblastic differentiation of MSCs. For example, multiple investigators have shown that the phosphorylation of FAK upon integrin binding leads to activation of the osteogenic transcription factor, Runx2/Cbfa-1, as well as enhanced expression of other osteoblastic markers [52, 54]. Future studies will be focused on examining the capacity of tri-component matrices to induce osteoblastic differentiation of MSCs and in vivo bone regeneration.

## Conclusion

The results presented in this study suggest that tri-component, bone-mimetic, PCL/col/HA scaffolds blend the advantageous mechanical properties of PCL with the favorable biochemical cues provided by the native bone molecules, collagen I and HA. As compared with scaffolds composed of col I, PCL or PCL/HA, tri-component scaffolds

supported better cell adhesion, spreading, proliferation and FAK activation. Tri-component scaffolds also adsorbed greater amounts of fibronectin and vitronectin from both serum and the bone microenvironment, thus providing additional ligands for cell surface integrins. Taken together, results from the current study suggest that tri-component PCL/col/HA matrices have high potential to serve as excellent supports for endogenous reparative cells that infiltrate into the implant site, as well as promising substrates for the delivery of exogenously-expanded stem cells.

#### Acknowledgements

The authors would like to thank Albert Tousson and the UAB High Resolution Imaging Facility for assistance in fluorescent imaging, the UAB NMR Facility for residual solvent testing, the Tulane University Center for Gene Therapy for providing lentivirus-transduced MSCs, and the UAB Bone Histomorphometry Core Facility for preparing sections for histology.

#### References

- [1] Brighton CT, Shaman P, Heppenstall RB, Esterhai Jr JL, Pollack SR, Friedenber ZB. Tibial nonunion treated with direct current, capacitive coupling, or bone graft. *Clin Orthop Relat Res.* 1995;321:223-34.
- [2] Fernyhough JC, Schimandle JJ, Weigel MC, Edwards CC, Levine AM. Chronic donor site pain complicating bone graft harvesting from the posterior iliac crest for spinal fusion. *Spine.* 1992;17:1474-80.
- [3] Goulet JA, Senunas LE, DeSilva GL, Greenfield ML. Autogenous iliac crest bone graft. Complications and functional assessment. *Clin Orthop Relat Res.* 1997;339:76-81.



- [4] Lee KJH, Roper JG, Wang JC. Demineralized bone matrix and spinal arthrodesis. *Spine J.* 2005;5:217-23.
- [5] Karsenty G. The genetic transformation of bone biology. *Genes Dev.* 1999;13:3037-51.
- [6] Ito Y, Hasuda H, Kamitakahara M, Ohtsuki C, Tanihara M, Kang IK, et al. A composite of hydroxyapatite with electrospun biodegradable nanofibers as a tissue engineering material. *J Biosci Bioeng.* 2005;100:43-9.
- [7] Wu Y, Hench LL, Du J, Choy KL, Guo J. Preparation of hydroxyapatite fibers by electrospinning technique. *J Am Ceram Soc.* 2004;87:1988-91.
- [8] Kim HW, Song JH, Kim HE. Nanofiber generation of gelatin-hydroxyapatite biomimetics for guided tissue regeneration. *Ad Func Mater.* 2005;15:1988-94.
- [9] Thomas V, Jagani S, Johnson K, Jose MV, Dean DR, Vohra YK, et al. Electrospun Bioactive Nanocomposite Scaffolds of Polycaprolactone and Nanohydroxyapatite for Bone Tissue Engineering. *J Nanosci Nanotechnol.* 2006;6:487-93.
- [10] Teng SH, Lee EJ, Wang P, Kim HE. Collagen/hydroxyapatite composite nanofibers by electrospinning. *Mater Lett.* 2008;62:3055-8.
- [11] Matthews JA, Wnek GE, Simpson DG, Bowlin GL. Electrospinning of collagen nanofibers. *Biomacromolecules.* 2002;3:232-8.
- [12] Zhong S, Teo WE, Zhu X, Beuerman RW, Ramakrishna S, Yung LYL. An aligned nanofibrous collagen scaffold by electrospinning and its effects on in vitro fibroblast culture. *J Biomed Mater Res A.* 2006; 79A: 456-463.
- [13] Ngiam M, Liao SS, Patil AJ, Cheng ZY, Chan CK, Ramakrishna S. The fabrication of nano-hydroxyapatite on PLGA and PLGA/collagen nanofibrous composite scaffolds and their effects in osteoblastic behavior for bone tissue engineering. *Bone.* 2009;45:4-16.
- [14] Venugopal J, Low S, Choon AT, Kumar TSS, Ramakrishna S. Mineralization of osteoblasts with electrospun collagen/hydroxyapatite nanofibers. *Journal of Materials Science-Materials in Medicine.* 2008;19:2039-46.
- [15] Salaszyk RM, Williams WA, Boskey A, Batorsky A, Plopper GE. Adhesion to vitronectin and collagen I promotes osteogenic differentiation of human mesenchymal stem cells. *Journal of Biomedicine and Biotechnology.* 2004;2004:24-34.
- [16] Marinucci L, Lilli C, Guerra M, Belcastro S, Becchetti E, Stabellini G, et al. Biocompatibility of collagen membranes crosslinked with glutaraldehyde or diphenylphosphoryl azide: an in vitro study. *Journal of Biomedical Materials Research Part A.* 2003;67:504-9.

- [17] van Wachem PB, van Luyn MJ, Olde Damink LH, Dijkstra PJ, Feijen J, Nieuwenhuis P. Biocompatibility and tissue regenerating capacity of crosslinked dermal sheep collagen. *J Biomed Mater Res.* 1994;28:353-63.
- [18] Heydarkhan-Hagvall S, Schenke-Layland K, Dhanasopon AP, Rofail F, Smith H, Wu BM, et al. Three-dimensional electrospun ECM-based hybrid scaffolds for cardiovascular tissue engineering. *Biomaterials.* 2008;29:2907-14.
- [19] Bezwada RS, Jamiolkowski DD, Lee IY, Agarwal V, Persivale J, Trenka-Benthin S, et al. Monocryl® suture, a new ultra-pliable absorbable monofilament suture. *Biomaterials.* 1995;16:1141-8.
- [20] Darney PD, Monroe SE, Klaisle CM, Alvarado A. Clinical evaluation of the Capronor contraceptive implant: preliminary report. *Am J Obstet Gynecol.* 1989;160:1292-5.
- [21] Woodward SC, Brewer PS, Moatamed F, Schindler A, Pitt CG. The intracellular degradation of poly (epsilon-caprolactone). *J Biomed Mater Res.* 1985;19:437-44.
- [22] Huang ZM, Zhang YZ, Kotaki M, Ramakrishna S. A review on polymer nanofibers by electrospinning and their applications in nanocomposites. *Composites Science and Technology.* 2003;63:2223-53.
- [23] Pham QP, Sharma U, Mikos AG. Electrospinning of polymeric nanofibers for tissue engineering applications: A review. *Tissue Engineering.* 2006;12:1197-211.
- [24] Murugan R, Ramakrishna S. Nano-featured scaffolds for tissue engineering: A review of spinning methodologies. *Tissue Engineering.* 2006;12:435-47.
- [25] Sill TJ, von Recum HA. Electro spinning: Applications in drug delivery and tissue engineering. *Biomaterials.* 2008;29:1989-2006.
- [26] Prabhakaran MP, Venugopal J, Ramakrishna S. Electrospun nanostructured scaffolds for bone tissue engineering. *Acta Biomaterialia.* 2009;5:2884-93.
- [27] Wutticharoenmongkol P, Sanchavanakit N, Pavasant P, Supaphol P. Preparation and characterization of novel bone scaffolds based on electrospun polycaprolactone fibers filled with nanoparticles. *Macromolecular Bioscience.* 2006;6:70-7.
- [28] Catledge SA, Clem WC, Shrikishen N, Chowdhury S, Stanishevsky AV, Koopman M, et al. An electrospun triphasic nanofibrous scaffold for bone tissue engineering. *Biomedical Materials.* 2007;2:142-50.
- [29] Tzaphlidou M. The role of collagen in bone structure: An image processing approach. *Micron.* 2005;36:593-601.

- [30] Thomas V, Dean DR, Jose MV, Mathew B, Chowdhury S, Vohra YK. Nanostructured biocomposite scaffolds based on collagen coelectrospun with nanohydroxyapatite. *Biomacromolecules*. 2007;8:631-7.
- [31] Kilpadi KL, Sawyer AA, Prince CW, Chang PL, Bellis SL. Primary human marrow stromal cells and Saos-2 osteosarcoma cells use different mechanisms to adhere to hydroxylapatite. *J Biomed Mater Res*. 2004;68A:273-285.
- [32] Hennessy KM, Clem WC, Phipps MC, Sawyer AA, Shaikh FM, Bellis SL. The effect of RGD peptides on osseointegration of hydroxyapatite biomaterials. *Biomaterials*. 2008;29:3075-83.
- [33] Discher DE, Janmey P, Wang YL. Tissue cells feel and respond to the stiffness of their substrate. *Science*. 2005;310:1139-43.
- [34] Butcher DT, Alliston T, Weaver VM. A tense situation: forcing tumour progression. *Nature Reviews Cancer*. 2009;9:108-22.
- [35] Shields KJ, Beckman MJ, Bowlin GL, Wayne JS. Mechanical properties and cellular proliferation of electrospun collagen type II. *Tissue Engineering*. 2004;10:1510-7.
- [36] Barnes CP, Pemble CW, Brand DD, Simpson DG, Bowlin GL. Cross-linking electrospun type II collagen tissue engineering scaffolds with carbodiimide in ethanol. *Tissue Engineering*. 2007;13:1593-605.
- [37] Engler AJ, Sen S, Sweeney HL, Discher DE. Matrix elasticity directs stem cell lineage specification. *Cell*. 2006;126:677-89.
- [38] Wang HB, Dembo M, Wang YL. Substrate flexibility regulates growth and apoptosis of normal but not transformed cells. *American Journal of Physiology- Cell Physiology*. 2000;279:1345-50.
- [39] Boland ED, Matthews JA, Pawlowski KJ, Simpson DG, Wnek GE, Bowlin GL. Electrospinning collagen and elastin: preliminary vascular tissue engineering. *Front Biosci*. 2004;9:1422-32.
- [40] Friess W, Lee G, Groves MJ. Insoluble collagen matrices for prolonged delivery of proteins. *Pharm Dev Technol*. 1996;1:185-93.
- [41] Li M, Mondrinos MJ, Gandhi MR, Ko FK, Weiss AS, Lelkes PI. Electrospun protein fibers as matrices for tissue engineering. *Biomaterials*. 2005;26:5999-6008.
- [42] Huang-Lee LL, Cheung DT, Nimni ME. Biochemical changes and cytotoxicity associated with the degradation of polymeric glutaraldehyde derived crosslinks. *J Biomed Mater Res*. 1990;24:1185-201.
- [43] Schmidt CE, Baier JM. Acellular vascular tissues: natural biomaterials for tissue repair and tissue engineering. *Biomaterials*. 2000;21:2215-31.

- [44] Lee JJ, Yu HS, Hong SJ, Jeong I, Jang JH, Kim HW. Nanofibrous membrane of collagen-polycaprolactone for cell growth and tissue regeneration. *Journal of Materials Science-Materials in Medicine*. 2009;20:1927-35.
- [45] Chuenjitkuntaworn B, Inrung W, Damrongsri D, Mekaapiruk K, Supaphol P, Pavasant P. Polycaprolactone/hydroxyapatite composite scaffolds: Preparation, characterization and in vitro and in vivo biological responses of human primary bone cells. *Journal of Biomedical Materials Research Part A*. 2010;94:241-51.
- [46] Gebb C, Hayman EG, Engvall E, Ruoslahti E. Interaction of vitronectin with collagen. *Journal of Biological Chemistry*. 1986;261:16698-703.
- [47] Engvall E, Ruoslahti E. Binding of soluble form of fibroblast surface protein, fibronectin, to collagen. *International Journal of Cancer*. 1977;20:1-5.
- [48] Giancotti FG. Integrin signaling: specificity and control of cell survival and cell cycle progression. *Current Opinion in Cell Biology*. 1997;9:691-700.
- [49] Moursi AM, Globus RK, Damsky CH. Interactions between integrin receptors and fibronectin are required for calvarial osteoblast differentiation in vitro. *Journal of Cell Science*. 1997;110:2187-96.
- [50] Schaller MD, Hildebrand JD, Shannon JD, Fox JW, Vines RR, Parsons JT. Autophosphorylation of the focal adhesion kinase, pp125FAK, directs SH2-dependent binding of pp60src. *Mol Cell Biol*. 1994;14:1680-8.
- [51] Wozniak MA, Modzelewska K, Kwong L, Keely PJ. Focal adhesion regulation of cell behavior. *Biochim Biophys Acta*. 2004;1692:103-19.
- [52] Salaszyk RM, Klees RF, Williams WA, Boskey A, Plopper GE. Focal adhesion kinase signaling pathways regulate the osteogenic differentiation of human mesenchymal stem cells. *Exp Cell Res*. 2007;313:22-37.
- [53] Wozniak MA, Desai R, Solski PA, Der CJ, Keely PJ. ROCK-generated contractility regulates breast epithelial cell differentiation in response to the physical properties of a three-dimensional collagen matrix. *J Cell Biol*. 2003;163:583-95.
- [54] Kundu AK, Putnam AJ. Vitronectin and collagen I differentially regulate osteogenesis in mesenchymal stem cells. *Biochem Biophys Res Commun*. 2006;347:347-57.

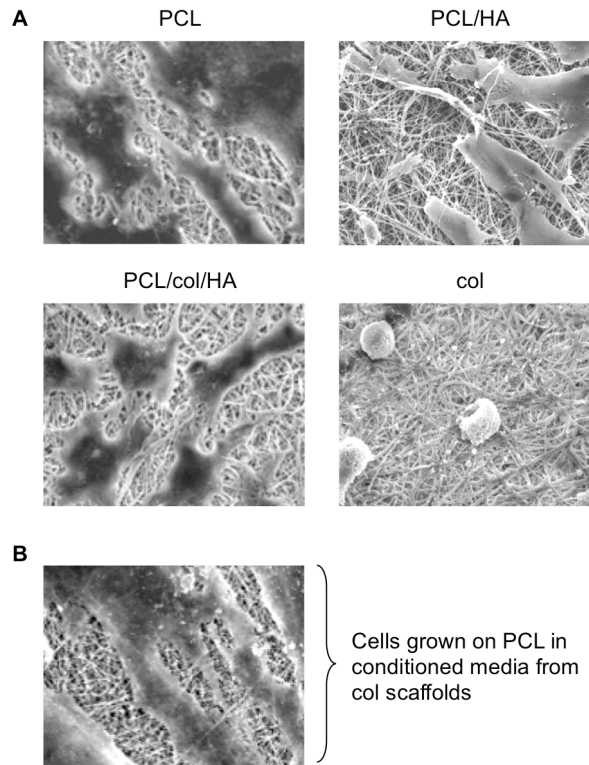


Figure 1. SEM images of MSCs cultured on nanofibrous scaffolds for 24 hours. A) Cell spreading was observed on PCL, PCL/HA, and PCL/col/HA scaffolds, but not on 100% collagen I (col). B) Col scaffolds (without cells) were incubated in culture media for 24 hrs to allow the potential release of soluble factors, and then the solution was collected. MSCs were suspended into this conditioned media, seeded onto PCL scaffolds, and allowed adhere in the media for 24 h. Under these conditions cell spreading was extensive, suggesting that lack of cell spreading on col substrates was not due to any soluble factors released from these scaffolds.

Note: From “Mesenchymal Stem Cell Responses to Bone-Mimetic Electrospun Matrices Composed of Polycaprolactone, Collagen I and Nanoparticulate Hydroxyapatite” by M.C. Phipps, W.C. Clem, S. A. Catledge, Y. Xu, K.M. Hennessy, V. Thomas, M. J. Jablonsky, S. Chowdhury, A. V. Stanishevsky, Y. K. Vohra, S. L. Bellis, 2011, *PLoS ONE*, 6, e16813. Copyright 2011 by Phipps et al. Reprinted with permission.

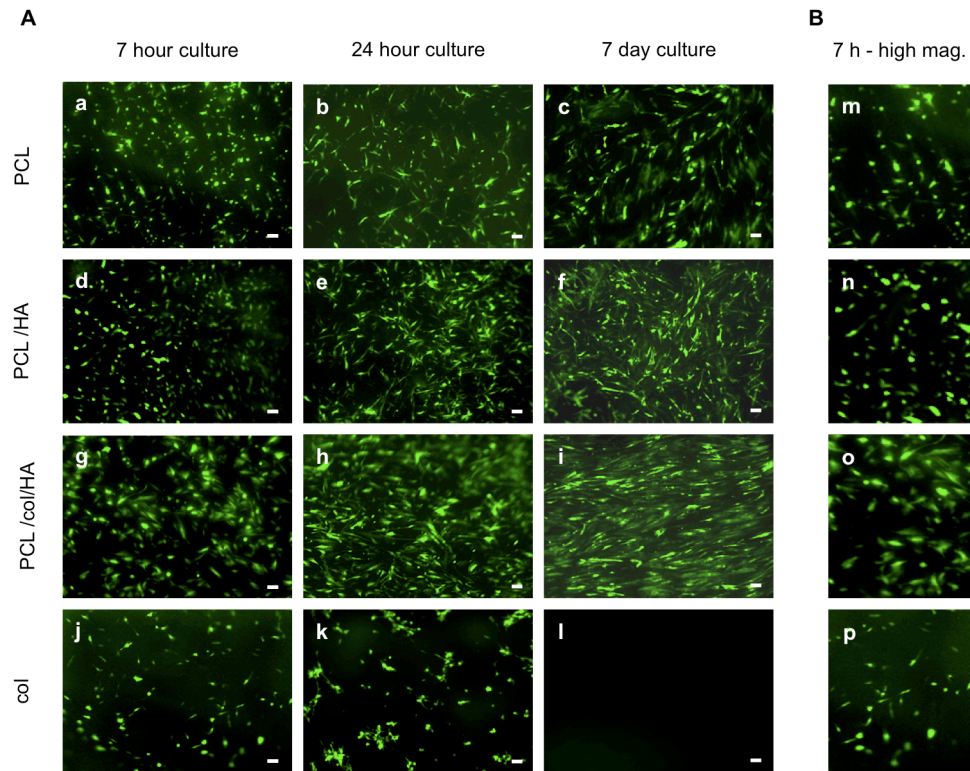


Figure 2. Live cell imaging of GFP-expressing MSCs seeded onto electrospun scaffolds. A) Cells were seeded onto scaffolds and imaged over varying time points. Panels a-c: PCL scaffolds; panels d-f: PCL/HA scaffolds; panels g-i: PCL/col/HA scaffolds and panels j-l: col scaffolds. Scale bar = 100  $\mu$ m. B) Higher magnification images of GFP-expressing MSCs at seven hours on electrospun scaffolds (panels m-p).

Note: From “Mesenchymal Stem Cell Responses to Bone-Mimetic Electrospun Matrices Composed of Polycaprolactone, Collagen I and Nanoparticulate Hydroxyapatite” by M.C. Phipps, W.C. Clem, S. A. Catledge, Y. Xu, K.M. Hennessy, V. Thomas, M. J. Jablonsky, S. Chowdhury, A. V. Stanishevsky, Y. K. Vohra, S. L. Bellis, 2011, *PLoS ONE*, 6, e16813. Copyright 2011 by Phipps et al. Reprinted with permission.

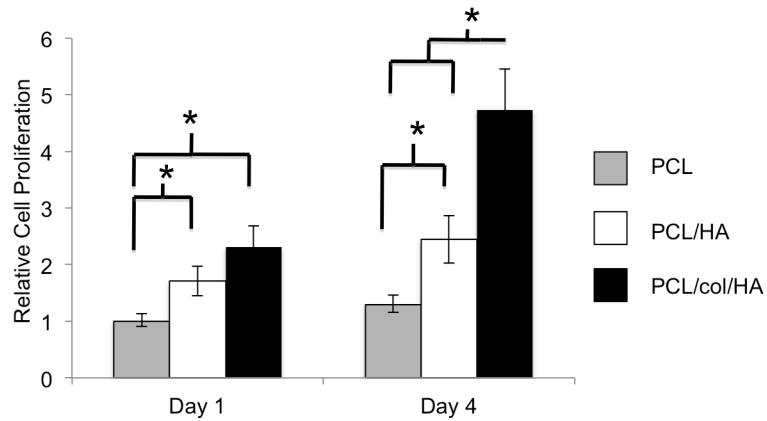


Figure 3. MTS assay quantifying cell proliferation on electrospun scaffolds of PCL, PCL/HA or PCL/col/HA. At day one, cell number was significantly higher on PCL/HA and PCL/col/HA scaffolds in comparison to PCL. By day four, PCL/HA was still significantly higher than PCL, and PCL/col/HA was significantly higher than PCL/HA and PCL. In addition, cell number on PCL/col/HA was significantly higher on day four than day one. An \* denotes  $p < 0.05$

Note: From “Mesenchymal Stem Cell Responses to Bone-Mimetic Electrospun Matrices Composed of Polycaprolactone, Collagen I and Nanoparticulate Hydroxyapatite” by M.C. Phipps, W.C. Clem, S. A. Catledge, Y. Xu, K.M. Hennessy, V. Thomas, M. J. Jablonsky, S. Chowdhury, A. V. Stanishevsky, Y. K. Vohra, S. L. Bellis, 2011, *PLoS ONE*, 6, e16813. Copyright 2011 by Phipps et al. Reprinted with permission.

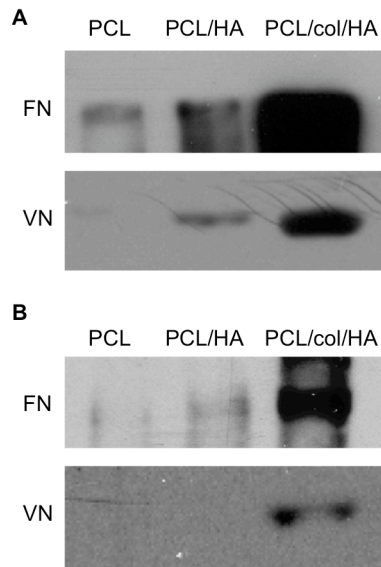


Figure 4. Adsorption of FN and VN by electrospun scaffolds. Scaffolds were coated with fetal bovine serum (A), or implanted into rat tibial osteotomies for 30 min (B). Scaffolds were then washed to remove loosely bound proteins, and proteins were subsequently desorbed by incubation in boiling SDS-containing solution. The amounts of FN and VN were evaluated by Western blot.

Note: From “Mesenchymal Stem Cell Responses to Bone-Mimetic Electrospun Matrices Composed of Polycaprolactone, Collagen I and Nanoparticulate Hydroxyapatite” by M.C. Phipps, W.C. Clem, S. A. Catledge, Y. Xu, K.M. Hennessy, V. Thomas, M. J. Jablonsky, S. Chowdhury, A. V. Stanishevsky, Y. K. Vohra, S. L. Bellis, 2011, *PLoS ONE*, 6, e16813. Copyright 2011 by Phipps et al. Reprinted with permission.



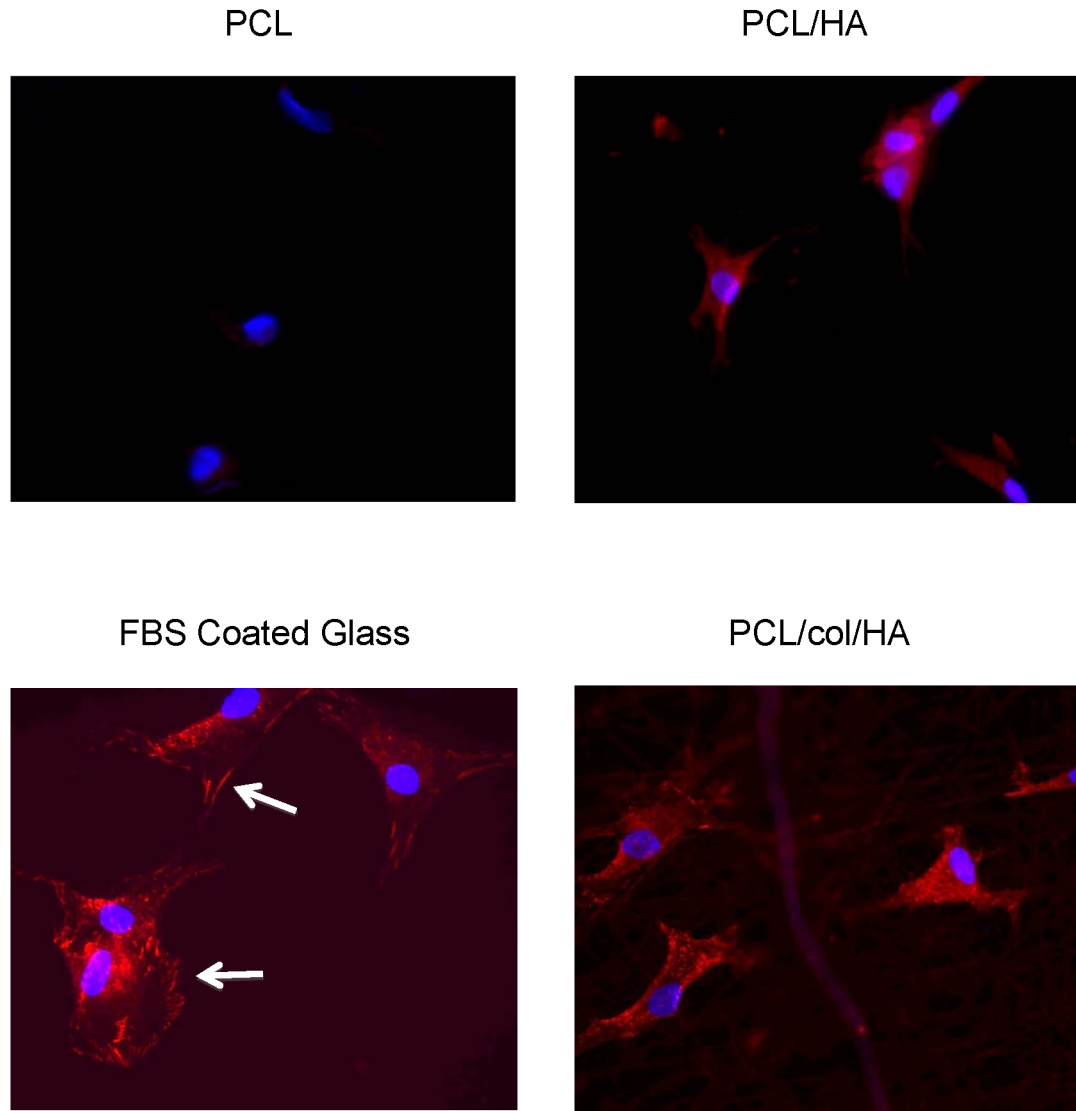


Figure 5. Immunostaining for phosphorylated focal adhesion kinase. MSCs were seeded onto glass coverslips coated with electrospun nanofibers, or with FBS as a control. After 5 hours, cells were fixed and stained for phosphorylated Focal Adhesion Kinase (red). Cells were counterstained with DAPI to show cell nuclei (blue). Cells seeded onto PCL/col/HA scaffolds were better spread, and exhibited greater amounts of punctuate pFAK staining (site pY397) as compared with cells on PCL or PCL/HA. Cells seeded onto FBS-coated glass coverslips displayed pFAK staining in focal adhesion-type structures (white arrows), as expected for cells grown on 2D surfaces.

Note: From “Mesenchymal Stem Cell Responses to Bone-Mimetic Electrospun Matrices Composed of Polycaprolactone, Collagen I and Nanoparticulate Hydroxyapatite” by M.C. Phipps, W.C. Clem, S. A. Catledge, Y. Xu, K.M. Hennessy, V. Thomas, M. J. Jablonsky, S. Chowdhury, A. V. Stanishevsky, Y. K. Vohra, S. L. Bellis, 2011, *PLoS ONE*, 6, e16813. Copyright 2011 by Phipps et al. Reprinted with permission.

INCREASING THE PORE SIZES OF BONE-MIMETIC ELECTROSPUN  
SCAFFOLDS COMPRISED OF POLYCAPROLACTONE, COLLAGEN I AND  
HYDROXYAPATITE TO ENHANCE CELL INFILTRATION

by

MATTHEW C. PHIPPS, WILLIAM C. CLEM, JESSICA M. GRUNDA, GREGORY A.  
CLINES, SUSAN L. BELLIS

*Biomaterials*, 2012 January; 33(2) 524-534

Copyright  
2011  
by  
Elsevier, Ltd

Used by permission

Format adapted for dissertation

## Abstract

Bone mimetic electrospun scaffolds consisting of polycaprolactone (PCL), collagen I and nanoparticulate hydroxyapatite (HA) have previously been shown to support the adhesion, integrin-related signaling and proliferation of mesenchymal stem cells (MSCs), suggesting these matrices serve as promising degradable substrates for osteoregeneration. However, the small pore sizes in electrospun scaffolds hinder cell infiltration *in vitro* and tissue in-growth into the scaffold *in vivo*, limiting their clinical potential. In this study, three separate techniques were evaluated for their capability to increase the pore size of the PCL/col I/nanoHA scaffolds: limited protease digestion, decreasing the fiber packing density during electrospinning, and inclusion of sacrificial fibers of the water-soluble polymer PEO. The PEO sacrificial fiber approach was found to be the most effective in increasing scaffold pore size. Furthermore, the use of sacrificial fibers promoted increased MSC infiltration into the scaffolds, as well as greater infiltration of endogenous cells within bone upon placement of scaffolds within calvarial organ cultures. These collective findings support the use of sacrificial PEO fibers as a means to increase the porosity of complex, bone-mimicking electrospun scaffolds, thereby enhancing tissue regenerative processes that depend upon cell infiltration, such as vascularization and replacement of the scaffold with native bone tissue.

## Introduction

Although significant advances have been made in the development of biomaterials for bone repair, there is still a pressing need for viable clinical alternatives to bone autografting [1], which is currently the gold standard treatment [2]. Autografting presents

multiple drawbacks for the patient, including increased surgery time, donor site pain, and limited quantity of harvestable bone [2-5]. Biomaterials capable of promoting osteoregeneration would provide a promising solution for many common clinical procedures, such as repair of long bone defects, spinal fusions, craniofacial and dental surgeries [6]. Some of the fundamental features of biomaterials thought to be important for effective bone regeneration include: (i) a biochemical composition and structure that supports osteogenic cell responses, (ii) appropriate kinetics of biodegradability, without any release of toxic byproducts, and (iii) a highly interconnected porous network that allows for proper tissue in-growth and vascularization of the biomaterial [7].

In order to engineer a successful osteoinductive material, many researchers have turned toward the process of electrospinning [8-12]. Electrospinning has garnered substantial attention in recent years due to the relatively simple fabrication process, combined with the significant potential to tailor these materials to mimic native bone matrices. Electrospun scaffolds have a nanofibrous structure with interconnecting pores and a large surface to volume ratio, resembling natural extracellular matrix (ECM), and are also amenable to the incorporation of biological factors that influence cellular fate [11, 13]. Several investigators have developed electrospun scaffolds that combine degradable polymers such as polycaprolactone (PCL) with native bone matrix molecules including collagen I and hydroxyapatite (HA) [13-18]. For example, we previously reported that scaffolds composed of blended PCL/collagen I nanofibers, with nanoparticles of HA distributed throughout the thickness of the matrix, promoted greater mesenchymal stem cell (MSC) adhesion, cell spreading, activation of focal adhesion kinase, and cell proliferation, as compared with scaffolds composed of PCL alone [19]. Thus, the PCL/col/HA

scaffolds represent promising substrates for supporting endogenous cells in a bone-healing environment, and also have potential utility as a delivery vehicle for exogenously expanded MSCs.

However, one known limitation of electrospun scaffolds is that the pore sizes within the matrices are typically too small to allow efficient cellular infiltration [20-24]. Migration of cells into a biodegradable scaffold is a crucial step for the success of the synthetic graft and the overall healing of the bone defect [20]. Additionally, the small pore sizes constrain vascularization of the biomaterial, which restricts nutrient delivery and waste removal, limiting the amount of tissue-ingrowth that can be supported [20]. To overcome this problem, numerous investigators have proposed mechanisms for increasing the average pore size of electrospun scaffolds with varying levels of success. Pham *et al.* addressed this issue by alternating layers of microfibers with nanofibers, however cell infiltration under static culture conditions was minimal [25]. Also, the decrease in the number of nanofibers resulting from this method caused diminished cell spreading. Others have used common engineering techniques of salt leaching [26, 27] or cryogenic electrospinning [28] and have achieved moderate success, however these techniques require advanced electrospinning set-ups and can also affect the surface properties of the nanofibers. Another potentially useful approach involves reducing the packing density of the electrospun scaffolds during the fabrication process [29], or alternatively, decreasing the packing density post-electrospinning by employing an ultrasonication method to mechanically separate the fibers, resulting in greater pore sizes and enhanced cellular infiltration [30]. Lastly, several investigators have explored co-electrospinning sacrificial fibers

along with stable fibers, thereby creating larger pores after removal of the sacrificial fibers; this strategy has been successful in facilitating cell infiltration [24, 31, 32].

Despite the many new electrospinning techniques developed to increase scaffold pore size, the vast majority of studies in this area have focused on scaffolds composed solely of synthetic polymers, which offer minimal biologic cues for cells. Therefore it is essential for these techniques to be adapted in order to engineer custom, complex matrices that incorporate biological molecules specific for their intended application. In this study, our goal was to compare various methods for increasing the pore size of bone-mimetic, PCL/col/HA (“TRI”) electrospun scaffolds in order to facilitate the infiltration of osteogenic cells.

## Materials and Methods

### *Preparation of Electrospun Scaffolds*

TRI component and PCL electrospun scaffolds were fabricated as described previously [19]. Briefly, electrospinning solutions of 50wt% PCL + 30wt% collagen I + 20wt% HA (TRI), and 100wt% PCL were dissolved in hexafluoroisopropanol (HFP, Sigma-Aldrich) so that the solid weight was 7.5% of the total solution weight. PEO was dissolved in HFP so that the solid weight was 5.5% of the total solution weight. PCL (MW = 100,000 Da) was purchased from Scientific Polymer Products (Ontario, NY), PEO (MW = 200,000 Da) was purchased from Polysciences, Inc. (Warrington, PA), lyophilized calf skin collagen I was from MP Biomedicals (Solon, OH), and HA nanoparticles (20-50nm) were purchased from Berkeley Advanced Biomaterials, Inc. (San Leandro, CA). The solutions were magnetically stirred at room temperature for over one

hour followed by brief sonication before loading into disposable 3cc syringes. A voltage of 22.5kV was applied using a high-voltage power supply (Gamma High Voltage Research, Ormond Beach, FL). The grounded aluminum collection plate (9cm diameter) was located 15cm from the tip of the electrically charged 27-gauge needle (Jensen Global Inc., Santa Barbara, CA). A syringe pump (Harvard Apparatus) was used to feed polymer solution into the needle at a flow rate of 2ml/h. The resulting samples were randomly arranged fibers deposited as a sheet with average thickness of 300 $\mu$ m. A Humboldt Boring Machine (Fisher) was then used to cut out electrospun scaffolds in fixed diameter circles to insure equal sample size. No chemical or radiation-induced cross-linking of PCL, PEO or collagen fibers was performed.

For studies aimed at reducing the packing density of electrospun scaffolds, a unique collecting plate was used. As shown in Figure 4A, a plastic petri dish (9cm diameter) was added to cover the grounded aluminum collecting plate. Twenty evenly spaced 19-gauge (1.5" length) needles (Jensen Global) were inserted perpendicularly through holes created in the petri dish, touching the aluminum plate underneath.

Following electrospinning, samples were placed under vacuum for 48 hours to remove the residual HFP solvent. Scaffolds were sterilized in 70% EtOH for one hour prior to use.

#### *Implantation of Scaffolds into Rat Tibiae*

PCL or TRI scaffolds were implanted into cortical defects created in rat tibias of four male Sprague-Dawley rats as previously described [33] (two rats per scaffold type). The wounds were closed with vicryl sutures, and buprenorphine was given as an analge-

sic. The tibiae, with implants in place, were retrieved after 7 days, fixed in 4% formalin, and embedded in poly(methylmethacrylate). Multiple 5 $\mu$ m sections were stained with Goldner's Trichrome, which stains mineralized tissue green, non-mineralized extracellular matrix red, and cell nuclei black. Low power survey images were acquired with a Nikon SMZ-U stereomicroscope. Higher magnification bright field images were acquired with a Nikon Eclipse TE2000-U. NIH guidelines for the care and use of laboratory animals (NIH publication #85-23 rev.1985) were observed, and all protocols were performed with prior approval from the University of Alabama Institutional Animal Care and Use Committee.

#### *Scanning Electron Microscopy (SEM) Imaging of Electrospun Scaffolds*

Electrospun scaffolds were visualized for fiber integrity and architecture using scanning electron microscopy. For collagenase treatment testing, scaffolds were placed in a collagenase solution (2mg/ml Roche Applied Sciences) for one week prior to being dried in increasing gradients of ethanol in water. SEM imaging was performed on a Philips 515 SEM with an accelerating voltage of 15kV.

In the subcutaneous skin pouch studies, scaffolds were implanted into dorsal subcutaneous sites of male Sprague-Dawley rats as described previously [34]. After one week, animals were sacrificed and implants were retrieved and washed. Scaffolds were dried in gradients of ethanol in water followed by a gradient of hexamethyldisilazane in ethanol. SEM imaging was performed on a Philips 515 SEM with an accelerating voltage of 15kV.



For reduced packing density studies, SEM imaging was performed on a Philips XL-30 SEM with an accelerating voltage of 10kV. Scaffolds were dried in a desiccator for 48 hours prior to imaging.

#### *Isolation and Culture of MSCs*

For *in vitro* infiltration studies, human MSCs were isolated from bone marrow donations, as previously described [35]. Briefly, cells were pelleted by centrifugation, resuspended in Dulbecco's Modified Eagle Medium (DMEM), and then applied to a His-topaque-1077 column (Sigma, St. Louis, MO). A density gradient was generated by centrifugation at 500g for 30 min. Cells from the DMEM/Histopaque interface were extracted with a syringe and seeded onto tissue culture dishes and cultured in DMEM containing 10% fetal bovine serum. Bone marrow samples were obtained with approval from the University of Alabama Institutional Review Board. For fluorescent studies, lentivirus-transduced human MSCs containing green fluorescent protein (GFP) were provided by the Tulane Center for Gene Therapy (New Orleans, LA).

#### *Collagenase Treatment of Electrospun Scaffolds*

TRI scaffolds were treated with a 2mg/ml collagenase solution at 37°C for one week. The dry weight of the scaffolds was measured before collagenase treatment, and then the scaffolds were dried in a dessicator before being weighed again. The change in mass is presented as the percent change between the initial and final weighing. 100% PCL scaffolds were used as control.

### *MSC Infiltration into Electrospun Scaffolds*

MSC infiltration into electrospun scaffolds was tested in two separate experiments. In the first, TRI or PCL scaffolds were treated with collagenase solution (2mg/ml) overnight prior to being sterilized in 70% ethanol for one hour. Scaffolds were placed in 24-well CellCrowns™ (Scaffdex, Tampere, Finland) to maintain scaffold orientation. GFP-expressing MSCs were seeded at a density of  $3.8 \times 10^4$  cells/cm<sup>2</sup> onto the top of the scaffolds and cultured in growth media (DMEM containing 4.5 g/L glucose, supplemented with 10% fetal bovine serum) at 37°C, exchanging media every 2-3 days. After two weeks, cells on the scaffolds were fixed in 70% EtOH prior to embedding the cell loaded scaffolds in frozen HistoPrep blocks (Fisher Scientific). 6µm sections were cut using a Leica cryostat. Sections were visualized using a Nikon fluorescent microscope for presence of GFP-expressing cells within the scaffold.

In the second cell infiltration assay, TRI/PEO or TRI scaffolds were washed overnight to remove PEO fibers prior to being sterilized in 70% ethanol for one hour. Scaffolds were again placed in 24-well CellCrown™ and MSCs were seeded at a density of  $5 \times 10^4$  cells/cm<sup>2</sup> onto the top of the scaffolds and cultured in growth media for one week. Cells were then fixed in 70% EtOH prior to embedding the cell-loaded scaffolds in frozen HistoPrep blocks. 6µm sections were cut using a Leica cryostat. Sections were stained with DAPI to visualize the location of cell nuclei.

### *Removal of Sacrificial Fibers of PEO*

After electrospinning, sacrificial fibers of PEO were removed from electrospun scaffolds by soaking in H<sub>2</sub>O overnight at room temperature. The removal of PEO fibers

was visualized by adding fluorescent dyes to the electrospinning solutions prior to electrospinning. The green fluorescent dye DiOC<sub>18</sub>(3) (Invitrogen Corp., Carlsbad, CA) was added to TRI solutions, and the red fluorescent dye DiIC<sub>18</sub>(3) (Invitrogen) was added to PEO solutions.

For percent mass loss studies, scaffolds were weighed before soaking in water for one week, then dried in a desiccator before being weighed again. The change in mass is presented as the percent change between the initial and final weighing.

#### *Measuring Pore Sizes of TRI/PEO Scaffolds*

TRI/PEO and TRI solutions were electrospun onto glass coverslips attached to the collecting plate. 0.05mL of solution was electrospun for all samples to ensure equal scaffold thickness. TRI solutions were fluorescently stained with DiOC<sub>18</sub>(3). After washing scaffolds, the fibers were visualized fluorescently using a Zeiss LSM 710 Confocal microscope. 10um sections were captured by stacking consecutive image slices. Images were analyzed using the Area Auto Detect feature on the NIS-Elements Basic Research software (Nikon Instruments Inc., Melville, NY). The macro was used to automatically detect boundaries and measure areas between fluorescent fibers of 25 pores manually selected at random for each image. Three images were analyzed per sample, two samples per group. All images were taken at 20x. Average pore size was calculated using the imaging software.

### *Infiltration of Cells from Calvarial Organ Cultures*

4-day-old Swiss White mice pups were euthanized via decapitation. The calvarial bones were excised as described by Mohammad et al. [36] and placed on top of a steel grid in 6-well plates. Electrospun scaffolds of TRI or TRI/PEO (soaked in water overnight to remove PEO) were placed on top of the calvaria. Calvaria were cultured in serum free media for eight days. Calvaria/scaffold constructs were then fixed in 70% EtOH and embedded in frozen HistoPrep blocks. 6 $\mu$ m sections were cut using a Leica cryostat. Sections were stained with DAPI to visualize the location of endogenous cell nuclei.

### *Statistics*

Percent mass loss studies were performed at least two independent times. MSC infiltration studies were performed two independent times in triplicate. Two representative microscopic fields were analyzed per sample, giving a total of 12 fields analyzed for each scaffold formulation. Organ culture studies were performed with seven samples per group. Two representative fields were analyzed per sample, giving a total of 14 fields analyzed for each scaffold type. Data sets were assessed using an unpaired Student's t-test parametric analysis, and data were reported as mean + standard deviation. A confidence level of at least 95% ( $p < 0.05$ ) was considered significant and denoted by “\*”. Additionally, ( $p < .0001$ ) was denoted by “\*\*\*”.

## Results

### *Controlled Degradation of Collagen Fibers*

Previous studies have shown that bone-mimetic electrospun scaffolds consisting of PCL, collagen I and nano HA (“TRI”) support MSC responses *in vitro* that are favorable for new bone formation [19]. However, it has become apparent that the small pore sizes within these scaffolds restrict cellular infiltration, consistent with most other types of electrospun scaffolds. As can be seen in Figure 1A, TRI scaffolds implanted into a cortical defect created in a rat tibia supported excellent new bone formation, and higher magnification images (Fig 1B) revealed that newly synthesized bone was in direct contact with the implant surface. However cells lined the surface of TRI scaffolds, with minimal infiltration into the scaffold (inset in Fig 1B).

To address this issue, we first tested whether the collagen present in the TRI scaffolds could be used to our advantage as a target for controlled degradation, thereby creating larger pores in order to facilitate cellular infiltration. We hypothesized that a limited treatment with collagenase solution could be employed to introduce selective fiber breaks (without completely eliminating collagen from the scaffolds). To test this, TRI scaffolds, and PCL scaffolds as a control, were treated with collagenase, and substrates were then analyzed by SEM to screen for the presence of fiber breakages. As shown in Figure 2A, SEM images of the treated scaffolds revealed breakage of fibers in the TRI (e) but not PCL (b) scaffolds. This cleavage of fibers in TRI scaffolds was also observed when scaffolds were placed into rat subcutaneous skin pouches, where they are exposed to endogenous collagenases (f). Additionally, the cleavage of collagen fibers was confirmed by comparing the dry-weight of scaffolds before and after treatment with collagenase solu-

tion *in vitro*. On average, TRI scaffolds lost 15.6% of their mass after one week, while PCL scaffolds exhibited no decrease in mass (Fig 2B).

#### *Cell Infiltration in Scaffolds Pre-Treated with Collagenase*

After observing that collagenase treatment creates specific fiber breakages in TRI scaffolds, thereby opening larger pores, we tested to see if this would facilitate cellular infiltration. MSCs that stably express GFP were seeded on top of TRI scaffolds that had been pre-treated with collagenase solution and then placed into Scaffdex CellCrown™ well inserts (to ensure the scaffold orientation was maintained). MSCs seeded onto the scaffolds were cultured in standard growth media. After two weeks of culture, the samples were fixed and scaffolds sectioned vertically to monitor migration of cells into the scaffold. As can be seen in Figure 3, panel b, the MSCs remained on the surface of the scaffolds, with negligible cellular infiltration observed.

Given the minimal level of cellular infiltration observed, we questioned whether or not the basal migration level of the GFP-MSCs was too low to observe infiltration into the scaffolds. To stimulate MSC migration, we coated the bottom side of the scaffolds with the chemo-attractant platelet derived growth factor (PDGF-BB), which has been shown to be a potent inducer of MSC migration [37-39]. By coating the underside of the scaffold with PDGF-BB, a chemo-attractive gradient was created through the scaffold for the MSCs. Despite the pretreatment of scaffolds with collagenase to increase pore sizes in addition to the inclusion of PDGF, there was still negligible cell infiltration at time points of two (Figure 3, panel c) and three weeks (not shown). Therefore it was apparent that this technique was not an adequate solution for facilitating robust cellular infiltration.

### *Reducing the Packing Density of Electrospun Fibers*

We next developed a modified electrospinning protocol aimed at decreasing the packing density of scaffold fibers. Specifically, a plastic petri dish was used to cover the normal aluminum collecting plate, and twenty evenly spaced holes were created in the petri dish, followed by the placement of 19 gauge needles through the holes touching the grounded collecting plate. A schematic of the collecting plate can be seen in Figure 4A. During electrospinning, the fibers were attracted to the grounded needles protruding from the petri dish, and bridged from one needle tip to the other. The limited amount of grounded points for fiber attachment reduced the packing density of the electrospun fibers, creating a more three dimensional scaffold with larger pore sizes. However, it was discovered that this three-dimensional scaffold fabrication technique was only successful with 100% PCL scaffolds, and could not be replicated with TRI scaffolds (Fig 4B). SEM confirmed that while the PCL scaffolds showed large pore distribution and channels, the TRI fibers remained densely packed (Fig 4C). Despite numerous modifications to the protocol, including changes to the solution composition and electrospinning conditions, as well as alterations in the collecting plate set-up, we failed to generate TRI scaffolds with the type of 3-dimensional architecture that was achievable with scaffolds composed of PCL alone. Given the importance of collagen I and nanoHA in stimulating MSC responses critical for osteogenesis, it seems unlikely that the greater porosity of PCL scaffolds spun with multiple grounded needles can compensate for the favorable biochemical signals provided by TRI scaffolds. Hence, alternative electrospinning methods were pursued.

### *Inclusion of Sacrificial PEO Fibers in Scaffolds*

As another method to increase the pore sizes of TRI scaffolds, the inclusion of sacrificial fibers of the water-soluble polymer poly(ethylene oxide) was evaluated. By simultaneously electrospinning separate solutions of PEO and TRI, a mixed scaffold was created. After fabrication, soaking the scaffolds in water washed away the sacrificial fibers, leaving just the TRI scaffold with voids where the PEO fibers had previously been. To facilitate the mixing of the fibers onto a flat collecting plate, a fixed gear motor was installed to rotate the collecting plate on an axis parallel to the electrospinning direction. By adding fluorescent dyes to the electrospinning solutions prior to electrospinning, fluorescent microscopy confirmed scaffolds were created with a mixture of two separate fibers, and that the fibers of PEO were removed after soaking in water, leaving just the TRI fibers (Fig 5A). Furthermore, the removal of PEO was confirmed by comparing the dry weight of the scaffolds before and after soaking them in water (Fig 5B).

### *Measuring the Pore Sizes of Electrospun Scaffolds*

To quantify the pore sizes of electrospun scaffolds created with sacrificial fibers of PEO, fluorescent confocal microscopy experiments were performed. Electrospun scaffolds of TRI or TRI/PEO were collected onto glass coverslips taped onto the rotating collecting plate. To ensure equal fiber distribution, equal volumes of TRI solution were electrospun. TRI solutions were stained with fluorescent dye (DiOC<sub>18</sub>(3)) prior to electrospinning. After soaking in water, scaffolds were imaged using a Zeiss confocal microscope. Individual scans of the samples were combined to create a 10 $\mu$ m thick picture.



NIS-Elements software was used to analyze the resulting images. 25 pores were selected at random using the Area Auto Detect feature. In Figure 6A, representative images are shown to illustrate boundary selection by the software. The mean pore size in TRI scaffolds created with sacrificial fibers of PEO was  $1826.11\mu\text{m}^2$ , significantly greater than the mean size of pores for TRI scaffolds created without PEO fibers ( $424\mu\text{m}^2$ ) (Fig 6B).

#### *MSC Infiltration in Scaffolds with PEO Fibers*

After successful fabrication of scaffolds consisting of separate TRI and PEO fibers, scaffolds were evaluated for the effect of PEO fiber removal on cellular infiltration. Electrospun scaffolds of TRI/PEO were first soaked in water overnight to remove the PEO fibers. Scaffolds were then loaded into Scaffoldex holders to maintain their orientation and seeded with MSCs. TRI scaffolds created without PEO were used as controls. After one week in culture, the samples were fixed and vertical sections of the scaffolds were stained with DAPI to visualize the nuclei of cells infiltrating into the scaffold. As can be seen in Figure 7A, MSCs were present within the interior of the TRI/PEO scaffolds, showing that removal of sacrificial fibers facilitated cellular infiltration. In comparison, MSCs were only present on the surface of TRI scaffolds created without PEO.

In order to quantify the amount of cellular infiltration observed in these experiments, a custom MATLAB script was created to process the images. Phase contrast and DAPI images were taken of the scaffold cross-sections and loaded into the MATLAB program. The phase contrast image was used in order to set the boundaries of the scaffold and calculate the thickness of the scaffold. The scaffold boundaries were then mapped onto the DAPI image, and the script calculated the distance from each cell nuclei to the

top of the scaffold. Results of this analysis showed that TRI scaffolds created with PEO had an average cell infiltration of 45.49 $\mu\text{m}$ , compared to 6.13 $\mu\text{m}$  for TRI scaffolds without PEO (Fig 7B), confirming that sacrificial fibers of PEO facilitate cellular infiltration of MSCs.

#### *Infiltration of Endogenous Cells from Calvarial Organ Cultures*

To examine the infiltration of endogenous cells from a bone microenvironment, a mouse organ culture model was used. This *ex-vivo* model has numerous advantages over *in vitro* cell migration assays. The excised calvariae retain the three-dimensional architecture of developing bones and also possess the relevant cell types found in bone, including osteoblasts, osteocytes, stromal and pre-osteoblastic cells [36, 40]. With all of these different cell types interacting with one another through paracrine and endocrine signaling molecules, this model provides a physiologically relevant environment to study cellular infiltration of bone cells. Excised calvariae from neonatal mice were placed into culture on top of a steel grid to keep them from floating and hold them at the liquid/air interface. TRI or TRI/PEO (previously soaked in water to remove PEO) scaffolds were placed directly on top of the calvariae, where they come into contact with the bone-lining cells. After 8 days in culture, the calvaria/scaffold constructs were fixed and vertical sections were stained with DAPI to show cellular nuclei. As can be seen in Figure 8A, TRI scaffolds created with sacrificial fibers of PEO showed greater cellular infiltration of cells from the mouse calvaria into the scaffold.

In order to quantify the distance traveled by infiltrating endogenous cells, a custom MATLAB script was used as outlined above. Results of this analysis showed that

cells on TRI/PEO scaffolds were able to infiltrate 63.15 $\mu$ m on average, compared to 20.06 $\mu$ m for cells on regular TRI scaffolds (Fig 8B). Collectively these results confirm that sacrificial fibers of PEO can be included in the electrospinning process in order to create electrospun scaffolds that facilitate the infiltration of MSCs and endogenous bone cells.

## Discussion

As the average age of the current population continues to increase, the need for bone grafts to repair skeletal defects will correspondingly rise [6]. Therefore, creating a synthetic bone graft that can replace or supplement autografted bone has become a major goal in the field of tissue engineering [7, 41]. One of the more promising techniques for fabricating a synthetic bone graft is the process of electrospinning, due to the ease in creating a nano-fibrous matrix that mimics natural ECM structure [42, 43]. Additionally, by combining synthetic and biological components, more complex, bone-mimetic scaffolds can be created that have tunable mechanical and resorbable properties (enabled by the synthetic polymer) while providing important biologic cues (from bone-derived molecules) to osteogenic cells [44]. As an example, several investigators have studied the incorporation of collagen I and hydroxyapatite into electrospun scaffolds since these two molecules comprise the principal constituents of bone ECM. These studies have shown that electrospun nanofibers that have incorporated HA [15, 16, 45] and/or collagen [17-19, 46] facilitate the adhesion, proliferation, and osteoblastic differentiation of bone cells *in vitro* as well as support robust bone formation *in vivo*.

Although these results show promise towards the end goal of creating a synthetic bone graft, there is a significant limitation associated with electrospun scaffolds. Due to the dense packing of electrospun nanofibers during the fabrication process, the resulting matrix has very small pore sizes, which hinders the infiltration of cells *in vitro* and limits tissue-ingrowth and vascularization *in vivo* [20, 21, 47]. In order to maximize the success of a biodegradable implant, the implant must support the infiltration of bone cells throughout the thickness of the material, allowing the implant to be replaced with native bone over time through the process of creeping substitution [48]. Additionally, vascularization of the biomaterial is an essential step in tissue healing, as this process provides the nutrients and oxygen needed for bone cells to survive, while facilitating removal of waste products from cell metabolism [20, 21, 47, 49]. Accordingly, a growing focus in the field of tissue engineering is to discover techniques that increase the mean pore sizes of electrospun scaffolds and thereby facilitate cellular infiltration.

In this study, we investigated several techniques for creating bone-mimetic TRI scaffolds that have permissive pore sizes for cellular infiltration. We initially observed that limited treatment of the bone-mimetic scaffolds with a collagenase solution *in vitro* created specific fiber breakages throughout the scaffold, thereby opening up larger pores. However, it was observed that the pores created by collagenase treatment were insufficient to allow MSC infiltration. As a second approach, we developed a modified electrospinning protocol with the goal of decreasing fiber packing density, creating larger pores between the fibers. Several groups have similarly attempted to decrease fiber-packing density using a variety of methods. Mitchell and Sanders reported the creation of a controlled electrospinning set-up in order to tightly control fiber diameter and inter-fiber

spacing [50, 51]. Although cell infiltration was not evaluated, it was found that the dielectric strength of the collecting plate had a significant effect on inter-fiber spacing. Vaquette and Cooper-White tested a number of patterned collecting plates, and determined that electrospun PCL fibers would collect along the patterns of the plate [51]. Some of these patterns could be used to create larger pores, and the resulting scaffolds facilitated infiltration of NIH 3T3 fibroblasts. Soliman et al. tested both micro- and nano-fiber meshes of either low or high density fiber packing and found that the microfiber low density fiber packing scaffolds supported the greatest cell infiltration of GFP-HUVECs [21]. Lastly, Blakeney et al. were able to significantly decrease the packing density of electrospun PCL scaffolds by using a custom collecting surface consisting of a spherical foam bowl with an array of embedded stainless steel probes [29]. The resulting electrospun scaffold possessed a fluffy, three-dimensional structure, which supported high levels of INS-1 cell infiltration *in vitro*. These collective results from multiple investigators provide excellent support for the concept of increasing pore size through controlled fiber packing, however it should be noted that all of these prior studies were performed with single polymer solutions (e.g. 100% PCL). In the current study, we created a unique collecting plate consisting of a 19 gauge needles protruding perpendicularly through a plastic petri dish. This strategy was very successful for scaffolds composed of 100% PCL; the scaffolds formed in biscuit-like sheets, with very loosely packed fibers between the sheets. Additionally, the scaffolds had a wide range of pore sizes and deep channels, creating a structure resembling natural trabecular bone. Unfortunately, these results could not be replicated using our bone-mimetic scaffolds, despite many adaptations to the protocol including changing the needle gauge, needle density, electrospinning voltage, solu-

tion viscosity, and the replacement of the plastic collecting plate with Styrofoam. Clearly there is a need for further studies aimed at adapting novel electrospinning protocols for use with complex scaffolds incorporating biologic molecules. In this regard, Hutmacher's group used a combination of electrospinning and electrospraying to create PCL/col electrospun scaffolds with pockets of hyaluronan gel; this approach was very effective in promoting infiltration of multiple cell types [22, 47].

Another emerging method for increasing scaffold porosity involves the incorporation of sacrificial fibers of PEO during the electrospinning process. This technique was first reported by Baker et al. [31], and its effectiveness has since been confirmed by others [24, 32]. However, to our knowledge, PEO fibers have yet to be utilized in conjunction with bone-mimetic fibers mixing collagen I, nanoHA and PCL, creating a complex, tissue-specific matrix. In the current study, composite fibers of PCL/col/HA were co-spun with separate fibers of PEO. Washing the scaffolds removed the PEO fibers, leaving larger voids in the matrix between the remaining PCL/col/HA fibers. Increased pore size was confirmed by fluorescent confocal microscope and NIS-Elements imaging software. In order to evaluate the effectiveness of using sacrificial fibers to promote cellular infiltration, MSCs were grown on the TRI scaffolds created with PEO fibers and the positions of nuclei on scaffold cross-sections were measured. It was observed that scaffolds created with PEO fibers were able to support a significantly greater level of cellular infiltration compared to scaffolds created without PEO fibers. These data establish that the inclusion of sacrificial fibers of PEO can be readily adapted to more complex electrospun scaffolds consisting of composite fibers designed to mimic a specific natural extracellular matrix. In future studies one important objective will be to test varying amounts of PEO in bone-

mimetic scaffolds, with the goal of tailoring PEO fiber number to control the degree of cell infiltration. Previous studies by others [31, 32] have shown a positive correlation between the degree of cell infiltration and the percentage of PEO within electrospun PCL scaffolds.

Although *in vitro* studies of cell infiltration are commonly employed to evaluate the effects of scaffold pore size, few investigators have monitored scaffold infiltration by endogenous cells within bone matrix. Due to the complexity of intact tissues, where numerous cell types and soluble factors cooperate to regulate cell and tissue responses, it can be difficult to accurately model bone cell behavior. Therefore we felt it was essential to examine cell infiltration in a more physiologically-relevant system. This was accomplished by using a mouse calvarial organ culture. In this *ex vivo* model, the calvaria retain the three-dimensional architecture of developing bones and also possess the relevant cell types found in bone, which constantly interact with one another in a bone microenvironment [36, 40]. Our results show that cells from the natural bone matrix interact favorably with the PCL/col/HA scaffolds; specifically, cells were able to migrate from the calvaria and attach to the surface of these scaffolds. Most importantly, significantly greater cell infiltration was observed in TRI matrices created with PEO fibers. These results provide strong evidence that matrices composed of PCL/col/HA are not only effective in promoting bone cell adhesion and survival, but the further inclusion of sacrificial PEO fibers represents a successful and technically straightforward method for enhancing porosity, leading to enhanced cell infiltration.

## Conclusion

In prior studies electrospun PCL/col/HA scaffolds were developed that supported greater MSC adhesion, signaling and proliferation as compared with scaffolds composed of PCL or collagen I alone, however the small pore sizes of these bone-mimetic scaffolds limited cell infiltration. In this investigation, we evaluated the efficacy of multiple techniques in increasing the pore size of the PCL/col/HA scaffolds, thereby enhancing cell infiltration. We found that incorporation of PEO sacrificial fibers in the electrospinning process facilitated MSC infiltration in vitro, as well as infiltration of endogenous cells when scaffolds were placed within calvarial organ cultures. While there is currently much interest in developing methods to increase the pore size of electrospun scaffolds, few of these have been adapted for use with multi-component scaffolds incorporating biologic molecules. Results from this study show that electrospinning PEO sacrificial fibers is a relatively simple approach that can be used with complex tissue-mimicking electrospun scaffolds to increase cell infiltration. More importantly, the enhanced cell infiltration achieved by incorporating PEO sacrificial fibers overcomes one of the major limitations of bone-mimetic PCL/col/HA matrices, which have already shown promise as supportive matrices for osteoregeneration.

## Acknowledgement

This research was supported by NIH/NIAMS grant R01AR51539 (SLB) and MC Phipps is supported by the NIH Nanotechnology in Biosensors and Bioengineering grant 5T32EB004312-04 (Vohra, YK). The authors gratefully acknowledge the Bone Histomorphometry Core Facility for their assistance with tissue processing and staining, the



High Resolution Imaging Facility for their assistance with confocal microscope imaging, the Central Analytical Facility (University of Alabama) and Robin Foley Ph.D. (UAB) for their assistance with SEM imaging. MC Phipps would also like to acknowledge the Howard Hughes Institute Med to Grad Fellowship program.

#### References

- [1] Hing KA. Bone repair in the twenty-first century: biology, chemistry or engineering? *Philos Transact A Math Phys Eng Sci.* 2004;362:2821-50.
- [2] Brighton CT, Shaman P, Heppenstall RB, Esterhai JL, Pollack SR, Friedenberg ZB. Tibial Nonunion Treated with Direct-Current, Capacitive Coupling, or Bone-Graft. *Clinical Orthopaedics and Related Research.* 1995:223-34.
- [3] Fernyhough JC, Schimandle JJ, Weigel MC, Edwards CC, Levine AM. Chronic Donor Site Pain Complicating Bone-Graft Harvesting from the Posterior Iliac Crest for Spinal-Fusion. *Spine.* 1992;17:1474-80.
- [4] Goulet JA, Senunas LE, DeSilva GL, Greenfield MLVH. Autogenous iliac crest bone graft - Complications and functional assessment. *Clinical Orthopaedics and Related Research.* 1997;339:76-81.
- [5] Giannoudis PV, Dinopoulos H, Tsiridis E. Bone substitutes: an update. *Injury.* 2005;36 Suppl 3:S20-7.
- [6] Brydone AS, Meek D, Maclaine S. Bone grafting, orthopaedic biomaterials, and the clinical need for bone engineering. *Proc Inst Mech Eng H.* 2010;224:1329-43.
- [7] Navarro M, Michiardi A, Castano O, Planell JA. Biomaterials in orthopaedics. *J R Soc Interface.* 2008;5:1137-58.
- [8] Huang ZM, Zhang YZ, Kotaki M, Ramakrishna S. A review on polymer nanofibers by electrospinning and their applications in nanocomposites. *Composites Science and Technology.* 2003;63:2223-53.
- [9] Pham QP, Sharma U, Mikos AG. Electrospinning of polymeric nanofibers for tissue engineering applications: A review. *Tissue Engineering.* 2006;12:1197-211.
- [10] Murugan R, Ramakrishna S. Nano-featured scaffolds for tissue engineering: A review of spinning methodologies. *Tissue Engineering.* 2006;12:435-47.
- [11] Prabhakaran MP, Venugopal J, Ramakrishna S. Electrospun nanostructured scaffolds for bone tissue engineering. *Acta Biomaterialia.* 2009;5:2884-93.

- [12] Venugopal J, Low S, Choon AT, Kumar TSS, Ramakrishna S. Mineralization of osteoblasts with electrospun collagen/hydroxyapatite nanofibers. *Journal of Materials Science-Materials in Medicine*. 2008;19:2039-46.
- [13] Wutticharoenmongkol P, Sanchavanakit N, Pavasant P, Supaphol P. Preparation and characterization of novel bone scaffolds based on electrospun polycaprolactone fibers filled with nanoparticles. *Macromolecular Bioscience*. 2006;6:70-7.
- [14] Catledge SA, Clem WC, Shrikishen N, Chowdhury S, Stanishevsky AV, Koopman M, et al. An electrospun triphasic nanofibrous scaffold for bone tissue engineering. *Biomedical Materials*. 2007;2:142-50.
- [15] Gupta D, Venugopal J, Mitra S, Giri Dev VR, Ramakrishna S. Nanostructured biocomposite substrates by electrospinning and electrospraying for the mineralization of osteoblasts. *Biomaterials*. 2009;30:2085-94.
- [16] Lao L, Wang Y, Zhu Y, Zhang Y, Gao C. Poly(lactide-co-glycolide)/hydroxyapatite nanofibrous scaffolds fabricated by electrospinning for bone tissue engineering. *J Mater Sci Mater Med*. 2011;22:1873-84.
- [17] Ekaputra AK, Zhou Y, Cool SM, Hutmacher DW. Composite electrospun scaffolds for engineering tubular bone grafts. *Tissue Eng Part A*. 2009;15:3779-88.
- [18] Chan CK, Liao S, Li B, Lareu RR, Larrick JW, Ramakrishna S, et al. Early adhesive behavior of bone-marrow-derived mesenchymal stem cells on collagen electrospun fibers. *Biomed Mater*. 2009;4:035006.
- [19] Phipps MC, Clem WC, Catledge SA, Xu Y, Hennessy KM, Thomas V, et al. Mesenchymal stem cell responses to bone-mimetic electrospun matrices composed of polycaprolactone, collagen I and nanoparticulate hydroxyapatite. *PLoS One*. 2011;6:e16813.
- [20] Karageorgiou V, Kaplan D. Porosity of 3D biomaterial scaffolds and osteogenesis. *Biomaterials*. 2005;26:5474-91.
- [21] Soliman S, Sant S, Nichol JW, Khabiry M, Traversa E, Khademhosseini A. Controlling the porosity of fibrous scaffolds by modulating the fiber diameter and packing density. *J Biomed Mater Res A*. 2011;96:566-74.
- [22] Ekaputra AK, Prestwich GD, Cool SM, Hutmacher DW. Combining electrospun scaffolds with electrosprayed hydrogels leads to three-dimensional cellularization of hybrid constructs. *Biomacromolecules*. 2008;9:2097-103.
- [23] Nerurkar NL, Sen S, Baker BM, Elliott DM, Mauck RL. Dynamic culture enhances stem cell infiltration and modulates extracellular matrix production on aligned electrospun nanofibrous scaffolds. *Acta Biomater*. 2011;7:485-91.

- [24] Milleret V, Simona B, Neuenschwander P, Hall H. Tuning electrospinning parameters for production of 3D-fiber-fleeces with increased porosity for soft tissue engineering applications. *Eur Cell Mater*. 2011;21:286-303.
- [25] Pham QP, Sharma U, Mikos AG. Electrospun poly(epsilon-caprolactone) microfiber and multilayer nanofiber/microfiber scaffolds: characterization of scaffolds and measurement of cellular infiltration. *Biomacromolecules*. 2006;7:2796-805.
- [26] Nam J, Huang Y, Agarwal S, Lannutti J. Improved cellular infiltration in electrospun fiber via engineered porosity. *Tissue Eng*. 2007;13:2249-57.
- [27] Wright LD, Andric T, Freeman JW. Utilizing NaCl to increase the porosity of electrospun materials. *Materials Science and Engineering C*. 2010;31:30-6.
- [28] Leong MF, Rasheed MZ, Lim TC, Chian KS. In vitro cell infiltration and in vivo cell infiltration and vascularization in a fibrous, highly porous poly(D,L-lactide) scaffold fabricated by cryogenic electrospinning technique. *Journal of Biomedical Materials Research Part A*. 2009;91:231-40.
- [29] Blakeney BA, Tambralli A, Anderson JM, Andukuri A, Lim DJ, Dean DR, et al. Cell infiltration and growth in a low density, uncompressed three-dimensional electrospun nanofibrous scaffold. *Biomaterials*. 2011;32:1583-90.
- [30] Lee JB, Jeong SI, Bae MS, Yang DH, Heo DN, Kim CH, et al. Highly Porous Electrospun Nanofibers Enhanced by Ultrasonication for Improved Cellular Infiltration. *Tissue Eng Part A*. 2011;17:2695-702.
- [31] Baker BM, Gee AO, Metter RB, Nathan AS, Marklein RA, Burdick JA, et al. The potential to improve cell infiltration in composite fiber-aligned electrospun scaffolds by the selective removal of sacrificial fibers. *Biomaterials*. 2008;29:2348-58.
- [32] Whited BM, Whitney JR, Hofmann MC, Xu Y, Rylander MN. Pre-osteoblast infiltration and differentiation in highly porous apatite-coated PLLA electrospun scaffolds. *Biomaterials*. 2011;32:2294-304.
- [33] Hennessy KM, Clem WC, Phipps MC, Sawyer AA, Shaikh FM, Bellis SL. The effect of RGD peptides on osseointegration of hydroxyapatite biomaterials. *Biomaterials*. 2008;29:3075-83.
- [34] Culpepper BK, Phipps MC, Bonvallet PP, Bellis SL. Enhancement of peptide coupling to hydroxyapatite and implant osseointegration through collagen mimetic peptide modified with a polyglutamate domain. *Biomaterials*. 2010;31:9586-94.
- [35] Kilpadi KL, Sawyer AA, Prince CW, Chang PL, Bellis SL. Primary human marrow stromal cells and Saos-2 osteosarcoma cells use different mechanisms to adhere to hydroxylapatite. *J Biomed Mater Res*. 2004;68A:273-85

- [36] Mohammad KS, Chirgwin JM, Guise TA. Assessing new bone formation in neonatal calvarial organ cultures. *Methods Mol Biol.* 2008;455:37-50.
- [37] Ozaki Y, Nishimura M, Sekiya K, Suehiro F, Kanawa M, Nikawa H, et al. Comprehensive analysis of chemotactic factors for bone marrow mesenchymal stem cells. *Stem Cells Dev.* 2007;16:119-29.
- [38] Allori AC, Sillon AM, Warren SM. Biological basis of bone formation, remodeling, and repair-part I: biochemical signaling molecules. *Tissue Eng Part B Rev.* 2008;14:259-73.
- [39] Alvarez RH, Kantarjian HM, Cortes JE. Biology of platelet-derived growth factor and its involvement in disease. *Mayo Clin Proc.* 2006;81:1241-57.
- [40] Garrett IR. Assessing bone formation using mouse calvarial organ cultures. *Methods Mol Med.* 2003;80:183-98.
- [41] Frohlich M, Grayson WL, Wan LQ, Marolt D, Drobic M, Vunjak-Novakovic G. Tissue engineered bone grafts: biological requirements, tissue culture and clinical relevance. *Curr Stem Cell Res Ther.* 2008;3:254-64.
- [42] Ifkovits JL, Sundararaghavan HG, Burdick JA. Electrospinning fibrous polymer scaffolds for tissue engineering and cell culture. *J Vis Exp.* 2009;32:10.3791/1589.
- [43] Li WJ, Tuan RS. Fabrication and application of nanofibrous scaffolds in tissue engineering. *Curr Protoc Cell Biol.* 2009;Chapter 25:Unit 25 2.
- [44] Nisbet DR, Forsythe JS, Shen W, Finkelstein DI, Horne MK. Review paper: a review of the cellular response on electrospun nanofibers for tissue engineering. *J Biomater Appl.* 2009;24:7-29.
- [45] Fu YC, Nie H, Ho ML, Wang CK, Wang CH. Optimized bone regeneration based on sustained release from three-dimensional fibrous PLGA/HAp composite scaffolds loaded with BMP-2. *Biotechnol Bioeng.* 2008;99:996-1006.
- [46] Lee JJ, Yu HS, Hong SJ, Jeong I, Jang JH, Kim HW. Nanofibrous membrane of collagen-polycaprolactone for cell growth and tissue regeneration. *J Mater Sci Mater Med.* 2009;20:1927-35.
- [47] Ekaputra AK, Prestwich GD, Cool SM, Hutmacher DW. The three-dimensional vascularization of growth factor-releasing hybrid scaffold of poly (varepsilon-caprolactone)/collagen fibers and hyaluronic acid hydrogel. *Biomaterials.* 2011;32:8108-17.
- [48] Nuss KM, von Rechenberg B. Biocompatibility issues with modern implants in bone - a review for clinical orthopedics. *Open Orthop J.* 2008;2:66-78.

- [49] Jain RK, Au P, Tam J, Duda DG, Fukumura D. Engineering vascularized tissue. *Nat Biotechnol.* 2005;23:821-3.
- [50] Mitchell SB, Sanders JE. A unique device for controlled electrospinning. *J Biomed Mater Res A.* 2006;78:110-20.
- [51] Vaquette C, Cooper-White JJ. Increasing electrospun scaffold pore size with tailored collectors for improved cell penetration. *Acta Biomater.* 2011;7:2544-57.

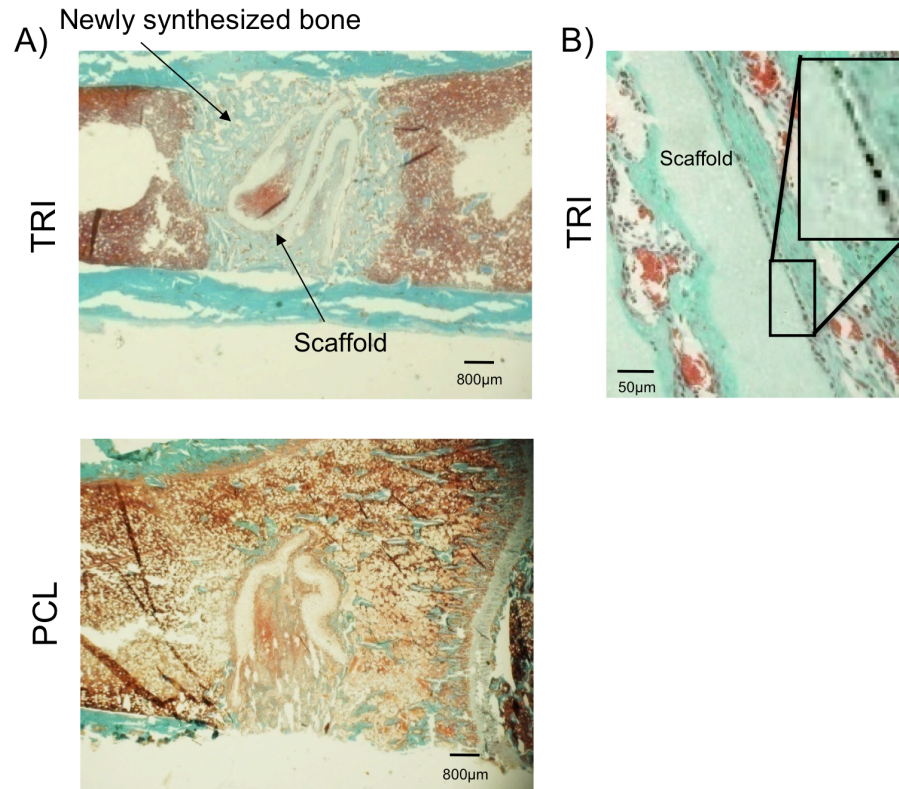


Figure 1. PCL/col/HA scaffolds (“TRI”), or scaffolds composed of 100% PCL, were implanted into a cortical defect in a rat tibia for seven days. A) Low magnification images of transverse sections stained with Goldner’s Trichrome show new bone stained light blue-green, soft tissue stained red, and cell nuclei stained black. TRI scaffolds supported robust new bone formation throughout the defect (A), especially in direct contact with the scaffold surface (B). However, endogenous cells can be seen lining the edge of scaffolds (B inset). The small pore sizes of electrospun TRI scaffolds hinder cell infiltration and tissue-ingrowth.

Note: From “Increasing the Pore Sizes of Bone-Mimetic Electrospun Scaffolds comprised of polycaprolactone , collagen I and hydroxyapatite to enhance cell infiltration” by M.C. Phipps, W.C. Clem, J.M. Grunda, G.A. Clines, S. L. Bellis, 2011, *Biomaterials*, 33, p. 526. Copyright 2012 by Elsevier et al. Reprinted with permission.

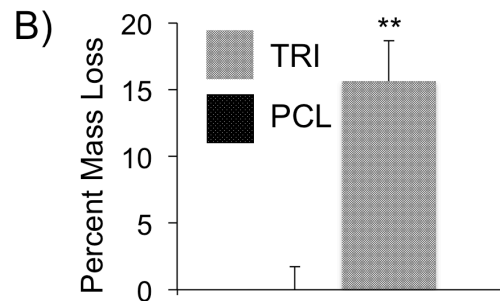
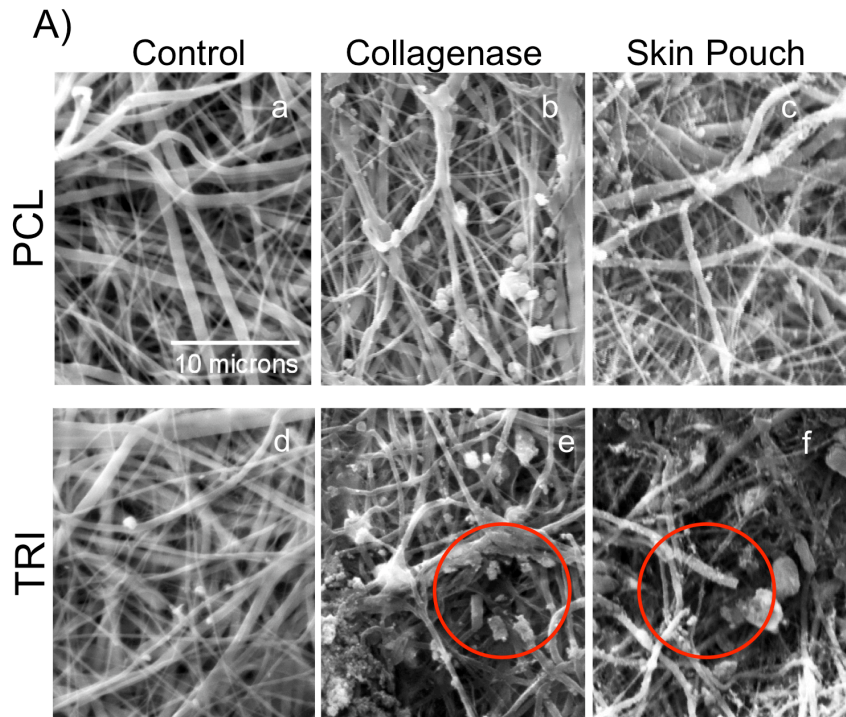


Figure 2. SEM images of selective cleavage of collagen I present in TRI scaffolds. A) Treatment with collagenase solution *in vitro* (b, e) or exposure to endogenous collagenases in a rat subcutaneous skin pouch (c, f) are able to cleave the collagen within fibers of TRI scaffolds creating larger pores (red circles), but have no effect on PCL scaffolds. B) Weighing the scaffolds before and after soaking in collagenase solution verified cleavage of collagen fibers in TRI scaffolds. An \*\* denotes  $p < .001$ .

Note: From “Increasing the Pore Sizes of Bone-Mimetic Electrospun Scaffolds comprised of polycaprolactone , collagen I and hydroxyapatite to enhance cell infiltration” by M.C. Phipps, W.C. Clem, J.M. Grunda, G.A. Clines, S. L. Bellis, 2011, *Biomaterials*, 33, p. 527. Copyright 2012 by Elsevier et al. Reprinted with permission.

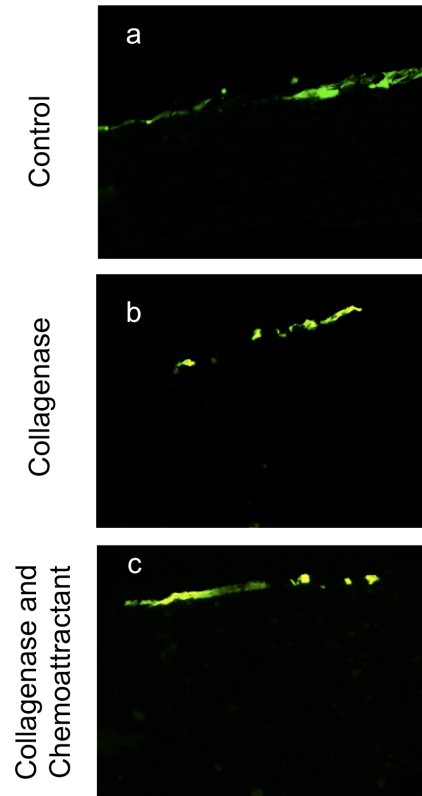


Figure 3. Pre-treating scaffolds with collagenase does not facilitate cell infiltration of MSCs *in vitro*. GFP-expressing MSCs were seeded onto TRI scaffolds previously treated with collagenase to create larger pores, or untreated scaffolds as a control. After two weeks, samples were fixed and sectioned to evaluate MSC infiltration into the scaffolds (a and b). Collagenase treatment did not facilitate significant cellular infiltration. In attempt to stimulate cellular infiltration, PDGF-BB, a known MSC chemoattractant, was added to the underside of scaffolds after collagenase treatment and prior to cell seeding. This was done to create a chemoattractive gradient through the scaffold. MSC infiltration remained minimal (c).

Note: From “Increasing the Pore Sizes of Bone-Mimetic Electrospun Scaffolds comprised of polycaprolactone , collagen I and hydroxyapatite to enhance cell infiltration” by M.C. Phipps, W.C. Clem, J.M. Grunda, G.A. Clines, S. L. Bellis, 2011, *Biomaterials*, 33, p. 528. Copyright 2012 by Elsevier et al. Reprinted with permission.



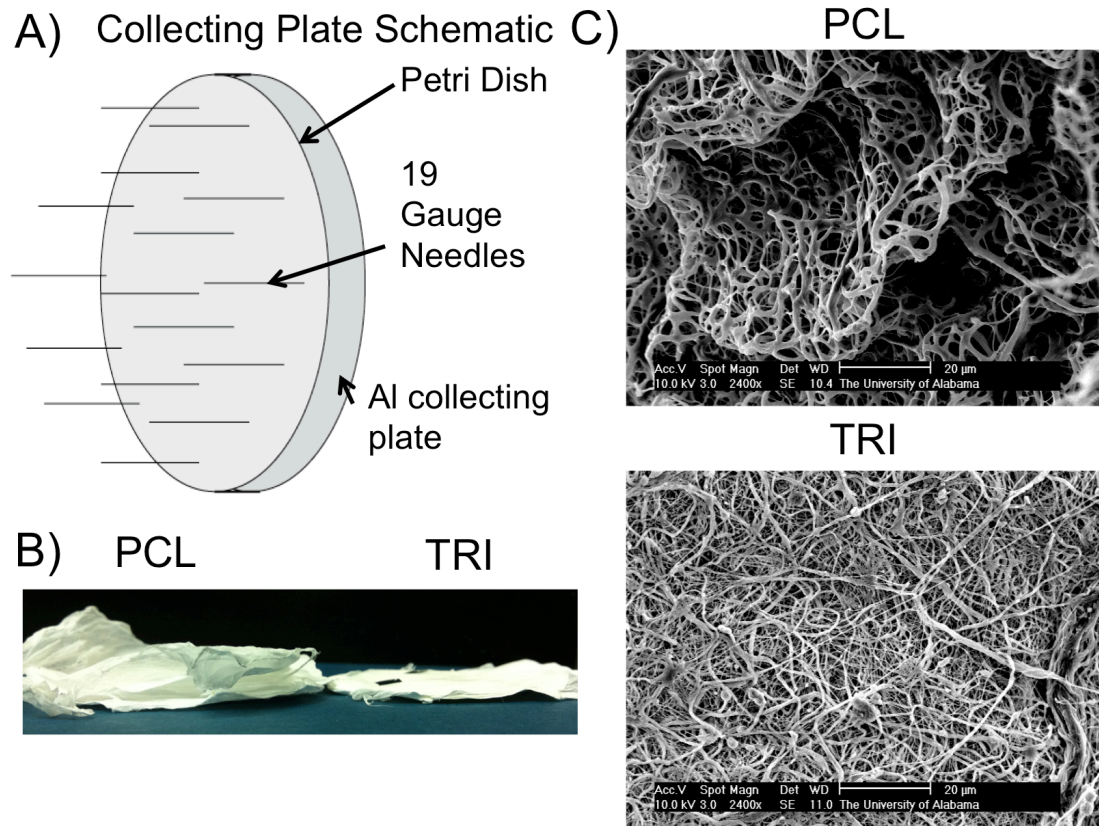


Figure 4. Decreasing the packing density of electrospun fibers. A unique collecting plate was used in order to decrease the packing density of electrospun fibers and therefore create larger pores (A). Although 100% PCL scaffolds formed in loosely packed layers (B) and possessed a favorable 3-dimensional architecture with deep channels (C), these results were not observed when TRI scaffolds were electrospun using the same collecting plate.

Note: From “Increasing the Pore Sizes of Bone-Mimetic Electrospun Scaffolds comprised of polycaprolactone , collagen I and hydroxyapatite to enhance cell infiltration” by M.C. Phipps, W.C. Clem, J.M. Grunda, G.A. Clines, S. L. Bellis, 2011, *Biomaterials*, 33, p. 529. Copyright 2012 by Elsevier et al. Reprinted with permission.

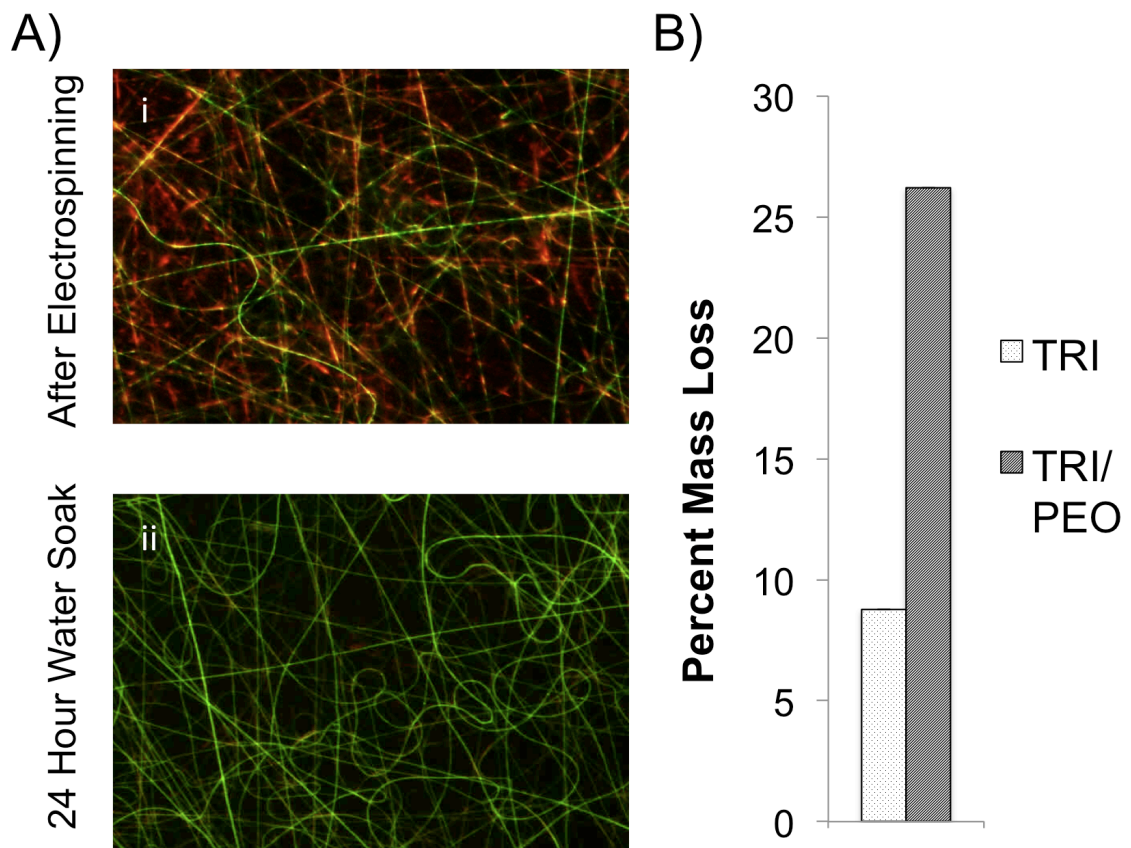


Figure 5. Removal of sacrificial electrospun fibers. A) As an alternative method to increase pore sizes, water-soluble fibers of PEO were incorporated into TRI scaffolds. Fluorescent dyes confirmed that separate fibers of PEO (Red) and TRI (Green) were intermixed in the scaffold (a). After washing scaffolds in water, PEO fibers were removed (b). B) Weighing the scaffolds before and after washing indicated removal of PEO fibers by mass loss.

Note: From “Increasing the Pore Sizes of Bone-Mimetic Electrospun Scaffolds comprised of polycaprolactone , collagen I and hydroxyapatite to enhance cell infiltration” by M.C. Phipps, W.C. Clem, J.M. Grunda, G.A. Clines, S. L. Bellis, 2011, *Biomaterials*, 33, p. 529. Copyright 2012 by Elsevier et al. Reprinted with permission.

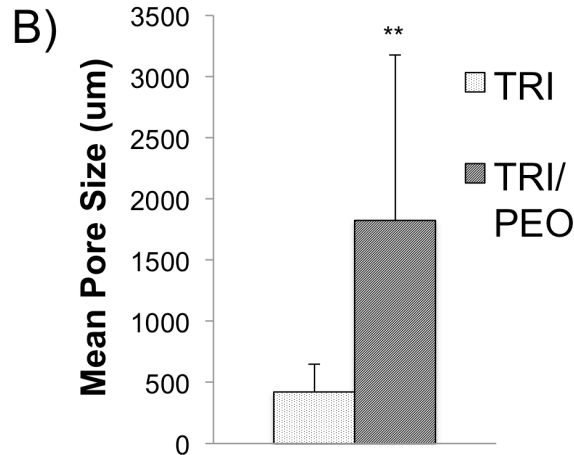
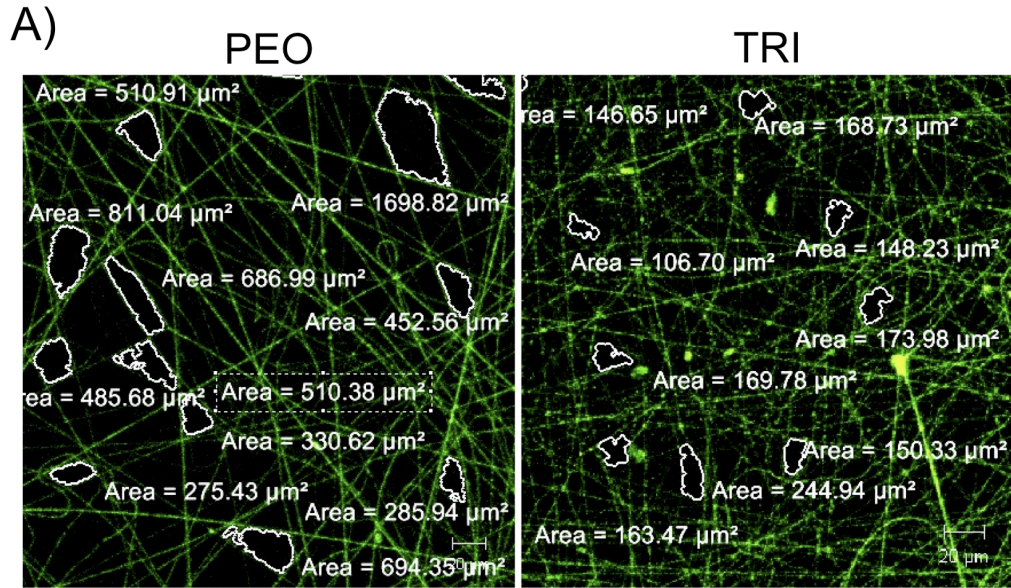


Figure 6. Mean pore size analysis of electrospun TRI and TRI/PEO scaffolds. A) Fluorescently stained TRI/PEO scaffolds (washed to remove PEO) or TRI scaffolds electrospun without PEO fibers were visualized using a Zeiss confocal microscope. The area of 25 pores manually selected at random were measured using the auto area detect feature of NIS-Elements software. B) The mean pore size of TRI/PEO scaffolds was significantly greater than TRI scaffolds. An \*\* denotes  $p < .0001$

Note: From “Increasing the Pore Sizes of Bone-Mimetic Electrospun Scaffolds comprised of polycaprolactone, collagen I and hydroxyapatite to enhance cell infiltration” by M.C. Phipps, W.C. Clem, J.M. Grunda, G.A. Clines, S. L. Bellis, 2011, *Biomaterials*, 33, p. 530. Copyright 2012 by Elsevier et al. Reprinted with permission.

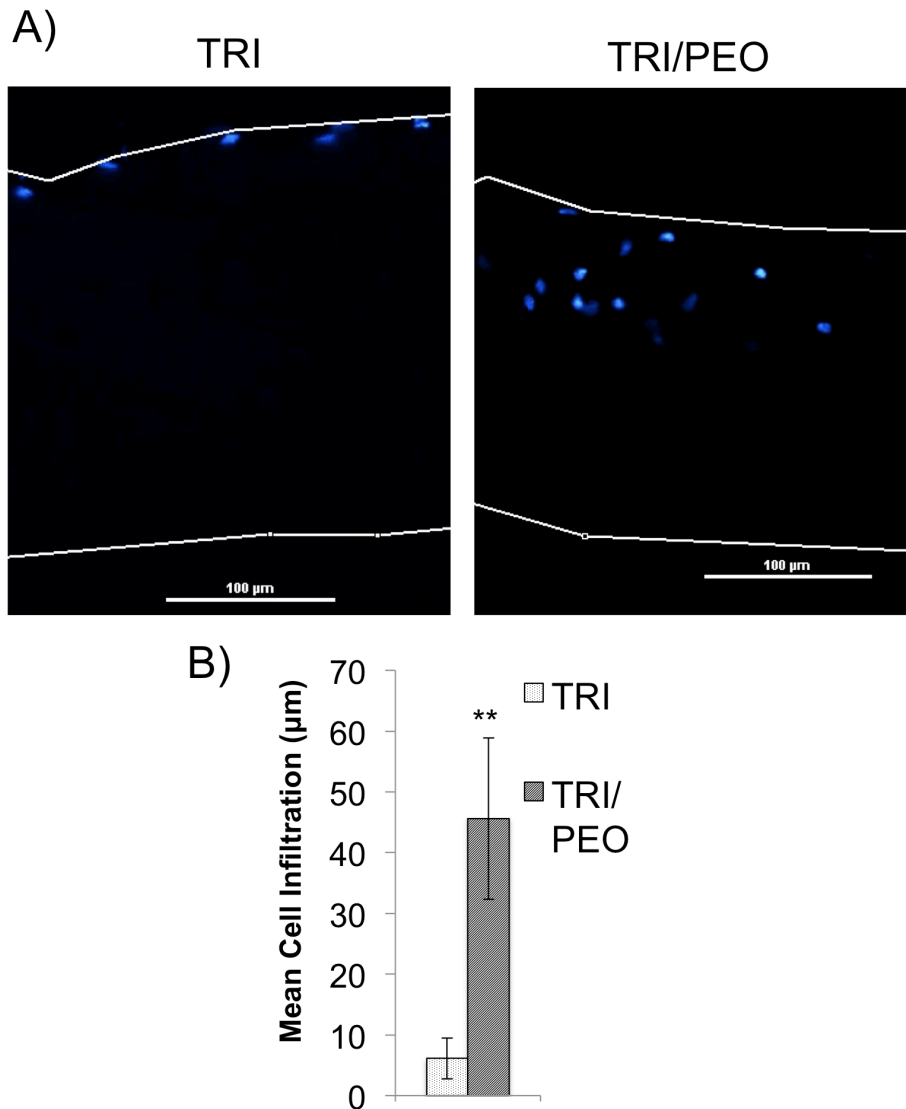


Figure 7. Electrospun scaffolds created with PEO fibers support cell infiltration of MSCs *in vitro*. After removal of PEO fibers from TRI/PEO scaffolds by washing, MSCs were seeded for one week. A) Scaffolds were sectioned and stained with DAPI to show cellular nuclei location. MSCs were able to infiltrate into the TRI/PEO scaffolds, but not TRI scaffolds, as seen by presence of nuclei within TRI/PEO scaffolds. B) Cell infiltration was quantified using a custom MatLab script. On average, MSCs seeded on TRI/PEO scaffolds migrated 45.59 $\mu\text{m}$  into the scaffold, significantly greater than infiltration on TRI scaffolds (6.13 $\mu\text{m}$ ). An \*\* denotes  $p < .0001$

Note: From “Increasing the Pore Sizes of Bone-Mimetic Electrospun Scaffolds comprised of polycaprolactone, collagen I and hydroxyapatite to enhance cell infiltration” by M.C. Phipps, W.C. Clem, J.M. Grunda, G.A. Clines, S. L. Bellis, 2011, *Biomaterials*, 33, p. 531. Copyright 2012 by Elsevier et al. Reprinted with permission.

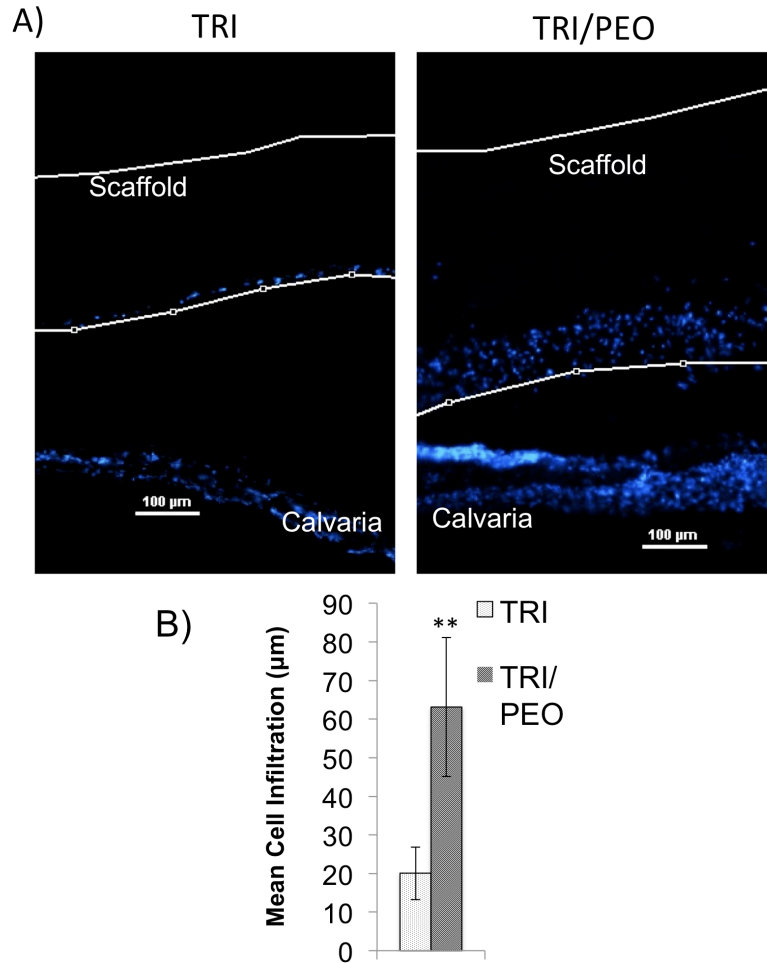


Figure 8. Electrospun scaffolds created with PEO fibers support infiltration of endogenous cells from calvarial organ cultures. After removal of PEO fibers from TRI/PEO scaffolds by washing, scaffolds were placed directly on top of excised calvaria from neonatal mice. After 8 days in culture, the scaffold/calvaria constructs were fixed and vertical sections were stained with DAPI to show cellular nuclei location (it should be noted that the apparent gap between the scaffold and the calvaria is an artifact introducing during processing and sectioning of the samples). A) Endogenous cells were observed within the TRI/PEO scaffolds, while remaining largely on the surface of TRI scaffolds. B) Cell infiltration was quantified using a custom MatLab script. On average, endogenous bone cells migrated 63.15μm into TRI/PEO scaffolds, which was significantly greater than infiltration levels observed on TRI scaffolds (20.06μm). An \*\* denotes  $p < .0001$

Note: From “Increasing the Pore Sizes of Bone-Mimetic Electrospun Scaffolds comprised of polycaprolactone , collagen I and hydroxyapatite to enhance cell infiltration” by M.C. Phipps, W.C. Clem, J.M. Grunda, G.A. Clines, S. L. Bellis, 2011, *Biomaterials*, 33, p. 532. Copyright 2012 by Elsevier et al. Reprinted with permission.

DELIVERY OF PLATELET-DERIVED GROWTH FACTOR AS A CHEMOTACTIC  
FACTOR FOR MESENCHYMAL STEM CELLS BY BONE-MIMETIC  
ELECTROSPUN SCAFFOLDS

by

MATTHEW C. PHIPPS, YUANYUAN XU, AND SUSAN L. BELLIS

*PLoS ONE*, 2012 July; 7(7) e40831

Copyright  
2012  
by  
Phipps et al.

Format adapted for dissertation

## Abstract

The recruitment of mesenchymal stem cells (MSCs) is a vital step in the bone healing process, and hence the functionalization of osteogenic biomaterials with chemotactic factors constitutes an important effort in the tissue engineering field. Previously we determined that bone-mimetic electrospun scaffolds composed of polycaprolactone, collagen I and nanohydroxyapatite (PCL/col/HA) supported greater MSC adhesion, proliferation and activation of integrin-related signaling cascades than scaffolds composed of PCL or collagen I alone. In the current study we investigated the capacity of bone-mimetic scaffolds to serve as carriers for delivery of an MSC chemotactic factor. In initial studies, we compared MSC chemotaxis toward a variety of molecules including PDGF-AB, PDGF-BB, BMP2, and a mixture of the chemokines SDF-1 $\alpha$ , CXCL16, MIP-1 $\alpha$ , MIP-1 $\beta$ , and RANTES. Transwell migration assays indicated that, of these factors, PDGF-BB was the most effective in stimulating MSC migration. We next evaluated the capacity of PCL/col/HA scaffolds, as compared with PCL scaffolds, to adsorb and release PDGF-BB. We found that significantly more PDGF-BB was adsorbed to, and subsequently released from, PCL/col/HA scaffolds, with sustained release extending over an 8-week interval. The PDGF-BB released was chemotactically active in transwell migration assays, indicating that bioactivity was not diminished by adsorption to the biomaterial. Complementing these studies, we developed a new type of migration assay in which the PDGF-BB-coated bone-mimetic substrates were placed 1.5 cm away from the cell migration front. These experiments confirmed the ability of PDGF-BB-coated PCL/col/HA scaffolds to induce significant MSC chemotaxis under more stringent conditions than standard types of migration assays. Our collective results substantiate the efficacy of

PDGF-BB in stimulating MSC recruitment, and further show that the incorporation of native bone molecules, collagen I and nanoHA, into electrospun scaffolds not only enhances MSC adhesion and proliferation, but also increases the amount of PDGF-BB that can be delivered from scaffolds.

## Introduction

Bone has a dramatic capacity for regeneration following injury, and undergoes constant remodeling during homeostasis. This remarkable regenerative process is initiated by recruitment and differentiation of progenitor cells of mesenchymal origin along with inflammatory cells in order to first form granulation tissue, followed by hyaline cartilage, endochondral ossification and finally the restoration of normal bone structure during remodeling. These activities are coordinated and controlled by an intricate system of growth factors and cytokines/chemokines, such as TGF- $\beta$ , PDGF, FGF-2, and BMP-2 [1].

Despite bone's regenerative capability, certain types of bone injuries or pathologies are not able to heal properly, and require intervention in the form of either bone grafts or engineered biomaterials that induce osteoregeneration. Biomaterials designed for bone repair typically serve as a carrier system for delivery of ex vivo-expanded mesenchymal stem cells (MSCs), or alternatively provide a supportive matrix for the attachment and growth of endogenous MSCs that migrate into the implant site. MSCs are multipotent cells within bone marrow (and other tissues) and these cells are a prime candidate for cell-based therapies involving regeneration of bone and other connective tissues [2]. Nonetheless, the inability to efficiently target these cells to selected tissues is a barrier to implementation of MSC therapy [3]. The identification of chemotactic factors for MSCs



is crucial in this regard, however there is less known concerning optimal chemoattractants for MSCs when compared with other cell types such as vascular or immune cells.

Platelet-Derived Growth Factor (PDGF) is a polypeptide growth factor that is secreted from cytokine-laden granules of aggregated platelets early after tissue injury [4, 5]. The active form of PDGF, consisting of either a homo- or heterodimer, functions by binding to cell-surface receptors on most cells of mesenchymal origin [6, 7], and participates in the development and remodeling of multiple tissue types, including bone [6]. The potent stimulatory effects of PDGF as a chemoattractant [8, 9] and a mitogen [10, 11], along with its ability to promote angiogenesis [12, 13], position it as a key regulatory molecule in tissue repair. PDGF has been studied in a variety of preclinical models for safety [14, 15] and tissue regeneration as well as clinical trials in periodontal and orthopedic patients [13, 16-18]. These combined studies have confirmed the effectiveness of PDGF in the repair of musculoskeletal tissue defects. However, the specific molecular mechanisms by which PDGF regulates the activity of multiple cell types to control tissue development require further elucidation. Much of the research in this area has focused on the role of PDGF in controlling vascularization of the nascent tissue forming within the wound site [19].

Despite its potency, the half-life of PDGF within blood is only a few minutes [20], indicating that a sustained local delivery of the growth factor will be critical to achieve clinical success. To date, PDGF has been utilized mostly with various carriers in animal models or clinical investigations to overcome the limitation of the short half-life. Examples of previous delivery strategies include: 1) encapsulating PDGF in porous scaffolds or microspheres [21-25], 2) a heparin-controlled delivery system [26], 3) modification of

PDGF with a collagen-binding motif for coupling to collagen carriers [27], and 4) chemical cross-linking of PDGF to demineralized bone matrix [28]. All of these approaches were successful to some degree in extending the PDGF release profile.

In the current study we tested whether delivery of PDGF from bone-mimetic electrospun scaffolds would be effective in stimulating MSC chemotaxis. Electrospinning is a promising and technically-straightforward approach for generating materials that have a porous, nanofibrous architecture similar to native extracellular matrix [29-33], and this method also allows synthesis of composite substrates incorporating native matrix molecules. Previously we reported that bone-mimetic electrospun scaffolds consisting of blended nanofibers of PCL and collagen I, with embedded nanoparticles of HA, supported greater MSC attachment, survival, proliferation and activation of integrin-related signaling cascades than scaffolds composed of either PCL or collagen I alone [34]. In addition, bone-mimetic scaffolds adsorbed increased amounts of the integrin-binding cell adhesive proteins, fibronectin and vitronectin, from serum, or following implantation into rat tibiae [34]. These results highlighted the benefit of blending the favorable mechanical properties of PCL with the biochemical cues provided by collagen I and nanoHA. We now show that electrospun scaffolds incorporating collagen I and nanoHA, as compared with scaffolds composed of PCL alone, adsorb and release greater quantities of PDGF-BB, leading to enhanced MSC chemotaxis.

## Materials and Methods

### *GFP-MSCs*

GFP-expressing human MSCs were obtained from Texas A&M University Health Sciences Center, Institute for Regenerative Medicine. The MSCs were analyzed extensively by the provider institute for cell growth characteristics, osteoblast, adipocyte, and chondrocyte lineage differentiation, and also selected surface markers using flow cytometry. Cells were cultured in  $\alpha$ MEM with 2mM L-Glutamine, and 16.5% Fetal Bovine Serum, as recommended by the provider. Some experiments used reduced serum media, as noted. Cells used in all experiments were passages 2-7.

### *PCL/col/HA Scaffold Preparation*

PCL/col/HA or 100% PCL scaffolds were prepared as described previously [34, 35]. Briefly, the tri-component scaffolds were electrospun from a 2 mL mixture of polycaprolactone (PCL, MW 100,000), type-I collagen from calf skin (col), and hydroxyapatite (HA) nanoparticles (20-70 nm in size) in a total of 0.262 grams with a dry weight ratio of 50:30:20, respectively, in hexafluoroisopropanol solvent (HFP) (Sigma-Aldrich, St Louis, MO). The polymer solution was filled in a syringe with a 27-gauge needle, placed in a syringe pump, and the solution was electrospun onto an aluminum foil-grounded target at rate of 2 mL/h under approximately 16-22 KV voltage (Gamma High Voltage Research, Ormond Beach, FL). After electrospinning, residual HFP solvent in the scaffolds was removed by placing scaffolds at room temperature in a vacuumed desiccator for 72 h. PCL, Col, and HA were purchased from Scientific Polymers (Ontario, NY), MP Biomedicals (Solon, OH), and Berkeley Advanced Biomaterials (Berkeley, CA), respectively.

### *Adsorption and Release of PDGF-BB from Scaffolds*

Purified recombinant human PDGF-BB (1.5 mg, Leinco Technologies Inc., St. Louis, MO) was passively absorbed to PCL/col/HA or PCL scaffolds (*diameter*=11 mm, *area* = 95 mm<sup>2</sup>) in 300 mL of PBS at 4°C for 24 h. The amount of PDGF-BB remaining in the solution after incubation with scaffolds (representing the unbound fraction) was measured using an ELISA kit (R&D Systems, Minneapolis, MN). PDGF-BB adsorption by the scaffolds was quantified by subtracting the unbound PDGF-BB from the total amount of protein initially added to the scaffolds (1.5 µg).

To measure release, scaffolds were coated with PDGF-BB as above, rinsed briefly with PBS, and then placed in 5 mL sterile plastic tubes containing 1mL of PBS, pH 7.2, containing 1% BSA. The scaffolds were incubated at 37°C with gentle agitation for 8 weeks. Samples of the supernatant were collected at varying time intervals, and the amount of released PDGF-BB in solution was quantified by ELISA. The release was calculated and expressed as the ng amount of PDGF-BB at a given time point.

### *Boyden Chamber Migration Assays*

Chemotaxis of human GFP-MSCs was performed in Boyden chamber units with transwell inserts (Corning Inc. Corning, NY), 6.5 mm in diameter with 8 mm pore size filters. To facilitate initial cell attachment, the upper side of the insert filter was pre-coated for 2 h at 37°C with the following solution: a minimum essential medium (αMEM, Invitrogen, Grand Island, NY) containing 1% fetal bovine serum (FBS) and 0.25% (w/v) bovine serum albumin (BSA). Serum-free αMEM with 0.25% BSA (hereafter designated as “assay media”) was placed into the lower wells of the Boyden chambers. For some trials, chemotactic factors were added to the assay media in the lower chambers; these

included PDGF-AB, and PDGF-BB, BMP-2, and a chemokine cocktail containing SDF-1a CXCL16, MIP-1a, MIP-1b, and RANTES (R&D Systems, Minneapolis, MN). After setting up the chambers with or without chemotactic factors, GFP-MSCs ( $4 \times 10^4$ ) were seeded into the upper chambers and allowed to migrate at 37°C for 20 h. The cells on the upper face of the filter (non-migrating cells) were then removed by wiping 3 times with a wet cotton wool swab. Transmigration of GFP-MSCs to the bottom surface of the filter was visualized by a fluorescent stereomicroscope Leica MZ16F (Leica Microsystems, Bullerlo Grove, IL). Quantification of migrated cells was performed by trypsinizing cells on the underside, and lysing cells in 1% Triton X-100 in 50 mM Tris-HCl buffer, pH 7.5 (“lysis buffer”). Fluorescence of the lysates, due to released GFP, was measured by fluorometry. Data shown in Figure 1A and B are representative of three independent runs, each performed in duplicate.

In addition to experiments performed with purified recombinant chemotactic factors, we monitored chemotaxis toward PDGF-BB that had been released from scaffolds. Specifically, the conditioned media was collected from PDGF-BB-coated scaffolds that had been incubated in serum-free  $\alpha$ MEM for 72 hr at 37°C with agitation. This solution was then placed in the lower chamber of a Boyden chamber, and migration of GFP-MSCs toward the PDGF-BB-containing conditioned media was monitored by measuring the fluorescence of cell lysates as described above. We also determined the concentration of released PDGF-BB within the media by ELISA. Purified PDGF-BB (10 ng/ml) and serum-free media were used as positive and negative controls, respectively. Three independent runs were performed in duplicate. Analysis of variance was carried out with StatPlus:mac LE (AnalystSoft Inc., [www.analystsoft.com](http://www.analystsoft.com)) with Tukey’s HSD post-hoc tests used to

make pair-wise comparisons between groups. A confidence level of at least 95% ( $p < .05$ ) was considered significant.

To validate the use of cell lysate fluorescence as a reporter for relative cell number, a standard curve was generated. GFP-MSCs were detached from tissue culture flasks by trypsinization and then counted with a hemocytometer. A defined number of cells was placed into an eppendorf tube and centrifuged. The supernatant was removed and the cell pellet resuspended in lysis buffer for 15 minutes at room temperature. Solution fluorescence of the released GFP was measured by fluorometry (Fig 1). Seven independent experiments were performed in duplicate with cells from passages 2-7. Linear regression and the coefficient of determination were determined using StatPlus:mac LE.

#### *GFP-MSC Proliferation on PDGF-BB Coated PCL/col/HA Scaffolds*

PCL/col/HA scaffolds were coated with either 0, 0.15, 0.3, or 1.5  $\mu\text{g}$  of PDGF-BB in 300  $\mu\text{L}$  of PBS at 4°C for 24 h. Scaffolds were washed in PBS prior to being seeded with  $4 \times 10^3$  GFP-MSCs in 500  $\mu\text{L}$  of reduced serum media (5% FBS). After 1 or 4 days of culture, cells were trypsinized from the scaffolds and then lysed in 1% Triton X-100 in 50 mM Tris-HCl buffer, pH 7.5. Solution fluorescence of the released GFP was measured by fluorometry. Three independent experiments were performed in duplicate.

#### *Modified MSC Migration Assay*

GFP-MSCs were seeded at  $8 \times 10^4$  cells/well in 8-well rectangular tissue culture plates (Nunc/Fisher Scientific, Pittsburg, PA), and allowed to establish confluence. A central line was then drawn horizontally across the wells (on the underside of the dish), and the cells in the upper half of each well (above the line) were removed using a cell scraper. After removal of the cells, a scaffold was placed into the cell free side of the

well at a distance 1.5 cm from the cell front created by the cell scraper. Specifically, scaffolds were pre-coated with or without 1.5 mg PDGF-BB for 24 hours, and then one scaffold per well was placed on a steel wire grid to suspend the scaffold in the media. The cultures containing scaffolds and GFP-MSCs were incubated at 37°C without further disturbance, which allowed the adsorbed PDGF-BB to release and diffuse through the media towards the cell front and stimulate migration. After 72 h of culture, cells were fixed, stained with DAPI, and migration was examined and imaged microscopically by using a fluorescent stereomicroscope Leica MZ16F.

To quantify cell migration, a total of 24 images were analyzed per sample (3 independent experiments performed in duplicate for a total of 6 wells per sample, 4 images per well). A custom MATLAB script was created to quantify the number and location of cells migrated across the cell front towards the scaffold. The script calculated the location of each cell nuclei that had migrated across the line created originally when manually removing cells. Cell number was analyzed using an unpaired Student's t-test parametric analysis and analysis of variance for cell migration distances was carried out with Stat-Plus:mac LE with Tukey's HSD post-hoc tests used to make pair-wise comparisons between groups. A confidence level of at least 95% ( $p < .05$ ) was considered significant.

## Results and Discussion

### *PDGF-BB is a Potent Chemotactic Factor for MSCs.*

The migration capacity of MSCs is influenced by a large range of growth factors, cytokines, and chemokines [8, 36, 37]. As a first step toward identifying an optimal chemotactic agent for delivery on bone-mimetic scaffolds, we used Boyden chamber assays to compare MSC migration in response to PDGF-AB, PDGF-BB, BMP2, or a chemokine

mixture containing SDF-1a, CXCL16, MIP-1a, MIP-1b and RANTES. Chemoattractants, or serum-free media as a negative control, were added to the lower wells of transwell chambers, and GFP-expressing human MSCs were seeded in the upper chamber. After a 20-hr incubation, migrated cells on the underside of the filter were lysed and solution fluorescence was quantified. As shown in Fig 2A, the two PDGF isoforms, PDGF-AB and PDGF-BB, induced markedly greater chemotaxis than the chemokine mixture, and PDGF-BB also induced considerably more chemotaxis compared to BMP-2 (Fig 2B). Additionally, MSC response to PDGF-BB was observed in a dose-dependent manner with 10ng/ml having the greatest effect (Fig 2C). These results are consistent with a growing literature suggesting that PDGF-BB is superior to BMP-2 or CC/CXC chemokines in stimulating chemotactic activity of human bone marrow-derived MSCs. For example, Ozaki et al. tested 26 different growth factors/chemokines, and of these PDGF-BB had the greatest effect on MSC chemotaxis in multiple assays. Additionally, anti-PDGF-BB antibodies were able to inhibit PDGF-BB induced MSC migration [8]. RANTES, MIP-1a and MIP-1b (CC family) or SDF-1a and CXCL16 (CXC family) are chemokines involved in recruitment of immune cells to areas of inflammation and their receptors have also been shown to be expressed by human MSCs [37]. In our study, MSCs exhibited a low level of migratory response to the cocktail of the chemokines, although the response was dose-dependent. Given this weak response, the individual chemotactic profile of each chemokine in the cocktail was not further tested. Our results are in agreement with the findings of Ponte et al., who observed limited MSC chemotaxis toward RANTES, SDF-1, or macrophage-derived chemokine (MDC) [36]. Intriguingly, in this same study pre-treatment of MSCs with TNF $\alpha$  significantly enhanced MSC migra-



tion toward RANTES and SDF-1, which prompted these authors to suggest that these chemokines may play important roles in MSC homing to inflamed tissue sites. The osteoinductive protein, BMP-2, has also been suggested to serve as a chemotactic factor for selected cell types, including bone-associated cells. For example, BMP-2 stimulates chemotaxis of human osteoblasts, bone-marrow derived osteoblasts, and human osteosarcoma cell lines [38]. However, in the current study BMP2 failed to elicit chemotaxis of MSCs. This may be due to phenotypic differences between MSCs and more differentiated osteoblastic cell types, or other variables relating to isolation or propagation of distinct cell cultures.

#### *Bone-Mimetic Scaffolds Adsorb Greater Amounts of PDGF-BB as Compared with PCL Scaffolds*

Prior studies from our group indicated that the inclusion of collagen I and nanoHA in electrospun PCL scaffolds increased the capacity of scaffolds to adsorb the adhesive proteins, fibronectin and vitronectin [34]. To evaluate the propensity of the bone-mimetic scaffolds to adsorb PDGF-BB, PCL/col/HA or PCL scaffolds were coated with solution containing 1.5 mg of PDGF-BB. We found that  $1.37 \text{ mg} \pm 0.02$  and  $0.83 \text{ mg} \pm 0.08$  of the protein were adsorbed to PCL/col/HA and PCL scaffolds, respectively, representing 91% and 55% of the total PDGF-BB in the starting solutions (Fig 3A). These results confirm that bone-mimetic scaffolds have an increased capacity for adsorbing PDGF-BB, relative to scaffolds composed of PCL alone.

*PCL/col/HA scaffolds release greater amounts of PDGF-BB over an 8-week time interval.*

To evaluate release kinetics, PCL/col/HA or PCL scaffolds coated with PDGF-BB, washed briefly, and then resuspended in PBS. At varying time points, samples of the conditioned PBS were collected and monitored for PDGF-BB release using an ELISA assay (Fig 3B). It was found that a rapid release of PDGF-BB occurred within the first 4 days from the scaffolds, with greater amounts released from PCL/col/HA scaffolds, consistent with the greater loading capacity of this material. Continuous release was observed over an 8 week interval, with levels declining gradually. At every time point, a greater amount of PDGF-BB was released from PCL/col/HA, as compared with PCL scaffolds. These data suggest that PCL/col/HA scaffolds are suitable carriers for PDGF-BB.

*PDGF-BB released from scaffolds stimulates MSC chemotaxis*

The adsorption of proteins onto biomaterial carriers can influence protein activity [39]; for example, many studies have shown that proteins can become denatured, or adopt altered conformations, when adsorbed to certain material surfaces. Thus it was important to test whether the PDGF-BB released from electrospun scaffolds was active. To this end, PCL/col/HA scaffolds were coated with PDGF-BB, washed briefly and then resuspended in serum-free media. After a 72-hr incubation, the conditioned media was collected and placed in the lower well of a transwell chamber. GFP-labelled MSCs were seeded into the upper chamber and allowed to migrate for 20 hrs. In addition, MSC migration was monitored in transwell chambers containing serum-free media with 10 ng/ml purified PDGF-BB (positive control) or serum-free media alone (negative control). As shown in

Fig 4, PDGF-BB released from scaffolds induced a significant level of MSC migration compared to serum-free media, and no significant difference in MSC migration was observed between released and purified PDGF-BB (10ng/ml). ELISA assays of the PDGF-BB released from scaffolds revealed a concentration of  $12.465 \pm 3.557$  ng/ml in the conditioned media used for Boyden chamber assays. These combined results show that the amount of PDGF-BB released from bone-mimetic scaffolds is sufficient to promote MSC migration, and also that adsorption to the scaffolds, and subsequent release, does not inhibit the bioactivity of the PDGF-BB.

#### *Mitogenic effects of PDGF-BB*

In addition to its chemotactic function, PDGF-BB is a known mitogen for many cell types including MSCs [40, 41]. Thus, we investigated whether MSCs would exhibit greater proliferation when adherent to PDGF-BB-coated scaffolds. PCL/col/HA scaffolds were pre-coated with varying concentrations of PDGF-BB and then GFP-MSCs were seeded onto the scaffolds and incubated for four days. Relative cell number was quantified by lysing cells and measuring fluorescence. As seen in Fig 5, no significant difference was observed between uncoated and PDGF-BB-coated samples. It is possible that this lack of effect may be due to the presence of suboptimal PDGF-BB concentrations for inducing mitosis. Alternatively, PDGF-BB may not be able to stimulate MSC proliferation beyond the level stimulated by PCL/col/HA scaffolds themselves, as we have previously shown that PCL/col/HA scaffolds promote significantly greater MSC proliferation than PCL scaffolds. While further studies will be needed to determine the reason for the lack of mitogenic activity of PDGF-BB when coupled to scaffolds, these

results suggest that under the conditions used in this study, the principal benefit of adsorbed PDGF-BB is in its function as a chemotactic, rather than proliferative, factor.

*PDGF-BB released from scaffolds stimulates MSC chemotaxis in a stringent migration assay.*

Boyden chamber assays represent a standard method for evaluating chemotaxis, however *in vivo*, chemotactic gradients may need to act over greater distances, and rapid dilution of the factors can occur. Accordingly, we developed a more stringent chemotaxis assay to better model the capacity of PDGF-BB-modified bone-mimetic scaffolds to influence endogenous MSC recruitment. As diagrammed in Fig 6A, MSCs were grown to confluence in rectangular tissue culture wells; a defined region of the cell cultures was then removed using a cell-scraper to create a distinct cell front. A PDGF-BB-coated PCL/col/HA scaffold, suspended on a steel wire grid, was placed at one end of the well, at a distance of 1.5 cm from the cell front. As controls, cell cultures were set up with a PCL/col/HA scaffold lacking PDGF-BB. After a 72 h incubation, DAPI staining of cell nuclei and subsequent fluorescent imaging revealed robust MSC migration toward the PCL/col/HA scaffolds coated with PDGF-BB, but very little toward uncoated PCL/col/HA scaffolds, indicating that PDGF-BB released from scaffolds was effective in stimulating chemotaxis even when the source of PDGF-BB was 1.5 cm from the cell front (Fig 6B). In addition, imaging of GFP-labeled MSCs showed that cells in wells with PDGF-BB-coated scaffolds exhibited an altered morphology (Fig 6C), consistent with the known effects of PDGF on cell shape [9, 42, 43]. In order to quantify the number and location of cells migrating beyond the original cell front, a custom MATLAB script was created to decrease processing time and remove user bias. The script used an

algorithm to locate clusters of connected pixels to identify DAPI-stained cell nuclei, and then calculated the distance from the center of the nuclei to the original cell front. Results from this analysis showed that wells with PDGF-BB-coated scaffolds had a significant increase ( $p < .0001$ ) in the total number of MSCs migrating beyond the original cell front (Fig 6D). As an additional measure of chemotaxis, we subdivided the area above the cell front into defined regions, and calculated the percentage of cells within each of these regions relative to the total number of cells that had crossed the central line. These data showed that cells exposed to PDGF-BB-releasing scaffolds migrated significantly greater distances than cells incubated with uncoated bone-mimetic scaffolds (Fig 6E). Finally, it is noteworthy that the tissue culture wells that the scaffolds were placed into contained 4.5 mL of media, resulting in a substantial dilution of the released PDGF-BB. Thus, PDGF-BB released from PCL/col/HA scaffolds can induce MSC migration under conditions of greater dilution and distance than typically employed in standard Boyden chamber assays.

### Conclusion

In the present study we show that bone-mimetic electrospun scaffolds composed of PCL, collagen I and nanoparticulate HA have a greater capacity to adsorb and release PDGF-BB than scaffolds composed of PCL alone, and release is sustained for at least 8 weeks. Furthermore, the PDGF-BB released from the PCL/col/HA scaffolds is effective in stimulating chemotactic migration of MSCs under stringent assay conditions. These collective results suggest that electrospun scaffolds incorporating the bone matrix molecules, collagen I and HA, not only provide favorable matrices for MSC attachment and proliferation, but also serve to concentrate and deliver growth/chemotactic factors, much

like native extracellular matrices. In sum, PDGF-BB-modified bone-mimetic scaffolds represent promising materials for bone regenerative therapies.

### Acknowledgements

This study received support from NIH grants R01AR51539 (SLB), and T32EB004312 (MCP predoctoral fellowship). MCP is a student in the HHMI Med-to-Grad doctoral program.

### References

- [1] Lieberman JR, Daluiski A, Einhorn TA. The role of growth factors in the repair of bone. Biology and clinical applications. *J Bone Joint Surg Am.* 2002;84-A:1032-44.
- [2] Phinney DG, Prockop DJ. Concise review: mesenchymal stem/multipotent stromal cells: the state of transdifferentiation and modes of tissue repair--current views. *Stem Cells* 2007;25:2896-902.
- [3] Karp JM, Leng Teo GS. Mesenchymal stem cell homing: the devil is in the details. *Cell Stem Cell.* 2009;4:206-16.
- [4] Trippel SB. Growth factors as therapeutic agents. *Instr Course Lect.* 1997;46:473-6.
- [5] Hart CE, Bailey M, Curtis DA, Osborn S, Raines E, Ross R, et al. Purification of PDGF-AB and PDGF-BB from human platelet extracts and identification of all three PDGF dimers in human platelets. *Biochemistry.* 1990;29:166-72.
- [6] Andrae J, Gallini R, Betsholtz C. Role of platelet-derived growth factors in physiology and medicine. *Genes Dev.* 2008;22:1276-312.
- [7] Fujii H, Kitazawa R, Maeda S, Mizuno K, Kitazawa S. Expression of platelet-derived growth factor proteins and their receptor alpha and beta mRNAs during fracture healing in the normal mouse. *Histochem Cell Biol* 1999;112:131-8.
- [8] Ozaki Y, Nishimura M, Sekiya K, Suehiro F, Kanawa M, Nikawa H, et al. Comprehensive analysis of chemotactic factors for bone marrow mesenchymal stem cells. *Stem Cells Dev.* 2007;16:119-29.
- [9] Heldin CH, Westermark B. Mechanism of action and in vivo role of platelet-derived growth factor. *Physiol Rev.* 1999;79:1283-316.

- [10] Kelly JD, Raines EW, Ross R, Murray MJ. The B chain of PDGF alone is sufficient for mitogenesis. *EMBO J.* 1985;4:3399-405.
- [11] Gruber R, Karreth F, Frommlet F, Fischer MB, Watzek G. Platelets are mitogenic for periosteum-derived cells. *J Orthop Res.* 2003;21:941-8.
- [12] Homsy J, Daud AI. Spectrum of activity and mechanism of action of VEGF/PDGF inhibitors. *Cancer Control.* 2007;14:285-94.
- [13] Hollinger JO, Hart CE, Hirsch SN, Lynch S, Friedlaender GE. Recombinant human platelet-derived growth factor: biology and clinical applications. *J Bone Joint Surg Am.* 2008;90 Suppl 1:48-54.
- [14] Solchaga LA, Hee CK, Roach S, Snel LB. Safety of recombinant human platelet-derived growth factor-BB in Augment((R)) Bone Graft. *J Tissue Eng.* 2012;3:2041731412442668.
- [15] Young CS, Bradica G, Hart CE, Karunanidhi A, Street RM, Schutte L, et al. Preclinical Toxicology Studies of Recombinant Human Platelet-Derived Growth Factor-BB Either Alone or in Combination with Beta-Tricalcium Phosphate and Type I Collagen. *J Tissue Eng.* 2011;2010:246215.
- [16] Graham S, Leonidou A, Lester M, Heliotis M, Mantalaris A, Tsiridis E. Investigating the role of PDGF as a potential drug therapy in bone formation and fracture healing. *Expert Opin Investig Drugs.* 2009;18:1633-54.
- [17] Solchaga LA, Hee CK, Aguiar DJ, Ratliff J, Turner AS, Seim HB, 3rd, et al. Augment bone graft products compare favorably with autologous bone graft in an ovine model of lumbar interbody spine fusion. *Spine (Phila Pa 1976).* 2012;37:E461-7.
- [18] Javed F, Al-Askar M, Al-Rasheed A, Al-Hezaimi K. Significance of the platelet-derived growth factor in periodontal tissue regeneration. *Arch Oral Biol.* 2011;56:1476-84.
- [19] Distler JH, Hirth A, Kurowska-Stolarska M, Gay RE, Gay S, Distler O. Angiogenic and angiostatic factors in the molecular control of angiogenesis. *Q J Nucl Med.* 2003;47:149-61.
- [20] Bowen-Pope DF, Malpass TW, Foster DM, Ross R. Platelet-derived growth factor in vivo: levels, activity, and rate of clearance. *Blood.* 1984;64:458-69.
- [21] Park YJ, Ku Y, Chung CP, Lee SJ. Controlled release of platelet-derived growth factor from porous poly(L-lactide) membranes for guided tissue regeneration. *J Control Release.* 1998;51:201-11.

- [22] Chen RR, Silva EA, Yuen WW, Mooney DJ. Spatio-temporal VEGF and PDGF delivery patterns blood vessel formation and maturation. *Pharm Res.* 2007;24:258-64.
- [23] Jin Q, Wei G, Lin Z, Sugai JV, Lynch SE, Ma PX, et al. Nanofibrous scaffolds incorporating PDGF-BB microspheres induce chemokine expression and tissue neogenesis in vivo. *PLoS One.* 2008;3:e1729.
- [24] Wei G, Jin Q, Giannobile WV, Ma PX. Nano-fibrous scaffold for controlled delivery of recombinant human PDGF-BB. *J Control Release.* 2006;112:103-10.
- [25] Richardson TP, Peters MC, Ennett AB, Mooney DJ. Polymeric system for dual growth factor delivery. *Nat Biotechnol.* 2001;19:1029-34.
- [26] Liao IC, Wan AC, Yim EK, Leong KW. Controlled release from fibers of polyelectrolyte complexes. *J Control Release.* 2005;104:347-58.
- [27] Lin H, Chen B, Sun W, Zhao W, Zhao Y, Dai J. The effect of collagen-targeting platelet-derived growth factor on cellularization and vascularization of collagen scaffolds. *Biomaterials.* 2006;27:5708-14.
- [28] Chen L, He Z, Chen B, Zhao Y, Sun W, Xiao Z, et al. Direct chemical cross-linking of platelet-derived growth factor-BB to the demineralized bone matrix improves cellularization and vascularization. *Biomacromolecules.* 2009;10:3193-8.
- [29] Pham QP, Sharma U, Mikos AG. Electrospinning of polymeric nanofibers for tissue engineering applications: a review. *Tissue Eng* 2006;12:1197-211.
- [30] Di Martino A, Liverani L, Rainer A, Salvatore G, Trombetta M, Denaro V. Electrospun scaffolds for bone tissue engineering. *Musculoskelet Surg.* 2011;95:69-80.
- [31] Jang JH, Castano O, Kim HW. Electrospun materials as potential platforms for bone tissue engineering. *Adv Drug Deliv Rev.* 2009;61:1065-83.
- [32] Prabhakaran MP, Ghasemi-Mobarakeh L, Ramakrishna S. Electrospun composite nanofibers for tissue regeneration. *J Nanosci Nanotechnol.* 2011;11:3039-57.
- [33] Holzwarth JM, Ma PX. Biomimetic nanofibrous scaffolds for bone tissue engineering. *Biomaterials.* 2011;32:9622-9.
- [34] Phipps MC, Clem WC, Catledge SA, Xu Y, Hennessy KM, Thomas V, et al. Mesenchymal stem cell responses to bone-mimetic electrospun matrices composed of polycaprolactone, collagen I and nanoparticulate hydroxyapatite. *PLoS One.* 2011;6:e16813.



- [35] Phipps MC, Clem WC, Grunda JM, Clines GA, Bellis SL. Increasing the pore sizes of bone-mimetic electrospun scaffolds comprised of polycaprolactone, collagen I and hydroxyapatite to enhance cell infiltration. *Biomaterials*. 2012;33:524-34.
- [36] Ponte AL, Marais E, Gallay N, Langonne A, Delorme B, Herault O, et al. The in vitro migration capacity of human bone marrow mesenchymal stem cells: comparison of chemokine and growth factor chemotactic activities. *Stem Cells*. 2007;25:1737-45.
- [37] Chamberlain G, Wright K, Rot A, Ashton B, Middleton J. Murine mesenchymal stem cells exhibit a restricted repertoire of functional chemokine receptors: comparison with human. *PLoS One*. 2008;3:e2934.
- [38] Lind M, Eriksen EF, Bunger C. Bone morphogenetic protein-2 but not bone morphogenetic protein-4 and -6 stimulates chemotactic migration of human osteoblasts, human marrow osteoblasts, and U2-OS cells. *Bone*. 1996;18:53-7.
- [39] Wilson CJ, Clegg RE, Leavesley DI, Percy MJ. Mediation of biomaterial-cell interactions by adsorbed proteins: a review. *Tissue Eng*. 2005;11:1-18.
- [40] Krattinger N, Applegate LA, Biver E, Pioletti DP, Caverzasio J. Regulation of proliferation and differentiation of human fetal bone cells. *Eur Cell Mater*. 2011;21:46-58.
- [41] Canalis E, Varghese S, McCarthy TL, Centrella M. Role of platelet derived growth factor in bone cell function. *Growth Regul*. 1992;2:151-5.
- [42] Betsholtz C, Johnsson A, Heldin CH, Westermark B. Efficient reversion of simian sarcoma virus-transformation and inhibition of growth factor-induced mitogenesis by suramin. *Proc Natl Acad Sci U S A*. 1986;83:6440-4.
- [43] Yang L, Lin C, Liu ZR. P68 RNA helicase mediates PDGF-induced epithelial mesenchymal transition by displacing Axin from beta-catenin. *Cell*. 2006;127:139-55.

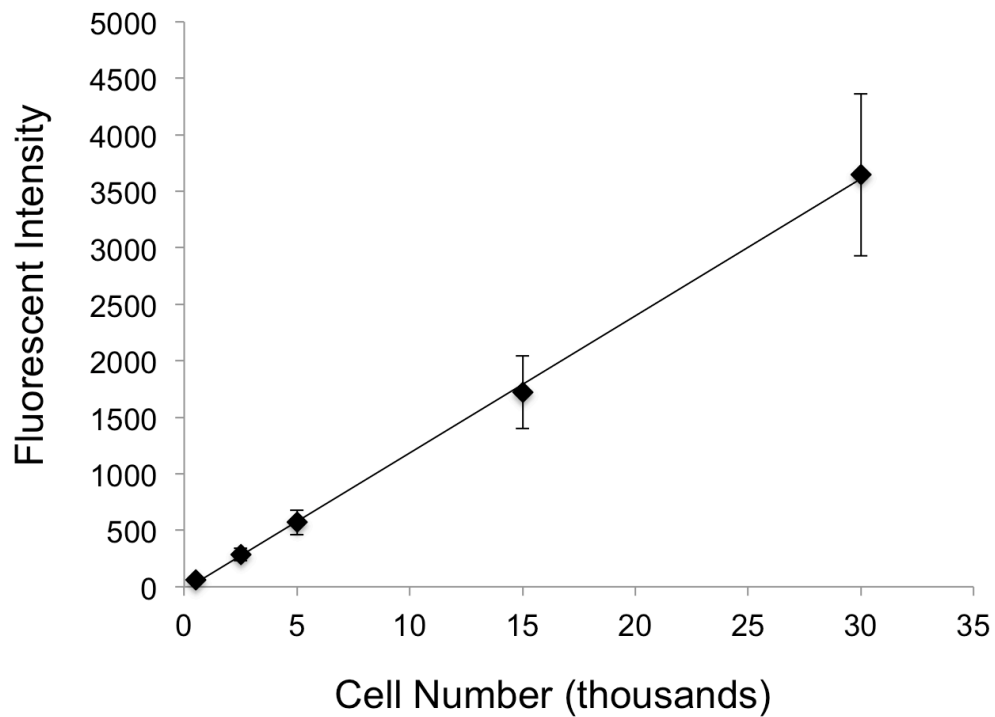


Figure 1. Standard curve of GFP fluorescent signal from lysed GFP-MSCs. GFP-MSCs were counted using a hemocytometer and set numbers of cells were spun down in a centrifuge. Cell pellets were lysed and solution fluorescence was measured by a fluorometer. The coefficient of determination for the linear regression was 0.999, showing a very strong linear correlation between GFP-MSC number and solution fluorescence.

Note: From “Delivery of Platelet-Derived Growth Factor as a Chemotactic Factor for Mesenchymal Stem Cells by Bone-Mimetic Electrospun Scaffolds” by M.C. Phipps, Y. Xu, J.M. Bellis, 2011, *PLoS ONE*, 7, e40831. Copyright 2012 by Phipps et al.

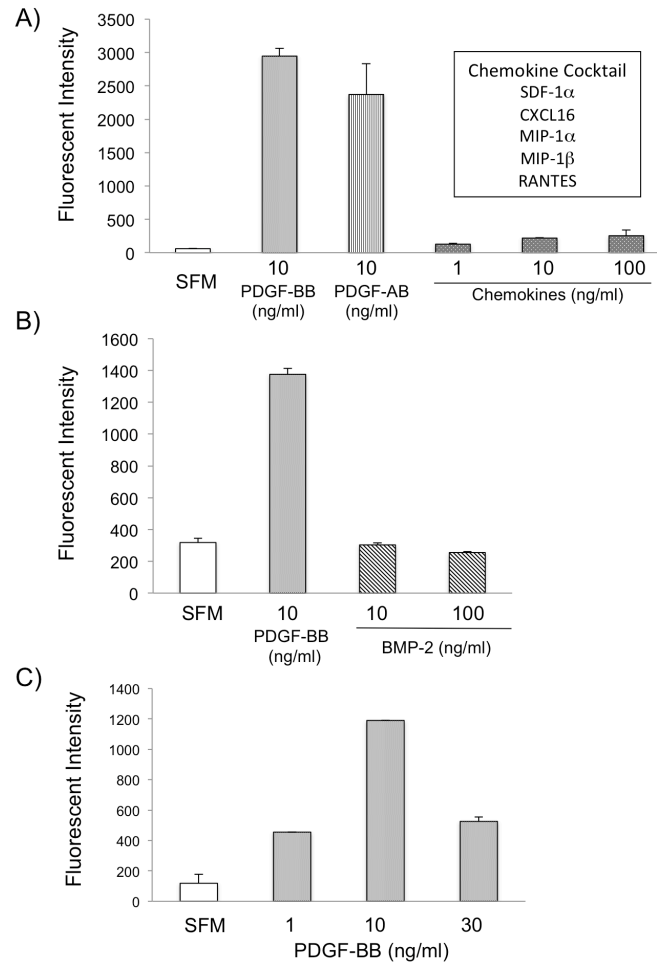


Figure 2. Chemotactic responses of MSCs. GFP-expressing MSCs ( $4 \times 10^4$ ) were seeded onto the top of transwell chambers, with various cytokines/chemokines placed in the bottom of the chambers, some wells contained serum-free media (SFM) as a negative control. After a 20 hr incubation at  $37^\circ\text{C}$ , the GFP-MSCs that had migrated across the transwell membrane were lysed and quantitated by fluorescence intensity of GFP. The following chemoattractants were evaluated: A) recombinant human PDGF-BB, PDGF-AB, or a mixture of SDF-1 $\alpha$ , CXCL16, MIP-1 $\alpha$ , MIP-1 $\beta$ , and RANTES, each at the indicated concentrations (ng/mL) (representative of 3 independent runs) B) PDGF-BB and BMP-2 (representative of 3 independent runs) and C), varying concentrations of PDGF-BB showing dose response.

Note: From "Delivery of Platelet-Derived Growth Factor as a Chemotactic Factor for Mesenchymal Stem Cells by Bone-Mimetic Electrospun Scaffolds" by M.C. Phipps, Y. Xu, J.M. Bellis, 2011, *PLoS ONE*, 7, e40831. Copyright 2012 by Phipps et al.

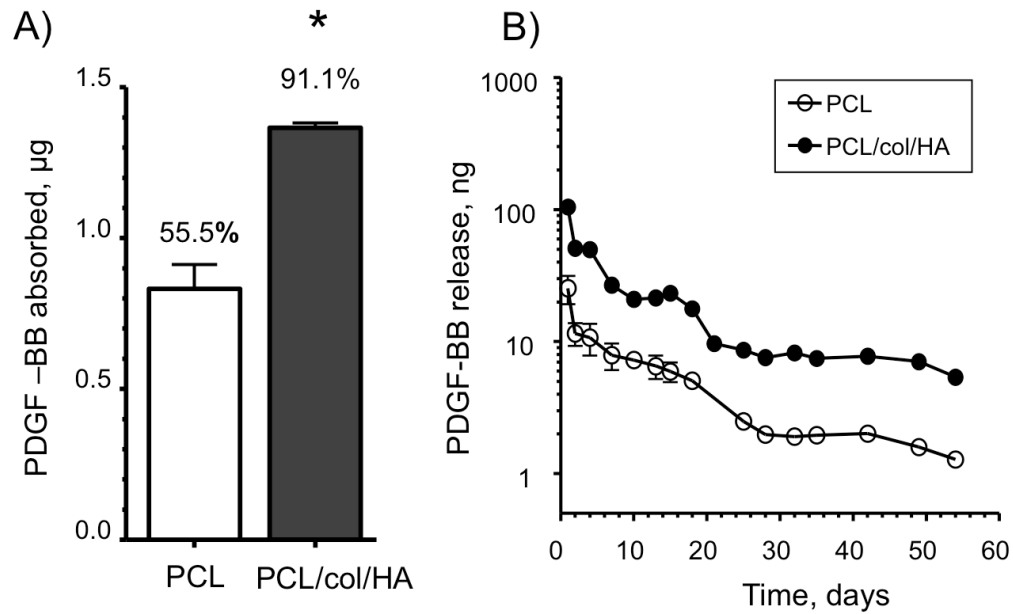


Figure 3. Adsorption and release of PDGF-BB from scaffolds. A) Scaffolds were incubated in PBS containing 1.5  $\mu\text{g}$  PDGF-BB for 24h at 4°C. ELISA assays were used to measure the unbound PDGF-BB in the supernatants. Adsorption of PDGF-BB to the scaffolds was determined by subtracting the unbound PDGF-BB from the 1.5 mg of PDGF-BB initially added. Data are from three independent experiments (\* denotes  $p < 0.01$ ). B) ELISAs were used to measure the amounts of PDGF-BB in conditioned PBS solution collected from the scaffolds at the indicated time intervals over a period of 8 weeks (for many of the data points, error bars are too small to be visualized).

Note: From “Delivery of Platelet-Derived Growth Factor as a Chemotactic Factor for Mesenchymal Stem Cells by Bone-Mimetic Electrospun Scaffolds” by M.C. Phipps, Y. Xu, J.M. Bellis, 2011, *PLoS ONE*, 7, e40831. Copyright 2012 by Phipps et al.

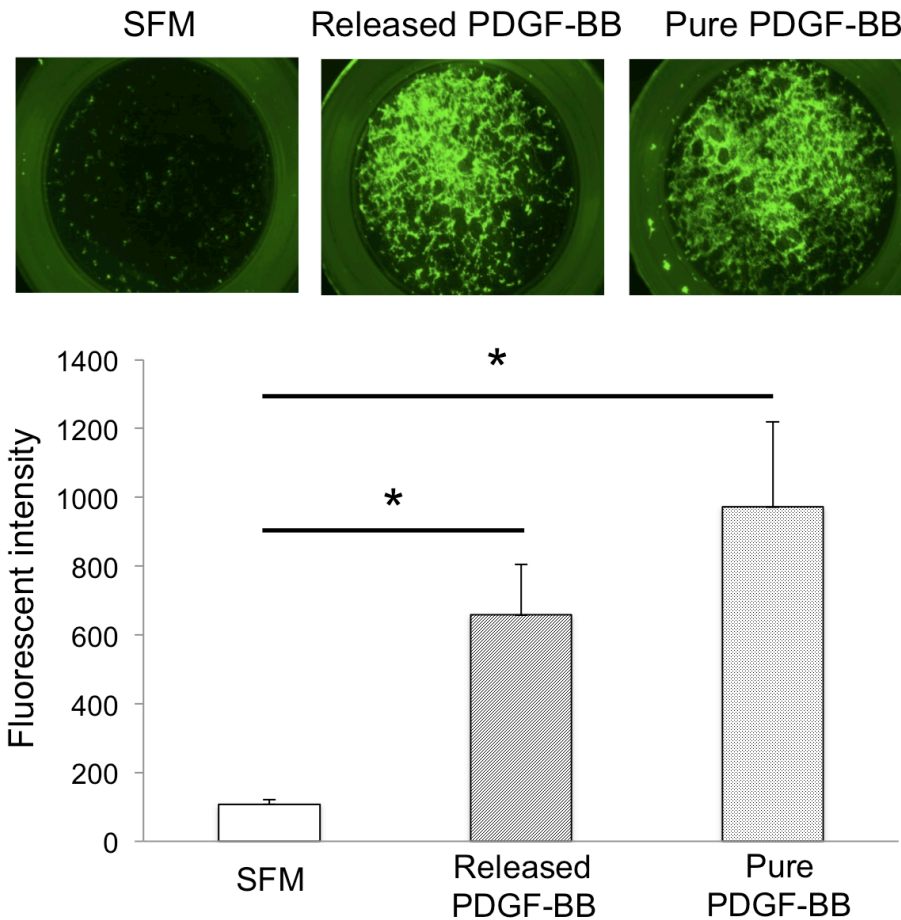


Figure 4. PDGF-BB released from PCL/col/HA scaffolds stimulates MSC chemotaxis. The lower wells of transwell chambers were filled with either purified PDGF-BB (10 ng/mL), serum-free medium (SFM) or PDGF-BB-containing conditioned media collected from PDGF-BB-coated PCL/col/HA scaffolds after 72 hrs. GFP-MSCs were seeded in the upper chambers and allowed to migrate for 20 hrs. After this interval, MSCs adherent to the underside of the transwells were visualized by fluorescent microscopy (top panel, representative images). In addition, MSC migration to the underside of the filter was quantified by lysing cells and measuring solution fluorescence (lower panel). Three independent experiments were performed for solution fluorescence. Analysis of variance with Tukey's HSD post-hoc was used to establish significance (\* denotes  $p < .01$ ).

Note: From "Delivery of Platelet-Derived Growth Factor as a Chemotactic Factor for Mesenchymal Stem Cells by Bone-Mimetic Electrospun Scaffolds" by M.C. Phipps, Y. Xu, J.M. Bellis, 2011, *PLoS ONE*, 7, e40831. Copyright 2012 by Phipps et al.

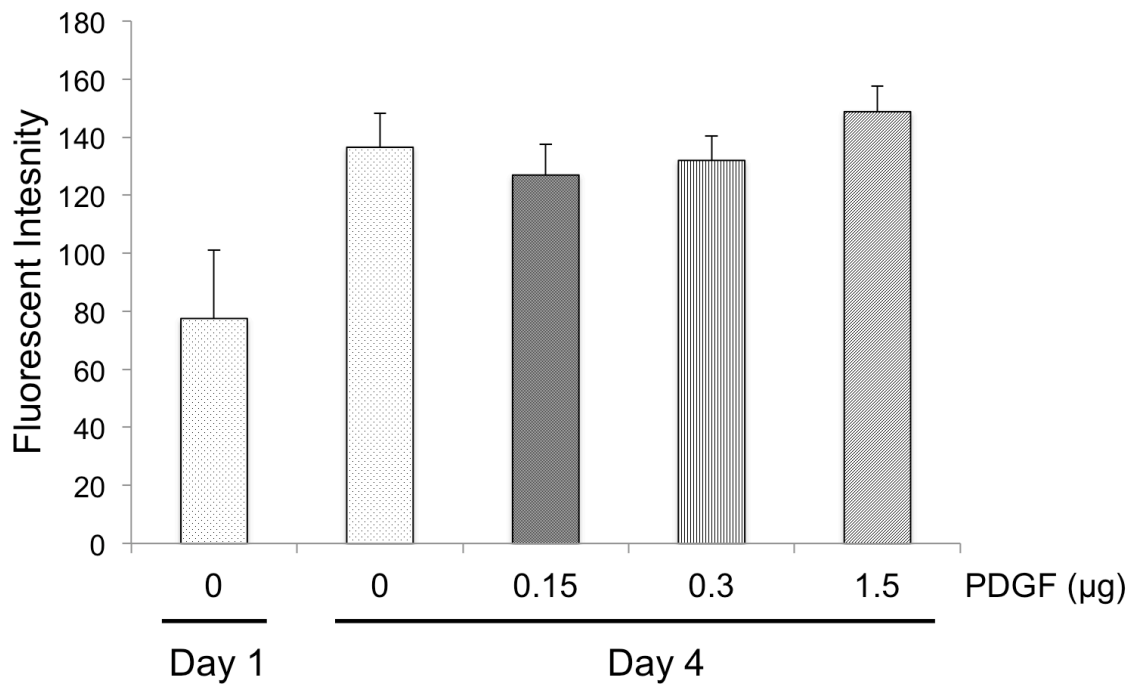


Figure 5. Mitogenic effects of PDGF-BB. GFP-MSCs ( $4 \times 10^3$ ) were seeded onto PCL/col/HA scaffolds and grown in reduced serum media (5% FBS). Cell number was measured at one day on PCL/col/HA scaffolds and four days for scaffolds pre-coated with varying concentrations of PDGF-BB. MSCs were lysed and solution fluorescence of the released GFP was measured.

Note: From “Delivery of Platelet-Derived Growth Factor as a Chemotactic Factor for Mesenchymal Stem Cells by Bone-Mimetic Electrospun Scaffolds” by M.C. Phipps, Y. Xu, J.M. Bellis, 2011, *PLoS ONE*, 7, e40831. Copyright 2012 by Phipps et al.

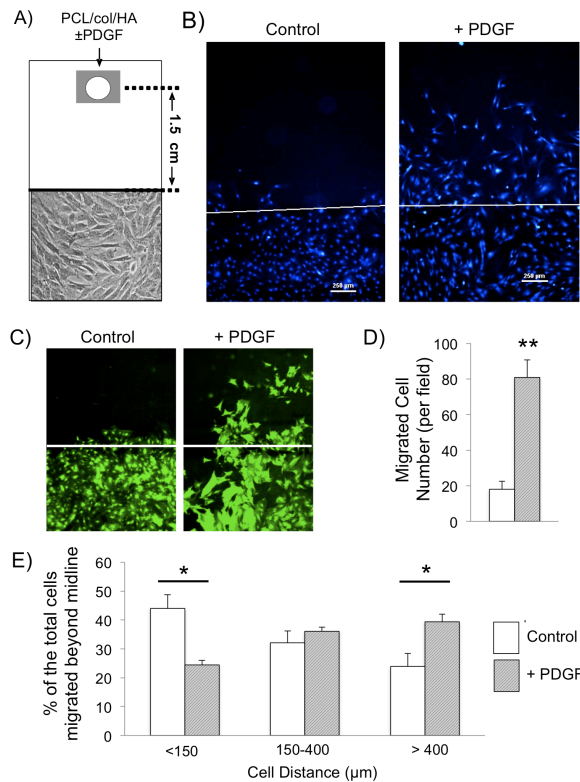


Figure 6. Released PDGF-BB induces chemotaxis of MSCs in a stringent migration assay. A) Schematic showing experimental set-up (not drawn to scale). GFP-MSCs were seeded in 8-well rectangular plates. After cell confluence was established, cells were completely removed from the top half of the well by scraping along a pre-drawn central line. Subsequently, a PDGF-BB-adsorbed PCL/col/HA/ scaffold, placed on a steel wire mesh, was placed 1.5 cm away from the cell front. As a control, some chambers were set up with PCL/col/HA scaffolds lacking PDGF-BB. B) After a 72 hr-incubation in the chambers described, MSCs were stained with DAPI and visualized by fluorescence microscopy. The original cell front created is denoted by a white line. C) GFP-images showing change in cell morphology of MSCs exposed to PDGF-BB. D) Significantly greater cell number was observed migrating toward PDGF-BB-coated scaffolds compared to uncoated. E) The images were further analyzed by counting the number of cells in three defined regions of distance beyond the original cell front. The distribution of cells in the PDGF-BB wells showed a greater percentage of the migrated cells were located in the region beyond 400 $\mu$ m. In comparison, the greatest percentage of migrated cells in the control wells were in the region below 150 $\mu$ m. A total of six samples were analyzed for each condition. An asterisk (\*) denotes significant differences observed with  $p < .01$ , (\*\*) denotes  $p < .0001$ .

Note: From “Delivery of Platelet-Derived Growth Factor as a Chemotactic Factor for Mesenchymal Stem Cells by Bone-Mimetic Electrospun Scaffolds” by M.C. Phipps, Y. Xu, J.M. Bellis, 2011, *PLoS ONE*, 7, e40831. Copyright 2012 by Phipps et al.

## CONCLUSIONS

To address the ever growing need for an off-the-shelf material capable of safely and effectively stimulating bone regeneration, a major goal in the field of tissue engineering is the development of advanced biomaterials that can support cellular responses consistent with new bone formation [19, 25]. Many currently available clinical products attempt to accomplish this goal using natural bone molecules, such as calcium phosphate minerals, collagen I, and osteoinductive factors. Studies have shown that calcium phosphate minerals, such as hydroxyapatite (HA), are highly osteoconductive [21, 121], and HA coatings on metal implants have been successfully used to improve implant osseointegration [122-124]. However, the resorption time of bulk HA is typically slower than new bone formation, leaving implanted particles at the defect site well beyond the necessary healing period [125]. Although this can be addressed through the combined use of HA with other calcium phosphates with faster resorption times, such as  $\beta$ -tricalcium phosphate (TCP) [125], these materials are limited in their use due to their lack of osteoinductive capability.

The other main constituent of natural bone, collagen I, has also been studied as a potential material for supporting new bone formation. Depending on processing techniques, collagen I can be used in a variety of forms, such as sponges [126, 127] and gels [128]. Although an important protein in cell adhesion, collagen I is rapidly degraded by proteases *in vivo*, and therefore it must be cross-linked [129] or incorporated into other materials with slower degradation rates in order to be effective [87]. Recently, collagen I



grafts have been investigated for their ability to deliver therapeutic agents, such as bone morphogenic protein 2 (BMP-2) [105, 130] and osteogenic protein 1 (OP-1) [131]. Collagen I is believed to be an effective drug delivery vehicle due to the known interactions between collagen I domains and other proteins, such as platelet-derived growth factor-BB (PDGF-BB) [132], allowing collagen I to sequester proteins from solution. However the release kinetics of these adsorbed proteins are often rapid *in vivo*, and this uncontrolled dissemination has the potential to trigger unwanted side effects and decrease the efficacy of the treatment. Accordingly, the primary focus of this dissertation has been to combine the natural bone molecules collagen I and HA in a nanofibrous matrix with tunable re-sorption times, thereby mimicking the composition of bone extracellular matrix, and potentially creating a more successful synthetic bone graft. Subsequently, we have evaluated the ability of our bone-mimetic matrix to deliver a chemotactic and mitogenic factor for mesenchymal stem cells, PDGF-BB.

In this study, the process of electrospinning was chosen to create our bone-mimetic scaffolds due to the relative ease in fabricating nanofibrous matrices with interconnected pores and a large surface to volume ratio, thereby mimicking the architecture of natural extracellular matrix [39, 133]. Electrospinning has received substantial recognition as a viable technique to create matrices specific for a variety of tissues, such as bone [134, 135], cartilage [136, 137], blood vessels [138, 139], and skin [140, 141]. A major advantage of the electrospinning technique is the ability to fabricate complex matrices, such as through guiding fiber alignment [142], the incorporation of natural cell ligands [143-145], and various methods for controlling the delivery of therapeutic agents [146, 147]. In order to investigate the use of electrospinning for our studies, our first aim

included the construction of an electrospinning apparatus in the laboratory. Numerous parameters, such as the flow rate of the solution, the voltage applied, and the distance between the needle and the collecting plate had to be optimized in order to create matrices with fiber diameters approximately 200nm in diameter, comparable in size to the collagen fiber bundles characteristic of natural bone matrix [41]. Additionally, using HA nanoparticles (20-50nm diameter) and sonication of the solution prior to electrospinning, we achieved a good dispersion of HA throughout the scaffold fibers, with minimal agglomeration [54]. The agglomeration of HA particles is a major problem in the field of electrospinning, and has led many investigators to passively coat the surface of their matrices with HA instead [49, 50, 148]. Successfully incorporating HA and collagen I into the electrospun solution creates a matrix entirely of bone-like fibers.

After optimizing the fabrication parameters, multiple scaffold formulations were tested for their ability to support MSCs *in vitro*, since the initial responses of these bone progenitor cells provide important information regarding the potential success of a synthetic bone graft [25]. The compositions of the scaffolds tested were 100% polycaprolactone (PCL), 80%PCL/20%HA, 50%PCL/30%col/20%HA, and 100% collagen I (col). We hypothesized that matrices containing collagen would present MSCs with natural integrin ligands, and therefore be the most successful at supporting MSC adhesion and survival. However it was observed that MSCs did not survive on 100% col matrices at 7 days [87]. Although we were initially surprised by these results, tensile testing of the scaffolds revealed that the lack of MSC survival on 100% col matrices was likely due to the low mechanical properties of our non-cross-linked 100% col matrices when wet. The matrices fell apart immediately upon application of mechanical force, below the limits of

detection by the dynamic mechanical analyzer. It has been shown that materials with an extremely low tensile modulus are not able to support cell adhesion and can even lead to the activation of cell apoptosis [58, 149-151]. Although the use of cross-linking agents has been reported to increase the mechanical properties of collagen biomaterials, the presence of residual cross-linking agents is capable of producing prolonged toxic effects [152]. Cross-linked collagen fibers also lead to a reduction in scaffold porosity, limiting the vascularization and tissue in-growth into the biomaterial [153].

As an alternative to chemical cross-linking, we have combined collagen I with HA and the biodegradable FDA approved polymer PCL, which has a much slower rate of degradation than collagen. It was found that these matrices possessed favorable mechanical properties for maintaining their integrity *in vitro* and *in vivo*, and supported greater integrin activation (as measured by FAK phosphorylation), adhesion and proliferation of MSCs compared to PCL/HA or 100% PCL scaffolds. Additionally, the incorporation of the collagen and HA within the electrospinning solution creates composite fibers throughout the biomaterial, continually providing cells with biological cues as they migrate within the scaffold and the scaffold resorbs. In comparison, many studies by others have simply coated the surfaces of electrospun polymer matrices with collagen I [52, 53, 154-156] or HA [148, 157], and while these studies have shown benefits on cell responses over uncoated polymer fibers, the coating is largely restricted to the outer layer of fibers. Therefore cells exposed to the interior of the scaffold via cell migration or scaffold degradation will not receive the benefits of these molecular signals.

Our findings that bone-mimetic matrices (BMM) supported greater MSC adhesion and proliferation relative to 100% PCL scaffolds was not surprising due to the colla-

gen I providing ligands for MSC integrins. It has been repeatedly shown that cell attachment to collagen I activates signaling cascades leading to firm cell adhesion, survival, and proliferation [66-68, 158]. However, we hypothesized that the HA nanoparticles were also playing an indirect role in these MSC responses. Our lab has previously shown that HA containing biomaterials are able to adsorb substantial quantities of proadhesive proteins, such as fibronectin and vitronectin, from blood and serum and these proteins subsequently support the binding of purified integrins and MSC adhesion [70, 71, 119]. Testing this hypothesis both *in vitro* and *in vivo*, our results show that electrospun matrices containing HA particles are able to adsorb greater quantities of proadhesive proteins from both serum and the bone microenvironment when compared to 100% PCL scaffolds. Additionally, bone-mimetic matrices containing HA and collagen I were able to adsorb greater quantities of protein than PCL/HA scaffolds. This is likely due to the known interactions between collagen I and some extracellular matrix proteins, including fibronectin [159] and vitronectin [160], leading to increases in their adsorption. The ability of a material to adsorb proadhesive proteins is an important characteristic of biomaterials, as they will quickly be coated with the patient's blood upon implantation, and the adsorbed proteins can then help facilitate cell adhesion.

As a result of the favorable responses observed from MSCs seeded on our bone-mimetic matrices *in vitro*, we decided to test the ability of these scaffolds to support bone formation *in vivo* in a rat tibia cortical defect. After one week of implantation, our findings that BMMs supported robust new bone formation throughout the defect and new bone was being deposited directly on the surface of the implant once again suggest the benefits of incorporating natural bone molecules in a nanofibrous matrix. In comparison,

defects with implanted PCL scaffolds showed primarily soft tissue formation around the implant. However, these experiments revealed the inability of endogenous cells to migrate within the electrospun matrices. Additional work in our lab as well as reports by others have confirmed that the pore sizes of electrospun nanofibrous matrices are too small to allow for cell infiltration [44, 83, 93, 94]. In order to maximize the success of a biodegradable bone matrix, the scaffold needs to facilitate cell infiltration and tissue in growth, thereby allowing the replacement of the synthetic bone graft with new bone through the process of creeping substitution [83].

In order to address this issue, the second goal of this thesis project was to develop a viable method for increasing the pore sizes of BMMs, creating matrices capable of facilitating cell infiltration. As noted, this has become a major issue for researchers using electrospinning for the creation of biomaterials for tissue regeneration. Numerous approaches have been reported as a means for increasing the mean pore size of electrospun scaffolds. These include the creation of larger pores through laser ablation [161], the incorporation of cell-mediated degradation sites [162], the inclusion of sacrificial particles [98, 100] or fibers for subsequent removal [101, 163], and the reduction of the packing density of electrospun fibers during fabrication [95], among other techniques. However, the majority of these studies have solely examined 100% synthetic matrices. Therefore, we tested multiple mechanisms to increase the pore sizes of our BMMs.

In natural ECM, cells cleave fibrous proteins via the secretion of proteases in order to create pores large enough to facilitate migration [164]. To model this mechanism, many researchers have incorporated specific protease domains within biomaterials, allowing cells to degrade the matrix and migrate into the interior [165, 166]. Similarly, we

hypothesized that the collagen in our BMMs could potentially provide domains for protease cleavage, opening larger pores for infiltration. Although treating our BMMs with collagenase *in vitro* created specific fiber breakages, culture of MSCs on BMMs pretreated with collagenase did not facilitate cell infiltration.

Next, we hypothesized that using a unique patterned collecting plate could potentially reduce the packing density of the electrospun fibers during fabrication. When electrospinning onto flat collecting plates, the fibers deposit tightly on top of each other in order to dissipate the charge they received from the power supply. The permittivity, or the amount of resistance to form an electric field in a medium, of the collecting plate largely determines the ability of the material to dissipate charge [167]. Therefore, a collecting plate capable of rapidly dissipating the positive electrical charge (low resistance) from a deposited fiber will permit the next deposited fibers to pack very tightly on top of one another. Alternatively, a collecting plate with a higher resistance will increase the amount of residual positive charge on deposited fibers. This residual charge will subsequently repel positively charged fibers collecting on top of it, thereby reducing the fiber packing density and potentially creating larger pores. Some examples of materials used in electrospinning collecting plates with reduced permittivity include air (patterned plates with gaps in between metal) [96, 97], Styrofoam [95], and polystyrene. Using a unique collecting plate that combined a flat polystyrene back with equally spaced stainless steel needles, we created 100% PCL matrices with advanced architecture, including deep channels and large pores. However, this scaffold structure could not be recapitulated with BMM fibers, despite testing changes to a variety of fabrication parameters. At this time, it is unclear why the inclusion of collagen I and HA prohibits the formation of matrices

with structures similar to that of 100% PCL fibers. Due to the numerous advantages previously described with the BMMs over PCL, this technique was not considered viable at this time. Future studies will be necessary to develop an effective technique for reducing the packing density of BMMs.

Lastly, we tested the addition of sacrificial fibers of polyethylene oxide (PEO), a water-soluble polymer that can be washed away after electrospinning. When electrospinning two separate solutions in the same direction, the positively charged fibers repel each other in the air, and therefore deposit on opposite sides of the collecting plate. To mix these fibers into one matrix, a fixed gear motor was added to continually rotate the grounded collecting plate at a low-RPM on an axis parallel to the direction of the electrospun fibers. After fabrication, washing away the PEO fibers leaves just the BMM with voids left by the sacrificial fibers, thereby creating larger pores. Our findings showed a significant increase in pore sizes of PEO/BMM scaffolds, with a mean pore size of  $\sim 25\mu\text{m}^2$ . This is comparable to the optimal cell infiltration pore size for biomaterials reported by Ratner et al. [85]. We observed that BMMs with sacrificial PEO fibers were able to facilitate a significant increase in the infiltration of MSCs *in vitro*. These results were encouraging, however we felt it was essential to study the infiltration of endogenous bone cells in a bone microenvironment, where multiple cell types are communicating and influencing each other through paracrine and autocrine signaling mechanisms. Using a mouse calvarial organ culture, which maintains the bone microenvironment with all relevant bone cells, including osteoblasts, osteoclasts, and stromal cells [168], a significant increase was observed in the number of endogenous bone cells migrating into BMM/PEO scaffolds. These results concur with a study by Baker et al, wherein PEO fibers success-

fully facilitated the infiltration of MSCs into matrices of aligned PCL fibers. In their study, it was found that increases in the percentage of sacrificial fibers in the scaffold were directly correlated with larger pore sizes and subsequently increased cell infiltration [101]. Therefore, we hypothesize that varying the amount of PEO in our matrices, which was slightly over 25% in the current study, has the potential to tune the relative amount of cell infiltration.

Our findings strongly suggest that BMMs are promising matrices for supporting new bone formation by providing cues for MSCs, and we have addressed a key limitation of inhibited cell infiltration through the incorporation of sacrificial fibers of PEO. However, in order to increase the therapeutic potential of our matrices, the third goal of this thesis project was to evaluate the capacity of BMMs to serve as a delivery vehicle for a biological molecule capable of improving patient prognosis. Due to the essential role of MSCs in the bone healing process, we hypothesized that local delivery of a chemotactic factor for MSCs would stimulate increased migration of MSCs to skeletal defects. This increase in bone building progenitor cells at the defect site would potentially increase the rate of new bone formation, thereby creating a more effective synthetic bone graft and improving clinical outcome [169]. Compared to many other cell types, such as inflammatory and immune cells, the optimal chemoattractants for MSCs are not as well understood [170]. We therefore studied the migration of MSCs *in vitro* in response to multiple growth factors and chemokines. Our findings strongly suggest that PDGF-BB is a robust stimulator of MSC migration. These results correlate with findings by others showing that PDGF-BB stimulated significantly greater amounts of MSC migration *in vitro* in comparison to a wide array of growth factors and chemokines [171, 172]. PDGF-BB has



also been shown to stimulate MSC proliferation *in vitro*, and the MSC secretion of vascular endothelial growth factor (VEGF). PDGF and VEGF are known to play an important role in the sprouting and formation of new blood vessels, therefore, local sustained delivery of PDGF-BB has the potential to stimulate angiogenesis in addition to MSC chemotaxis and proliferation, adding to its therapeutic potential [11].

Currently, PDGF-BB is FDA approved for clinical use in combination with  $\beta$ -TCP in periodontal procedures (GEM-21S<sup>®</sup>, Osteohealth) and awaiting FDA approval for foot and ankle fusion procedures (Augment, BioMimetic Therapeutics Inc.). However, the rapid dissemination of PDGF-BB from  $\beta$ -TCP (100% release after 90 minutes *in vitro* [118]) may limit the therapeutic efficacy of the PDGF, which has a short half-life in blood. Since it is speculated that prolonged release of PDGF will further stimulate MSC proliferation and angiogenesis, other researchers have been investigating methods for controlling the release of PDGF from various delivery vehicles, such as heparin-conjugated scaffolds [147], PLGA microspheres [173], and a photo-crosslinked PVA hydrogel [174]. These studies report release times from several days to months *in vitro*, showing a wide range of possibilities based on the delivery vehicle used.

In the current study, we investigated the passive adsorption of PDGF-BB onto our BMMs and found that BMMs adsorbed significantly more PDGF-BB from solution than PCL scaffolds. This is likely due to the known ability of HA to adsorb proteins from solution, as well as the reported interactions between PDGF and collagen I [132]. Additionally, PDGF-BB released from the scaffolds maintained its bioactivity, stimulating robust MSC chemotaxis in transwell assays, as well as a custom, stringent assay designed to better represent cell migration *in vivo* where released PDGF is diluted in greater volumes

and required to stimulate cells at farther distances than a transwell assay. Lastly, release of PDGF-BB was sustained for 8 weeks with agitation *in vitro*, suggesting that BMMs are promising carriers for PDGF-BB, although additional studies are needed to fully elucidate the safety and efficacy of delivering PDGF-BB from BMMs *in vivo*.

Based on the findings presented in this study, we postulate that electrospun matrices consisting of collagen I, nanoparticulate HA, and PCL are promising materials for use in many clinical applications of bone regeneration. Additionally, the tailoring of BMMs, such as varying the percentage of PEO fibers, provides a means to customize the matrix for specific applications. For example, BMMs without PEO, and therefore small pore sizes, are well suited for use as cell-occlusive membranes in ridge augmentation for dental implants. These membranes, currently comprised solely of collagen I, are necessary to isolate the bone healing environment from invading gingiva tissue, allowing the jaw bone to regrow and support a dental implant [175]. In comparison, BMMs with PEO are promising substrates for many procedures requiring a biodegradable substrate that will be replaced by natural bone, such as spinal fusion and non-routine tibia fractures. The inclusion of PDGF, and potentially other growth factors, provides a means to further increase the bone healing response and patient prognosis.

Future studies are essential to develop a greater understanding of the delivery of PDGF-BB from BMMs prior to clinical use. In particular, animal models will need to be developed to study the ability of BMMs to deliver PDGF *in vivo*. For example, implantation of BMMs coated with radiolabeled PDGF-BB will provide a means to measure the release kinetics of PDGF in a bone defect [118]. Based on these results, the amount of PDGF-BB loaded onto the scaffolds may be adjusted to maintain an optimal release of

growth factor. Additionally, BMMs could potentially be used to deliver multiple therapeutic agents. Other researchers have investigated the co-delivery of PDGF-BB with other growth factors, such as BMP-7 [176], basic fibroblast growth factor [177], and VEGF/TGF- $\beta$  [178] in order to stimulate multiple pathways of bone healing. Concurrent studies in our lab have begun to investigate the delivery of a bioactive BMP-2 peptide with a specific domain capable of tightly anchoring to HA particles. We hypothesize that co-delivery of passively adsorbed PDGF-BB, which will provide a bolus release to stimulate MSC chemotaxis, and tightly anchored BMP-2 peptides, capable of inducing the osteogenic differentiation of invading MSCs, has the potential to synergistically stimulate new bone formation. To examine the co-delivery of PDGF-BB and a bioactive BMP-2 peptide, it will be necessary to look at their adsorption onto and release from BMMs, followed by studying the effect of these growth factors on MSC migration, proliferation, and osteoblastic differentiation *in vitro*. Finally, animal models will be needed to study the ability of BMMs to co-deliver these factors and stimulate new bone formation.

In conclusion, the main focus of this thesis project was the development, adaptation and application of an engineered matrix for use as a synthetic bone graft. The results presented demonstrate that nanofibrous scaffolds consisting of the natural bone matrix molecules collagen I and HA, with the biodegradable polymer PCL and sacrificial fibers of PEO create encouraging biomaterials for bone regenerative applications. Additionally, these matrices show promise for their use as delivery vehicles for PDGF-BB and potentially other growth factors. Ultimately, the local sustained delivery of osteoinductive factors from a bone-mimetic matrix capable of supporting new bone formation has the po-

tential to provide therapeutic benefit in numerous clinical procedures where increased or guided bone regeneration is needed.

## GENERAL LIST OF REFERENCES

- [1] Clarke B. Normal bone anatomy and physiology. *Clin J Am Soc Nephrol.* 2008;3 Suppl 3:S131-9.
- [2] McKibbin B. The biology of fracture healing in long bones. *J Bone Joint Surg Br.* 1978;60-B:150-62.
- [3] Caplan AI. Mesenchymal stem cells. *J Orthop Res.* 1991;9:641-50.
- [4] Pittenger MF, Mackay AM, Beck SC, Jaiswal RK, Douglas R, Mosca JD, et al. Multilineage potential of adult human mesenchymal stem cells. *Science.* 1999;284:143-7.
- [5] Caplan AI. Review: mesenchymal stem cells: cell-based reconstructive therapy in orthopedics. *Tissue Eng.* 2005;11:1198-211.
- [6] Conget PA, Minguell JJ. Phenotypical and functional properties of human bone marrow mesenchymal progenitor cells. *J Cell Physiol.* 1999;181:67-73.
- [7] Dominici M, Le Blanc K, Mueller I, Slaper-Cortenbach I, Marini F, Krause D, et al. Minimal criteria for defining multipotent mesenchymal stromal cells. The International Society for Cellular Therapy position statement. *Cytotherapy.* 2006;8:315-7.
- [8] Liu ZJ, Zhuge Y, Velazquez OC. Trafficking and differentiation of mesenchymal stem cells. *J Cell Biochem.* 2009;106:984-91.
- [9] Caplan AI. The mesengenic process. *Clin Plast Surg.* 1994;21:429-35.
- [10] Devescovi V, Leonardi E, Ciapetti G, Cenni E. Growth factors in bone repair. *Chir Organi Mov.* 2008;92:161-8.
- [11] Hollinger JO, Hart CE, Hirsch SN, Lynch S, Friedlaender GE. Recombinant human platelet-derived growth factor: biology and clinical applications. *J Bone Joint Surg Am.* 2008;90 Suppl 1:48-54.
- [12] Bielby R, Jones E, McGonagle D. The role of mesenchymal stem cells in maintenance and repair of bone. *Injury.* 2007;38 Suppl 1:S26-32.

- [13] Chen Y, Shao JZ, Xiang LX, Dong XJ, Zhang GR. Mesenchymal stem cells: a promising candidate in regenerative medicine. *Int J Biochem Cell Biol.* 2008;40:815-20.
- [14] Bonewald LF. Establishment and characterization of an osteocyte-like cell line, MLO-Y4. *J Bone Miner Metab.* 1999;17:61-5.
- [15] Boyle WJ, Simonet WS, Lacey DL. Osteoclast differentiation and activation. *Nature.* 2003;423:337-42.
- [16] Brighton CT, Sugioka Y, Hunt RM. Cytoplasmic structures of epiphyseal plate chondrocytes. Quantitative evaluation using electron micrographs of rat costochondral junctions with special reference to the fate of hypertrophic cells. *J Bone Joint Surg Am.* 1973;55:771-84.
- [17] Brighton CT, Hunt RM. Histochemical localization of calcium in the fracture callus with potassium pyroantimonate. Possible role of chondrocyte mitochondrial calcium in callus calcification. *J Bone Joint Surg Am.* 1986;68:703-15.
- [18] Dimitriou R, Tsiridis E, Giannoudis PV. Current concepts of molecular aspects of bone healing. *Injury.* 2005;36:1392-404.
- [19] Brydone AS, Meek D, Maclaine S. Bone grafting, orthopaedic biomaterials, and the clinical need for bone engineering. *Proc Inst Mech Eng H.* 2010;224:1329-43.
- [20] Panagiotis M. Classification of non-union. *Injury.* 2005;36 Suppl 4:S30-7.
- [21] Nandi SK, Roy S, Mukherjee P, Kundu B, De DK, Basu D. Orthopaedic applications of bone graft & graft substitutes: a review. *Indian J Med Res.* 2010;132:15-30.
- [22] Fernyhough JC, Schimandle JJ, Weigel MC, Edwards CC, Levine AM. Chronic Donor Site Pain Complicating Bone-Graft Harvesting from the Posterior Iliac Crest for Spinal-Fusion. *Spine.* 1992;17:1474-80.
- [23] Goulet JA, Senunas LE, DeSilva GL, Greenfield MLVH. Autogenous iliac crest bone graft - Complications and functional assessment. *Clinical Orthopaedics and Related Research.* 1997;339:76-81.
- [24] Urist MR. Bone: formation by autoinduction. *Science.* 1965;150:893-9.
- [25] Navarro M, Michiardi A, Castano O, Planell JA. Biomaterials in orthopaedics. *J R Soc Interface.* 2008;5:1137-58.
- [26] Macaya D, Spector M. Injectable hydrogel materials for spinal cord regeneration: a review. *Biomed Mater.* 2012;7:012001.
- [27] Salinas CN, Anseth KS. Mesenchymal stem cells for craniofacial tissue regeneration: designing hydrogel delivery vehicles. *J Dent Res.* 2009;88:681-92.

- [28] Prestwich GD. Hyaluronic acid-based clinical biomaterials derived for cell and molecule delivery in regenerative medicine. *J Control Release*. 2011;155:193-9.
- [29] Gkioni K, Leeuwenburgh SC, Douglas TE, Mikos AG, Jansen JA. Mineralization of hydrogels for bone regeneration. *Tissue Eng Part B Rev*. 2010;16:577-85.
- [30] Chuenjitkuntaworn B, Inrung W, Damrongsri D, Mekaapiruk K, Supaphol P, Pavasant P. Polycaprolactone/hydroxyapatite composite scaffolds: preparation, characterization, and in vitro and in vivo biological responses of human primary bone cells. *J Biomed Mater Res A*. 2010;94:241-51.
- [31] Draghi L, Resta S, Pirozzolo MG, Tanzi MC. Microspheres leaching for scaffold porosity control. *J Mater Sci Mater Med*. 2005;16:1093-7.
- [32] Johnson T, Bahrapourian R, Patel A, Mequanint K. Fabrication of highly porous tissue-engineering scaffolds using selective spherical porogens. *Biomed Mater Eng*. 2010;20:107-18.
- [33] Mikos AG, Sarakinos G, Leite SM, Vacanti JP, Langer R. Laminated three-dimensional biodegradable foams for use in tissue engineering. *Biomaterials*. 1993;14:323-30.
- [34] Suh SW, Shin JY, Kim J, Beak CH, Kim DI, Kim H, et al. Effect of different particles on cell proliferation in polymer scaffolds using a solvent-casting and particulate leaching technique. *ASAIO J*. 2002;48:460-4.
- [35] Huang ZM, Zhang YZ, Kotaki M, Ramakrishna S. A review on polymer nanofibers by electrospinning and their applications in nanocomposites. *Composites Science and Technology*. 2003;63:2223-53.
- [36] Pham QP, Sharma U, Mikos AG. Electrospinning of polymeric nanofibers for tissue engineering applications: A review. *Tissue Engineering*. 2006;12:1197-211.
- [37] Murugan R, Ramakrishna S. Nano-featured scaffolds for tissue engineering: A review of spinning methodologies. *Tissue Engineering*. 2006;12:435-47.
- [38] Sill TJ, von Recum HA. Electro spinning: Applications in drug delivery and tissue engineering. *Biomaterials*. 2008;29:1989-2006.
- [39] Wutticharoenmongkol P, Sanchavanakit N, Pavasant P, Supaphol P. Preparation and characterization of novel bone scaffolds based on electrospun polycaprolactone fibers filled with nanoparticles. *Macromolecular Bioscience*. 2006;6:70-7.
- [40] Li WJ, Tuan RS. Fabrication and application of nanofibrous scaffolds in tissue engineering. *Curr Protoc Cell Biol*. 2009;Chapter 25:Unit 25 2.
- [41] Tzaphlidou M. The role of collagen in bone structure: An image processing approach. *Micron*. 2005;36:593-601.

- [42] Teo WE, Ramakrishna S. A review on electrospinning design and nanofibre assemblies. *Nanotechnology*. 2006;17:R89-R106.
- [43] Ebersole GC, Buettmann EG, Macewan MR, Tang ME, Frisella MM, Matthews BD, et al. Development of novel electrospun absorbable polycaprolactone (PCL) scaffolds for hernia repair applications. *Surg Endosc*. 2012;26:2717-28.
- [44] Soliman S, Sant S, Nichol JW, Khabiry M, Traversa E, Khademhosseini A. Controlling the porosity of fibrous scaffolds by modulating the fiber diameter and packing density. *J Biomed Mater Res A*. 2011;96:566-74.
- [45] Alves da Silva ML, Martins A, Costa-Pinto AR, Costa P, Faria S, Gomes M, et al. Cartilage tissue engineering using electrospun PCL nanofiber meshes and MSCs. *Biomacromolecules*. 2010;11:3228-36.
- [46] Aviss KJ, Gough JE, Downes S. Aligned electrospun polymer fibres for skeletal muscle regeneration. *Eur Cell Mater*. 2010;19:193-204.
- [47] Hiep NT, Lee BT. Electro-spinning of PLGA/PCL blends for tissue engineering and their biocompatibility. *J Mater Sci Mater Med*. 2010;21:1969-78.
- [48] Toyokawa N, Fujioka H, Kokubu T, Nagura I, Inui A, Sakata R, et al. Electrospun synthetic polymer scaffold for cartilage repair without cultured cells in an animal model. *Arthroscopy*. 2010;26:375-83.
- [49] Liu W, Yeh YC, Lipner J, Xie J, Sung HW, Thomopoulos S, et al. Enhancing the stiffness of electrospun nanofiber scaffolds with a controlled surface coating and mineralization. *Langmuir*. 2011;27:9088-93.
- [50] Dinarvand P, Seyedjafari E, Shafiee A, Jandaghi AB, Doostmohammadi A, Fathi MH, et al. New approach to bone tissue engineering: simultaneous application of hydroxyapatite and bioactive glass coated on a poly(L-lactic acid) scaffold. *ACS Appl Mater Interfaces*. 2011;3:4518-24.
- [51] Wojtowicz AM, Shekaran A, Oest ME, Dupont KM, Templeman KL, Hutmacher DW, et al. Coating of biomaterial scaffolds with the collagen-mimetic peptide GFOGER for bone defect repair. *Biomaterials*. 2010;31:2574-82.
- [52] Truong YB, Glattauer V, Briggs KL, Zappe S, Ramshaw JA. Collagen-based layer-by-layer coating on electrospun polymer scaffolds. *Biomaterials*. 2012;33:9198-204.
- [53] Shabani I, Haddadi-Asl V, Soleimani M, Seyedjafari E, Babaeijandaghi F, Ahmadbeigi N. Enhanced infiltration and biomineralization of stem cells on collagen-grafted three-dimensional nanofibers. *Tissue Eng Part A*. 2011;17:1209-18.



- [54] Catledge SA, Clem WC, Shrikishen N, Chowdhury S, Stanishevsky AV, Koopman M, et al. An electrospun triphasic nanofibrous scaffold for bone tissue engineering. *Biomedical Materials*. 2007;2:142-50.
- [55] Woodward SC, Brewer PS, Moatamed F, Schindler A, Pitt CG. The intracellular degradation of poly(epsilon-caprolactone). *J Biomed Mater Res*. 1985;19:437-44.
- [56] Darney PD, Monroe SE, Klaisle CM, Alvarado A. Clinical evaluation of the Capronor contraceptive implant: preliminary report. *Am J Obstet Gynecol*. 1989;160:1292-5.
- [57] Bezwada RS, Jamiolkowski DD, Lee IY, Agarwal V, Persivale J, Trenka-Benthin S, et al. Monocryl suture, a new ultra-pliable absorbable monofilament suture. *Biomaterials*. 1995;16:1141-8.
- [58] Engler AJ, Sen S, Sweeney HL, Discher DE. Matrix elasticity directs stem cell lineage specification. *Cell*. 2006;126:677-89.
- [59] Bosnakovski D, Mizuno M, Kim G, Takagi S, Okumura M, Fujinaga T. Chondrogenic differentiation of bovine bone marrow mesenchymal stem cells (MSCs) in different hydrogels: influence of collagen type II extracellular matrix on MSC chondrogenesis. *Biotechnol Bioeng*. 2006;93:1152-63.
- [60] Curran JM, Chen R, Hunt JA. The guidance of human mesenchymal stem cell differentiation in vitro by controlled modifications to the cell substrate. *Biomaterials*. 2006;27:4783-93.
- [61] Zhao X, Hadjiargyrou M. Induction of cell migration in vitro by an electrospun PDGF-BB/PLGA/PEG-PLA nanofibrous scaffold. *J Biomed Nanotechnol*. 2011;7:823-9.
- [62] Huang YC, Liu TJ. Mobilization of mesenchymal stem cells by stromal cell-derived factor-1 released from chitosan/tripolyphosphate/fucoidan nanoparticles. *Acta Biomater*. 2012;8:1048-56.
- [63] Choo T, Marino V, Bartold PM. Effect of PDGF-BB and beta-tricalcium phosphate (beta-TCP) on bone formation around dental implants: a pilot study in sheep. *Clin Oral Implants Res*. 2011;00: 1-9.
- [64] Shao Z, Zhang X, Pi Y, Wang X, Jia Z, Zhu J, et al. Polycaprolactone electrospun mesh conjugated with an MSC affinity peptide for MSC homing in vivo. *Biomaterials*. 2012;33:3375-87.
- [65] McBeath R, Pirone DM, Nelson CM, Bhadriraju K, Chen CS. Cell shape, cytoskeletal tension, and RhoA regulate stem cell lineage commitment. *Dev Cell*. 2004;6:483-95.

- [66] Salaszyk RM, Williams WA, Boskey A, Batorsky A, Plopper GE. Adhesion to vitronectin and collagen I promotes osteogenic differentiation of human mesenchymal stem cells. *Journal of Biomedicine and Biotechnology*. 2004;2004:24-34.
- [67] Wozniak MA, Modzelewska K, Kwong L, Keely PJ. Focal adhesion regulation of cell behavior. *Biochim Biophys Acta*. 2004;1692:103-19.
- [68] Salaszyk RM, Klees RF, Williams WA, Boskey A, Plopper GE. Focal adhesion kinase signaling pathways regulate the osteogenic differentiation of human mesenchymal stem cells. *Exp Cell Res*. 2007;313:22-37.
- [69] Kilpadi KL, Chang PL, Bellis SL. Hydroxylapatite binds more serum proteins, purified integrins, and osteoblast precursor cells than titanium or steel. *J Biomed Mater Res*. 2001;57:258-67.
- [70] Sawyer AA, Hennessy KM, Bellis SL. Regulation of mesenchymal stem cell attachment and spreading on hydroxyapatite by RGD peptides and adsorbed serum proteins. *Biomaterials*. 2005;26:1467-75.
- [71] Hennessy KM, Clem WC, Phipps MC, Sawyer AA, Shaikh FM, Bellis SL. The effect of RGD peptides on osseointegration of hydroxyapatite biomaterials. *Biomaterials*. 2008;29:3075-83.
- [72] Jaiswal N, Haynesworth SE, Caplan AI, Bruder SP. Osteogenic differentiation of purified, culture-expanded human mesenchymal stem cells in vitro. *J Cell Biochem*. 1997;64:295-312.
- [73] Rickard DJ, Sullivan TA, Shenker BJ, Leboy PS, Kazhdan I. Induction of rapid osteoblast differentiation in rat bone marrow stromal cell cultures by dexamethasone and BMP-2. *Dev Biol*. 1994;161:218-28.
- [74] Knutsen R, Wergedal JE, Sampath TK, Baylink DJ, Mohan S. Osteogenic protein-1 stimulates proliferation and differentiation of human bone cells in vitro. *Biochem Biophys Res Commun*. 1993;194:1352-8.
- [75] Hanada K, Dennis JE, Caplan AI. Stimulatory effects of basic fibroblast growth factor and bone morphogenetic protein-2 on osteogenic differentiation of rat bone marrow-derived mesenchymal stem cells. *J Bone Miner Res*. 1997;12:1606-14.
- [76] Mizuno M, Kuboki Y. TGF-beta accelerated the osteogenic differentiation of bone marrow cells induced by collagen matrix. *Biochem Biophys Res Commun*. 1995;211:1091-8.
- [77] Isogai Y, Akatsu T, Ishizuya T, Yamaguchi A, Hori M, Takahashi N, et al. Parathyroid hormone regulates osteoblast differentiation positively or negatively depending on the differentiation stages. *J Bone Miner Res*. 1996;11:1384-93.

- [78] Pountos I, Georgouli T, Henshaw K, Bird H, Jones E, Giannoudis PV. The effect of bone morphogenetic protein-2, bone morphogenetic protein-7, parathyroid hormone, and platelet-derived growth factor on the proliferation and osteogenic differentiation of mesenchymal stem cells derived from osteoporotic bone. *J Orthop Trauma*. 2010;24:552-6.
- [79] Myers TJ, Granero-Molto F, Longobardi L, Li T, Yan Y, Spagnoli A. Mesenchymal stem cells at the intersection of cell and gene therapy. *Expert Opin Biol Ther*. 2010;10:1663-79.
- [80] Bruder SP, Jaiswal N, Ricalton NS, Mosca JD, Kraus KH, Kadiyala S. Mesenchymal stem cells in osteobiology and applied bone regeneration. *Clin Orthop Relat Res*. 1998:S247-56.
- [81] Takeuchi Y, Suzawa M, Kikuchi T, Nishida E, Fujita T, Matsumoto T. Differentiation and transforming growth factor-beta receptor down-regulation by collagen-alpha2beta1 integrin interaction is mediated by focal adhesion kinase and its downstream signals in murine osteoblastic cells. *J Biol Chem*. 1997;272:29309-16.
- [82] Mizuno M, Fujisawa R, Kuboki Y. Type I collagen-induced osteoblastic differentiation of bone-marrow cells mediated by collagen-alpha2beta1 integrin interaction. *J Cell Physiol*. 2000;184:207-13.
- [83] Karageorgiou V, Kaplan D. Porosity of 3D biomaterial scaffolds and osteogenesis. *Biomaterials*. 2005;26:5474-91.
- [84] Singh L, Kumar V, Ratner BD. Generation of porous microcellular 85/15 poly (DL-lactide-co-glycolide) foams for biomedical applications. *Biomaterials*. 2004;25:2611-7.
- [85] Galperin A, Long TJ, Ratner BD. Degradable, thermo-sensitive poly(N-isopropyl acrylamide)-based scaffolds with controlled porosity for tissue engineering applications. *Biomacromolecules*. 2010;11:2583-92.
- [86] Hutmacher DW. Scaffolds in tissue engineering bone and cartilage. *Biomaterials*. 2000;21:2529-43.
- [87] Phipps MC, Clem WC, Catledge SA, Xu Y, Hennessy KM, Thomas V, et al. Mesenchymal stem cell responses to bone-mimetic electrospun matrices composed of polycaprolactone, collagen I and nanoparticulate hydroxyapatite. *PLoS One*. 2011;6:e16813.
- [88] Alvarez Perez MA, Guarino V, Cirillo V, Ambrosio L. In vitro mineralization and bone osteogenesis in poly(epsilon-caprolactone)/gelatin nanofibers. *J Biomed Mater Res A*. 2012;100:3008-19.

- [89] Venugopal JR, Giri Dev VR, Senthilram T, Sathiskumar D, Gupta D, Ramakrishna S. Osteoblast mineralization with composite nanofibrous substrate for bone tissue regeneration. *Cell Biol Int*. 2011;35:73-80.
- [90] Kasoju N, Bora U. Silk fibroin based biomimetic artificial extracellular matrix for hepatic tissue engineering applications. *Biomed Mater*. 2012;7:045004.
- [91] Neal RA, McClugage SG, Link MC, Sefcik LS, Ogle RC, Botchwey EA. Laminin nanofiber meshes that mimic morphological properties and bioactivity of basement membranes. *Tissue Eng Part C Methods*. 2009;15:11-21.
- [92] Blit PH, Battiston KG, Yang M, Paul Santerre J, Woodhouse KA. Electrospun elastin-like polypeptide enriched polyurethanes and their interactions with vascular smooth muscle cells. *Acta Biomater*. 2012;8:2493-503.
- [93] Phipps MC, Clem WC, Grunda JM, Clines GA, Bellis SL. Increasing the pore sizes of bone-mimetic electrospun scaffolds comprised of polycaprolactone, collagen I and hydroxyapatite to enhance cell infiltration. *Biomaterials*. 2012;33:524-34.
- [94] Ekaputra AK, Prestwich GD, Cool SM, Hutmacher DW. Combining electrospun scaffolds with electrosprayed hydrogels leads to three-dimensional cellularization of hybrid constructs. *Biomacromolecules*. 2008;9:2097-103.
- [95] Blakeney BA, Tambralli A, Anderson JM, Andukuri A, Lim DJ, Dean DR, et al. Cell infiltration and growth in a low density, uncompressed three-dimensional electrospun nanofibrous scaffold. *Biomaterials*. 2011;32:1583-90.
- [96] Vaquette C, Cooper-White JJ. Increasing electrospun scaffold pore size with tailored collectors for improved cell penetration. *Acta Biomater*. 2011;7:2544-57.
- [97] Zhu X, Cui W, Li X, Jin Y. Electrospun fibrous mats with high porosity as potential scaffolds for skin tissue engineering. *Biomacromolecules*. 2008;9:1795-801.
- [98] Nam J, Huang Y, Agarwal S, Lannutti J. Improved cellular infiltration in electrospun fiber via engineered porosity. *Tissue Eng*. 2007;13:2249-57.
- [99] Wright LD, Andric T, Freeman JW. Utilizing NaCl to increase the porosity of electrospun materials. *Materials Science and Engineering C*. 2010;31:30-6.
- [100] Leong MF, Rasheed MZ, Lim TC, Chian KS. In vitro cell infiltration and in vivo cell infiltration and vascularization in a fibrous, highly porous poly(D,L-lactide) scaffold fabricated by cryogenic electrospinning technique. *Journal of Biomedical Materials Research Part A*. 2009;91:231-40.
- [101] Baker BM, Gee AO, Metter RB, Nathan AS, Marklein RA, Burdick JA, et al. The potential to improve cell infiltration in composite fiber-aligned electrospun scaffolds by the selective removal of sacrificial fibers. *Biomaterials*. 2008;29:2348-58.

- [102] Milleret V, Simona B, Neuenschwander P, Hall H. Tuning electrospinning parameters for production of 3D-fiber-fleeces with increased porosity for soft tissue engineering applications. *Eur Cell Mater*. 2011;21:286-303.
- [103] Solheim E. Growth factors in bone. *Int Orthop*. 1998;22:410-6.
- [104] Walker DH, Wright NM. Bone morphogenetic proteins and spinal fusion. *Neurosurg Focus*. 2002;13:e3.
- [105] McKay WF, Peckham SM, Badura JM. A comprehensive clinical review of recombinant human bone morphogenetic protein-2 (INFUSE Bone Graft). *Int Orthop*. 2007;31:729-34.
- [106] Woo EJ. Adverse events reported after the use of recombinant human bone morphogenetic protein 2. *J Oral Maxillofac Surg*. 2012;70:765-7.
- [107] Crawford CH, 3rd, Carreon LY, McGinnis MD, Campbell MJ, Glassman SD. Perioperative complications of recombinant human bone morphogenetic protein-2 on an absorbable collagen sponge versus iliac crest bone graft for posterior cervical arthrodesis. *Spine (Phila Pa 1976)*. 2009;34:1390-4.
- [108] Lavery K, Hawley S, Swain P, Rooney R, Falb D, Alaoui-Ismaili MH. New insights into BMP-7 mediated osteoblastic differentiation of primary human mesenchymal stem cells. *Bone*. 2009;45:27-41.
- [109] Vaccaro AR, Whang PG, Patel T, Phillips FM, Anderson DG, Albert TJ, et al. The safety and efficacy of OP-1 (rhBMP-7) as a replacement for iliac crest autograft for posterolateral lumbar arthrodesis: minimum 4-year follow-up of a pilot study. *Spine J*. 2008;8:457-65.
- [110] Yu NY, Schindeler A, Peacock L, Mikulec K, Baldock PA, Ruys AJ, et al. In vivo local co-delivery of recombinant human bone morphogenetic protein-7 and pamidronate via poly-D, L-lactic acid. *Eur Cell Mater*. 2010;20:431-41.
- [111] Wei G, Jin Q, Giannobile WV, Ma PX. The enhancement of osteogenesis by nano-fibrous scaffolds incorporating rhBMP-7 nanospheres. *Biomaterials*. 2007;28:2087-96.
- [112] Xian L, Wu X, Pang L, Lou M, Rosen CJ, Qiu T, et al. Matrix IGF-1 maintains bone mass by activation of mTOR in mesenchymal stem cells. *Nat Med*. 2012;18:1095-101.
- [113] Wang F, Song YL, Li CX, Li DH, Zhang HP, Ma AJ, et al. Sustained release of insulin-like growth factor-1 from poly(lactide-co-glycolide) microspheres improves osseointegration of dental implants in type 2 diabetic rats. *Eur J Pharmacol*. 2010;640:226-32.

- [114] Chen FM, Zhao YM, Wu H, Deng ZH, Wang QT, Zhou W, et al. Enhancement of periodontal tissue regeneration by locally controlled delivery of insulin-like growth factor-I from dextran-co-gelatin microspheres. *J Control Release*. 2006;114:209-22.
- [115] Andrae J, Gallini R, Betsholtz C. Role of platelet-derived growth factors in physiology and medicine. *Genes Dev*. 2008;22:1276-312.
- [116] Solchaga LA, Hee CK, Aguiar DJ, Ratliff J, Turner AS, Seim HB, 3rd, et al. Augment bone graft products compare favorably with autologous bone graft in an ovine model of lumbar interbody spine fusion. *Spine (Phila Pa 1976)*. 2012;37:E461-7.
- [117] Solchaga LA, Hee CK, Roach S, Snel LB. Safety of recombinant human platelet-derived growth factor-BB in Augment((R)) Bone Graft. *J Tissue Eng*. 2012;3:2041731412442668.
- [118] Young CS, Ladd PA, Browning CF, Thompson A, Bonomo J, Shockley K, et al. Release, biological potency, and biochemical integrity of recombinant human platelet-derived growth factor-BB (rhPDGF-BB) combined with Augment(TM) Bone Graft or GEM 21S beta-tricalcium phosphate (beta-TCP). *J Control Release*. 2009;140:250-5.
- [119] Hennessy KM, Pollot BE, Clem WC, Phipps MC, Sawyer AA, Culpepper BK, et al. The effect of collagen I mimetic peptides on mesenchymal stem cell adhesion and differentiation, and on bone formation at hydroxyapatite surfaces. *Biomaterials*. 2009;30:1898-909.
- [120] Davies JE. In vitro modeling of the bone/implant interface. *Anat Rec*. 1996;245:426-45.
- [121] LeGeros RZ. Properties of osteoconductive biomaterials: calcium phosphates. *Clin Orthop Relat Res*. 2002:81-98.
- [122] Burr DB, Mori S, Boyd RD, Sun TC, Blaha JD, Lane L, et al. Histomorphometric assessment of the mechanisms for rapid ingrowth of bone to HA/TCP coated implants. *J Biomed Mater Res*. 1993;27:645-53.
- [123] Cook SD, Thomas KA, Dalton JE, Volkman TK, Whitecloud TS, 3rd, Kay JF. Hydroxylapatite coating of porous implants improves bone ingrowth and interface attachment strength. *J Biomed Mater Res*. 1992;26:989-1001.
- [124] Karabatsos B, Myerthall SL, Fornasier VL, Binnington A, Maistrelli GL. Osseointegration of hydroxyapatite porous-coated femoral implants in a canine model. *Clin Orthop Relat Res*. 2001:442-9.
- [125] Bohner M. Calcium orthophosphates in medicine: from ceramics to calcium phosphate cements. *Injury*. 2000;31 Suppl 4:37-47.

- [126] Geiger M, Li RH, Friess W. Collagen sponges for bone regeneration with rhBMP-2. *Adv Drug Deliv Rev.* 2003;55:1613-29.
- [127] Speer DP, Chvapil M, Volz RG, Holmes MD. Enhancement of healing in osteochondral defects by collagen sponge implants. *Clin Orthop Relat Res.* 1979;326-35.
- [128] Wakitani S, Kimura T, Hirooka A, Ochi T, Yoneda M, Yasui N, et al. Repair of rabbit articular surfaces with allograft chondrocytes embedded in collagen gel. *J Bone Joint Surg Br.* 1989;71:74-80.
- [129] Marinucci L, Lilli C, Guerra M, Belcastro S, Becchetti E, Stabellini G, et al. Biocompatibility of collagen membranes crosslinked with glutaraldehyde or diphenylphosphoryl azide: an in vitro study. *Journal of Biomedical Materials Research Part A.* 2003;67:504-9.
- [130] Glassman SD, Carreon LY, Djurasovic M, Campbell MJ, Puno RM, Johnson JR, et al. RhBMP-2 versus iliac crest bone graft for lumbar spine fusion: a randomized, controlled trial in patients over sixty years of age. *Spine (Phila Pa 1976).* 2008;33:2843-9.
- [131] Papanna MC, Al-Hadithy N, Somanchi BV, Sewell MD, Robinson PM, Khan SA, et al. The use of bone morphogenetic protein-7 (OP-1) in the management of resistant non-unions in the upper and lower limb. *Injury.* 2012;43:1135-40.
- [132] Somasundaram R, Schuppan D. Type I, II, III, IV, V, and VI collagens serve as extracellular ligands for the isoforms of platelet-derived growth factor (AA, BB, and AB). *J Biol Chem.* 1996;271:26884-91.
- [133] Prabhakaran MP, Venugopal J, Ramakrishna S. Electrospun nanostructured scaffolds for bone tissue engineering. *Acta Biomater.* 2009;5:2884-93.
- [134] Gupta D, Venugopal J, Mitra S, Giri Dev VR, Ramakrishna S. Nanostructured biocomposite substrates by electrospinning and electrospraying for the mineralization of osteoblasts. *Biomaterials.* 2009;30:2085-94.
- [135] Ekaputra AK, Zhou Y, Cool SM, Hutmacher DW. Composite electrospun scaffolds for engineering tubular bone grafts. *Tissue Eng Part A.* 2009;15:3779-88.
- [136] Kazemnejad S, Akhondi MM, Soleimani M, Zarnani AH, Khanmohammadi M, Darzi S, et al. Characterization and chondrogenic differentiation of menstrual blood-derived stem cells on a nanofibrous scaffold. *Int J Artif Organs.* 2012;35:55-66.
- [137] Shafiee A, Soleimani M, Chamheidari GA, Seyedjafari E, Dodel M, Atashi A, et al. Electrospun nanofiber-based regeneration of cartilage enhanced by mesenchymal stem cells. *J Biomed Mater Res A.* 2011;99:467-78.

- [138] Zhang X, Xu Y, Thomas V, Bellis SL, Vohra YK. Engineering an antiplatelet adhesion layer on an electrospun scaffold using porcine endothelial progenitor cells. *J Biomed Mater Res A*. 2011;97:145-51.
- [139] Ruder C, Sauter T, Becker T, Kratz K, Hiebl B, Jung F, et al. Viability, proliferation and adhesion of smooth muscle cells and human umbilical vein endothelial cells on electrospun polymer scaffolds. *Clin Hemorheol Microcirc*. 2012;50:101-12.
- [140] Kim HL, Lee JH, Lee MH, Kwon BJ, Park JC. Evaluation of Electrospun (1,3)-(1,6)-beta-D-Glucans/Biodegradable Polymer as Artificial Skin for Full-Thickness Wound Healing. *Tissue Eng Part A*. 2012; Epub ahead of print.
- [141] Sundaramurthi D, Vasanthan KS, Kuppan P, Krishnan UM, Sethuraman S. Electrospun nanostructured chitosan-poly(vinyl alcohol) scaffolds: a biomimetic extracellular matrix as dermal substitute. *Biomed Mater*. 2012;7:045005.
- [142] Brown TD, Slotosch A, Thibaudeau L, Taubenberger A, Loessner D, Vaquette C, et al. Design and fabrication of tubular scaffolds via direct writing in a melt electrospinning mode. *Biointerphases*. 2012;7:13.
- [143] Teng SH, Lee EJ, Wang P, Kim HE. Collagen/hydroxyapatite composite nanofibers by electrospinning. *Materials Letters*. 2008;62:3055-8.
- [144] Matthews JA, Wnek GE, Simpson DG, Bowlin GL. Electrospinning of collagen nanofibers. *Biomacromolecules*. 2002;3:232-8.
- [145] Ngiam M, Liao SS, Patil AJ, Cheng ZY, Chan CK, Ramakrishna S. The fabrication of nano-hydroxyapatite on PLGA and PLGA/collagen nanofibrous composite scaffolds and their effects in osteoblastic behavior for bone tissue engineering. *Bone*. 2009;45:4-16.
- [146] Su Y, Su Q, Liu W, Lim M, Venugopal JR, Mo X, et al. Controlled release of bone morphogenetic protein 2 and dexamethasone loaded in core-shell PLLACL-collagen fibers for use in bone tissue engineering. *Acta Biomater*. 2012;8:763-71.
- [147] Lee J, Yoo JJ, Atala A, Lee SJ. The effect of controlled release of PDGF-BB from heparin-conjugated electrospun PCL/gelatin scaffolds on cellular bioactivity and infiltration. *Biomaterials*. 2012;33:6709-20.
- [148] Nandakumar A, Yang L, Habibovic P, van Blitterswijk C. Calcium phosphate coated electrospun fiber matrices as scaffolds for bone tissue engineering. *Langmuir*. 2010;26:7380-7.
- [149] Discher DE, Janmey P, Wang YL. Tissue cells feel and respond to the stiffness of their substrate. *Science*. 2005;310:1139-43.



- [150] Butcher DT, Alliston T, Weaver VM. A tense situation: forcing tumour progression. *Nature Reviews Cancer*. 2009;9:108-22.
- [151] Wang HB, Dembo M, Wang YL. Substrate flexibility regulates growth and apoptosis of normal but not transformed cells. *American Journal of Physiology-Cell Physiology*. 2000;279:C1345-C50.
- [152] van Wachem PB, van Luyn MJ, Olde Damink LH, Dijkstra PJ, Feijen J, Nieuwenhuis P. Biocompatibility and tissue regenerating capacity of crosslinked dermal sheep collagen. *J Biomed Mater Res*. 1994;28:353-63.
- [153] Heydarkhan-Hagvall S, Schenke-Layland K, Dhanasopon AP, Rofail F, Smith H, Wu BM, et al. Three-dimensional electrospun ECM-based hybrid scaffolds for cardiovascular tissue engineering. *Biomaterials*. 2008;29:2907-14.
- [154] Gustafsson Y, Haag J, Jungebluth P, Lundin V, Lim ML, Baiguera S, et al. Viability and proliferation of rat MSCs on adhesion protein-modified PET and PU scaffolds. *Biomaterials*. 2012;33:8094-103.
- [155] Hong SG, Kim GH. Mechanically improved electrospun PCL biocomposites reinforced with a collagen coating process: preparation, physical properties, and cellular activity. *Bioprocess Biosyst Eng*. 2012; Epub ahead of print.
- [156] Duan Y, Wang Z, Yan W, Wang S, Zhang S, Jia J. Preparation of collagen-coated electrospun nanofibers by remote plasma treatment and their biological properties. *J Biomater Sci Polym Ed*. 2007;18:1153-64.
- [157] Kim IA, Rhee SH. Apatite coating of electrospun PLGA fibers using a PVA vehicle system carrying calcium ions. *J Biomater Sci Polym Ed*. 2010;21:1127-41.
- [158] Jokinen J, Dadu E, Nykvist P, Kapyla J, White DJ, Ivaska J, et al. Integrin-mediated cell adhesion to type I collagen fibrils. *J Biol Chem*. 2004;279:31956-63.
- [159] Engvall E, Ruoslahti E. Binding of soluble form of fibroblast surface protein, fibronectin, to collagen. *International Journal of Cancer*. 1977;20:1-5.
- [160] Gebb C, Hayman EG, Engvall E, Ruoslahti E. Interaction of vitronectin with collagen. *Journal of Biological Chemistry*. 1986;261:16698-703.
- [161] McCullen SD, Gittard SD, Miller PR, Pourdeyhimi B, Narayan RJ, Lobo EG. Laser ablation imparts controlled micro-scale pores in electrospun scaffolds for tissue engineering applications. *Ann Biomed Eng*. 2011;39:3021-30.
- [162] Tambralli A, Blakeney B, Anderson J, Kushwaha M, Andukuri A, Dean D, et al. A hybrid biomimetic scaffold composed of electrospun polycaprolactone nanofibers and self-assembled peptide amphiphile nanofibers. *Biofabrication*. 2009;1:025001.

- [163] Whited BM, Whitney JR, Hofmann MC, Xu Y, Rylander MN. Pre-osteoblast infiltration and differentiation in highly porous apatite-coated PLLA electrospun scaffolds. *Biomaterials*. 2011;32:2294-304.
- [164] Murphy G, Gavrilovic J. Proteolysis and cell migration: creating a path? *Curr Opin Cell Biol*. 1999;11:614-21.
- [165] Gobin AS, West JL. Cell migration through defined, synthetic ECM analogs. *FASEB J*. 2002;16:751-3.
- [166] Lutolf MP, Hubbell JA. Synthetic biomaterials as instructive extracellular microenvironments for morphogenesis in tissue engineering. *Nat Biotechnol*. 2005;23:47-55.
- [167] Mitchell SB, Sanders JE. A unique device for controlled electrospinning. *J Biomed Mater Res A*. 2006;78:110-20.
- [168] Mohammad KS, Chirgwin JM, Guise TA. Assessing new bone formation in neonatal calvarial organ cultures. *Methods Mol Biol*. 2008;455:37-50.
- [169] Phinney DG. Biochemical heterogeneity of mesenchymal stem cell populations: clues to their therapeutic efficacy. *Cell Cycle*. 2007;6:2884-9.
- [170] Karp JM, Leng Teo GS. Mesenchymal stem cell homing: the devil is in the details. *Cell Stem Cell*. 2009;4:206-16.
- [171] Ozaki Y, Nishimura M, Sekiya K, Suehiro F, Kanawa M, Nikawa H, et al. Comprehensive analysis of chemotactic factors for bone marrow mesenchymal stem cells. *Stem Cells Dev*. 2007;16:119-29.
- [172] Ponte AL, Marais E, Gallay N, Langonne A, Delorme B, Herault O, et al. The in vitro migration capacity of human bone marrow mesenchymal stem cells: comparison of chemokine and growth factor chemotactic activities. *Stem Cells*. 2007;25:1737-45.
- [173] Wei G, Jin Q, Giannobile WV, Ma PX. Nano-fibrous scaffold for controlled delivery of recombinant human PDGF-BB. *J Control Release*. 2006;112:103-10.
- [174] Bourke SL, Al-Khalili M, Briggs T, Michniak BB, Kohn J, Poole-Warren LA. A photo-crosslinked poly(vinyl alcohol) hydrogel growth factor release vehicle for wound healing applications. *AAPS PharmSci*. 2003;5:E33.
- [175] Parrish LC, Miyamoto T, Fong N, Mattson JS, Cerutis DR. Non-bioabsorbable vs. bioabsorbable membrane: assessment of their clinical efficacy in guided tissue regeneration technique. A systematic review. *J Oral Sci*. 2009;51:383-400.

- [176] Zhang Y, Cheng N, Miron R, Shi B, Cheng X. Delivery of PDGF-B and BMP-7 by mesoporous bioglass/silk fibrin scaffolds for the repair of osteoporotic defects. *Biomaterials*. 2012;33:6698-708.
- [177] Tengood JE, Ridenour R, Brodsky R, Russell AJ, Little SR. Sequential delivery of basic fibroblast growth factor and platelet-derived growth factor for angiogenesis. *Tissue Eng Part A*. 2011;17:1181-9.
- [178] Reyes R, De la Riva B, Delgado A, Hernandez A, Sanchez E, Evora C. Effect of triple growth factor controlled delivery by a brushite-PLGA system on a bone defect. *Injury*. 2012;43:334-42.


APPENDIX A

INSTITUTIONAL REVIEW BOARD FOR HUMAN USE APPROVAL FORM

DATE: August 27, 2012

MEMORANDUM

TO: Matthew Phipps  
Principal Investigator

FROM: Cari Oliver, CIP   
Assistant Director, UAB OIRB

RE: Request for Determination—Human Subjects Research  
**IRB Protocol #N120815001– Development of Electrospun Bone – Mimetic  
Matrices for Bone Regenerative Applications**

A member of the Office of the IRB has reviewed your application for Designation of Not Human Subjects Research for above referenced proposal.

The reviewer has determined that this proposal is **not** subject to FDA regulations and is **not** Human Subjects Research. Note that any changes to the project should be resubmitted to the Office of the IRB for determination.

470 Administration Building  
701 20th Street South  
205.934.3789  
Fax 205.934.1301  
irb@uab.edu

The University of  
Alabama at Birmingham  
Mailing Address:  
AB 470  
1530 3RD AVE S  
BIRMINGHAM AL 35294-0104

APPENDIX B

INSTITUTIONAL ANIMAL CARE AND USE COMMITTEE APPROVAL FORMS




THE UNIVERSITY OF ALABAMA AT BIRMINGHAM

*Institutional Animal Care and Use Committee (IACUC)*

NOTICE OF RENEWAL

**DATE:** November 22, 2010

**TO:** SUSAN L BELLIS, Ph.D.  
MCLM-982A 0005  
FAX: (205) 975-9028

**FROM:**   
Judith A. Kapp, Ph.D., Chair  
Institutional Animal Care and Use Committee (IACUC)

**SUBJECT:** Title: Functionalizing Hydroxyapatite with Proadhesive Peptides  
Sponsor: NIH  
Animal Project Number: 101107667

As of November 22, 2010, the animal use proposed in the above referenced application is renewed. The University of Alabama at Birmingham Institutional Animal Care and Use Committee (IACUC) approves the use of the following species and numbers of animals:

Species	Use Category	Number in Category
Rats	B	200

Animal use must be renewed by November 13, 2011. Approval from the IACUC must be obtained before implementing any changes or modifications in the approved animal use.

**Please keep this record for your files, and forward the attached letter to the appropriate granting agency.**

Refer to Animal Protocol Number (APN) 101107667 when ordering animals or in any correspondence with the IACUC or Animal Resources Program (ARP) offices regarding this study. If you have concerns or questions regarding this notice, please call the IACUC office at (205) 934-7692.

**Institutional Animal Care and Use Committee**  
CH19 Suite 403  
933 19<sup>th</sup> Street South  
205.934.7692  
FAX 205.934.1188

Mailing Address:  
CH19 Suite 403  
1530 3RD AVE S  
BIRMINGHAM AL 35294-0019



THE UNIVERSITY OF ALABAMA AT BIRMINGHAM

*Institutional Animal Care and Use Committee (IACUC)*

**MEMORANDUM**

**DATE:** September 21, 2011

**TO:** SUSAN L BELLIS, Ph.D.  
MCLM-982A 0005  
FAX: (205) 975-9028

**FROM:**   
Judith A. Kapp, Ph.D., Chair  
Institutional Animal Care and Use Committee (IACUC)

**SUBJECT:** NOTICE OF APPROVAL - Please forward this notice to the appropriate granting agency.

---

The following application was approved by the University of Alabama at Birmingham Institutional Animal Care and Use Committee (IACUC) on September 21, 2011.

Title of Application: Designing Electrospun Scaffolds for Stimulating Bone Formation

Fund Source: Internal

This institution has an Animal Welfare Assurance on file with the Office of Laboratory Animal Welfare (OLAW), is registered as a Research Facility with the USDA, and is accredited by the Association for Assessment and Accreditation of Laboratory Animal Care International (AAALAC).

**Institutional Animal Care and Use Committee**  
CH19 Suite 403  
933 19<sup>th</sup> Street South  
205.934.7692  
FAX 205.934.1188

Mailing Address:  
CH19 Suite 403  
1530 3RD AVE S  
BIRMINGHAM AL 35294-0019